

Portland State University

PDXScholar

Dissertations and Theses


Dissertations and Theses

Winter 3-11-2016

Acid-Base Equilibria in Organic-Solvent/Water Mixtures and Their Relevance to Gas/Particle Partitioning in the Atmosphere and in Tobacco Smoke

Julia Lynn DeGagne
Portland State University

Follow this and additional works at: https://pdxscholar.library.pdx.edu/open_access_etds

 Part of the [Chemicals and Drugs Commons](#), and the [Civil and Environmental Engineering Commons](#)

Let us know how access to this document benefits you.

Recommended Citation

DeGagne, Julia Lynn, "Acid-Base Equilibria in Organic-Solvent/Water Mixtures and Their Relevance to Gas/Particle Partitioning in the Atmosphere and in Tobacco Smoke" (2016). *Dissertations and Theses*. Paper 2733.

<https://doi.org/10.15760/etd.2729>

This Thesis is brought to you for free and open access. It has been accepted for inclusion in Dissertations and Theses by an authorized administrator of PDXScholar. Please contact us if we can make this document more accessible: pdxscholar@pdx.edu.

Acid-Base Equilibria in Organic-Solvent/Water Mixtures and Their Relevance to Gas/Particle

Partitioning in the Atmosphere and in Tobacco Smoke

by

Julia Lynn DeGagné

A thesis submitted in partial fulfillment of the
requirements for the degree of

Master of Science
in
Civil and Environmental Engineering

Thesis Committee:
James F. Pankow, Chair
Scott Wells
Dean Atkinson

Portland State University
2016

Abstract

Acid-base equilibria in organic particulate matter (PM) are poorly understood, but have important implications for air quality and public health. First, acid-base reactions in organic particulate matter affect the gas/particle partitioning of organic compounds in the atmosphere, and these processes are not currently represented in atmospheric and climate change models. Second, the acid-base balance of tobacco smoke affects the amount of nicotine absorbed by the smoker, and a greater understanding of this balance would help to relate cigarette smoke composition to the addictive properties of cigarettes. This work presents data related to both air quality and tobacco smoke modeling.

The gas/particle partitioning behavior of organic acids and bases is highly dependent on acid-base equilibria and speciation between neutral and ionic forms, because ionic compounds do not volatilize. Descriptions of acid dissociation behavior in atmospheric PM have, to date, focused primarily on phases in which the solvent is water; however, atmospheric PM may include up to 90% organic matter. Data is presented here describing the acid dissociation behavior of organic acids and protonated amines in organic/aqueous mixtures (chosen to approximate the characteristics of organic PM) with varying levels of water content. In such mixtures, the preferential solvation of ions and neutral molecules (by the aqueous portion or the organic portion, respectively) affects the acid-base equilibria of the solutes. It is demonstrated that neutralization reactions between acids and bases that create ions are likely to have non-negligible effects on gas/particle partitioning under certain atmospheric conditions. Thus, including acid-base reactions in organic gas/particle partitioning models could result in a greater proportion of acidic and

basic compounds partitioning to the particulate phase. In addition, the acid dissociation constants (pK_a values) of atmospherically-relevant acids and bases vary with water content. Specifically, as water content increases, the pK_a values of organic acids decrease dramatically, while the pK_a values of protonated amines changes only slightly. This situation can result in drastically different speciations and partitioning behavior depending on water content.

This second part of this work reports some of the data needed to develop an acid-base balance for tobacco smoke PM using electroneutrality as a governing principle. Five brands of cigarettes were sampled and the smoke PM extracted. Cations (sodium, potassium, and ammonia) and anions (organic acids, nitrate, nitrite, and chloride) were measured using ion chromatography. Ammonia and organic acids were also re-measured after the acidification of the sample in order to determine whether “bound” forms of these compounds exist in cigarette PM. Weak acids were determined by acid-base titration to determine whether or not all of the weak acids (including organic acids) had been accounted for by the ion chromatography. Weak bases were also determined by acid-base titration, and the majority of weak base is expected to be accounted for by total nicotine (to be measured in a separate analysis). In terms of total acidic species and total basic species, two of the five cigarette brands measured were relatively basic, and three were relatively acidic. Between 50% and 89% of the titrated acids were accounted for by the anionic species measured in ion chromatography. Based on samples tested after sample acidification, about half of the potential ammonia in tobacco smoke PM exists in “bound” form. The speciation of weak acids and bases in tobacco smoke PM cannot be determined

from this data alone, because the equilibrium constants of acid-base reactions are not understood in complex organic media. The data presented here, when combined with data from free-base and total nicotine analyses, represent a first step toward a predictive model of acid-base behavior in tobacco smoke PM.

“...solvents, in spite of appearing at first to be indifferent, are by no means inert; they can greatly influence the course of chemical reactions. This statement is full of consequences...”

- Nikolai Menschutkin, 1890

Acknowledgements

I would like to vehemently thank everyone who supported me in my research over the past two years. Much gratitude goes to my research advisor, James Pankow, for sending me down this fascinating rabbit hole, and for his constant encouragement of my academic and professional development. This project wouldn't have been possible without my friends and colleagues Amy Devita-McBride, Chris Motti, Ben Walker, and Clarissa Chumfong— I'm very thankful for their help with data collection. I am cheerfully indebted to Wentai Luo, whose advice, patience, and general calming presence have prevented several lab-related mistakes. I am also grateful to Dr. David Peyton and Rob Jensen for their time and assistance with the NMR analysis. As always, I owe the most to Marc who takes care of everything.

Table of Contents

Abstract	i
Acknowledgements	v
List of Tables	vii
List of Figures	viii
1. Introduction: Acid-Base Chemistry and Gas/Particle Partitioning in Organic Aerosol Systems	1
1.1. General Characteristics of Aerosol Particulate Matter	2
1.2. Equilibrium Gas/Particle Partitioning of Acids and Bases to Organic PM	4
1.3. Acid-Base Chemistry in Non-Aqueous Systems	9
2. Acid-Base Chemistry in Simulated Atmospheric OPM	12
2.1. Background	12
2.2. Methods	15
2.2.1. Solution Design	15
2.2.2. Acid-Base Titrations	16
2.2.3. NMR Experiments	20
2.3. Results	23
2.4. Discussion	26
3. Acid-Base Chemistry of Tobacco Smoke PM	30
3.1. Background	30
3.1.1. Free Base Nicotine, Nicotine Delivery, and Tobacco Smoke “pH”	30
3.1.2. Toward a Comprehensive Acid-Base Balance of Tobacco Smoke PM	32
3.1.3. “Stealth” Acids and Bases	34
3.2. Methods	35
3.2.1. Sampling and Extraction	35
3.2.2. Acid-Base Titrations	38
3.2.3. Ion Chromatography	42
3.3. Results	43
3.4. Discussion	54
4. Conclusions	57
5. References	59
6. Appendices	69
6.1. Appendix A: ¹ HNMR and HSQC Spectra for Simulated Organic PM	69
6.2. Appendix B: Titration Curves for Tobacco Smoke PM	73
6.3. Appendix C: ¹ HNMR Data for Acetic Acid and Nicotine in 95% IPA	76
6.4. Appendix D: Ion Chromatograms	79

List of Tables

Table 1. Properties of the solvents chosen for the liquid mixture to simulate atmospheric organic PM.....	15
Table 2. Concentrations of the three solvent components used in titration and NMR experiments.....	17
Table 3. Concentrations of solutes representing partitioning compounds used in titration and NMR experiments.....	17
Table 4. Fraction of hexanoic acid and benzylamine that are ionized in 1:1 molar solutions consisting of various portions of organic solvent.....	26
Table 5. Range of analytical method and linear calibration curve R^2 values for tobacco smoke PM analytes quantified using ion chromatography.....	43
Table 6. Measured WTPM extracted from two cigarettes of each brand, and total weak acids and total weak bases measured by titration.....	44
Table 7. Cation concentrations measured in the first five puffs for five cigarette brands.....	47
Table 8. Cation concentrations measured after acidification in the first five puffs for five cigarette brands.....	47
Table 9. Anion concentrations measured in the first five puffs for five cigarette brands.....	48
Table 10. Anion concentrations measured after acidification in the first five puffs for five cigarette brands.....	49

List of Figures

Figure 1. Formation of organic particulate matter.	3
Figure 2. Partitioning behavior in neutral and partially-ionized acids and bases.	9
Figure 3. Unprotonated and protonated forms of benzylamine and hexanoic acid.	22
Figure 4. ¹ HNMR spectra of fully protonated and fully unprotonated hexanoic acid (0.05M) and benzylamine (0.05M).....	22
Figure 5. Titration curves for 0.06F hexanoic acid dissolved in solutions consisting of between 5% and 94% (by volume) organic solvent.....	24
Figure 6. Titration curves for 0.05F benzylamine dissolved in solutions consisting of between 5% and 94% (by volume) organic solvent.....	25
Figure 7. The three forms of nicotine potentially present in solution.....	30
Figure 8. Cigarette smoking apparatus used for sampling of tobacco smoke PM.....	37
Figure 9. Example of a tobacco smoke titration curve and the slope of the titration curve.	40
Figure 10. Measured titratable acids and bases in the first five puffs (plus lighting puff) for five cigarette brands.	44
Figure 11. Identified and unidentified weak acids in the first five puffs (plus lighting puff) for five cigarette brands.....	46
Figure 12. Total measured acids less total measured bases in the first five puffs (plus lighting puff) for five cigarette brands.....	50
Figure 13. Concentrations of strong base tracers (sodium and potassium, shown as positive values) and strong acid tracers (chloride and nitrate, shown as negative values) in the first five puffs (plus lighting puff) for five cigarette brands.	51
Figure 14. Concentrations of ammonium in initial and acidified samples in the first five puffs (plus lighting puff) for five cigarette brands.....	52
Figure 15. Concentrations of acetate and formate in initial and acidified samples in the first five puffs (plus lighting puff) for five cigarette brands.....	53

1. Introduction: Acid-Base Chemistry and Gas/Particle Partitioning in Organic Aerosol Systems

The acid-base chemistry of aerosol particulate matter (PM) affects the equilibrium partitioning of chemical compounds from the gas to the particulate phase. This chemistry includes the dissociation of acids, the protonation of bases, and the formation of salts.

The proportion of organic versus inorganic material in a solvent system such as aerosol PM affects the dissociation constants of acids and protonated bases. These dissociation constants, together with the pH of the particulate phase, determine the ratio of the ionized form of each compound to its “free” (neutral) form. Because only the neutral form is “free” to partition to the gas phase, gas/particle equilibrium partitioning is shifted toward the particulate phase for a given compound when the acid-base equilibrium of the particulate phase favors ionization for that compound.

This thesis explores the importance of acid-base chemistry to two distinct areas of current interest involving gas/particle partitioning to PM: 1.) the representation of relevant physical and chemical processes in atmospheric equilibrium partitioning models, and 2.) the characterization of acids and bases in tobacco smoke. In the first case, it is demonstrated experimentally that significant portions of organic acids and bases can undergo acid-base reactions and become ionized in solvents with compositional and chemical characteristics similar to those of some types of atmospheric PM. This ionization represents a potential mechanism (currently unrepresented in atmospheric models representing partitioning to organic PM) by which atmospheric organics may

enter the particulate phase. In the second case, a compositional analysis of tobacco smoke PM in terms of acids, bases, and ions provides some of the data needed to characterize the acid-base balance of tobacco smoke. This acid-base balance has been historically difficult to measure, yet it has important implications for the bioavailability of nicotine in tobacco smoke and its addictive properties.

1.1. General Characteristics of Aerosol Particulate Matter

Aerosol particulate matter is complex, and is made up of both organic and inorganic components originating from a wide variety of emissions sources. Primary organic aerosol (POA) consists of directly emitted organic particles from combustion or some other source (Kanakidou et al., 2005; Zhang et al., 2015). Secondary organic aerosol (SOA) often forms via the oxidation (primarily by hydroxyl radicals) of reactive volatile organic gases to less-volatile compounds, which condense onto existing suspended particulate matter or form new particles (Hallquist et al., 2009; Kroll and Seinfeld, 2008; Ziemann and Atkinson, 2012) (Figure 1). Suspended PM usually contains both POA and SOA, along with inorganic components such as acids, water, and some crustal materials (Kanakidou et al., 2005; Zhang et al., 2015). All of these PM constituents may be distributed in various morphologies made up of multiple phases. These phases may be solid, liquid, or semisolid (Abramson et al., 2013), and, depending on atmospheric conditions, a liquid phase may separate into additional phases; e.g. a primarily aqueous/hydrophilic/polar phase and a primarily organic/hydrophobic/nonpolar phase

(Arp et al., 2008; Chang and Pankow, 2006; Ciobanu et al., 2009; Song et al., 2012; Wania et al., 2015; You and Bertram, 2015; Zuend and Seinfeld, 2012).

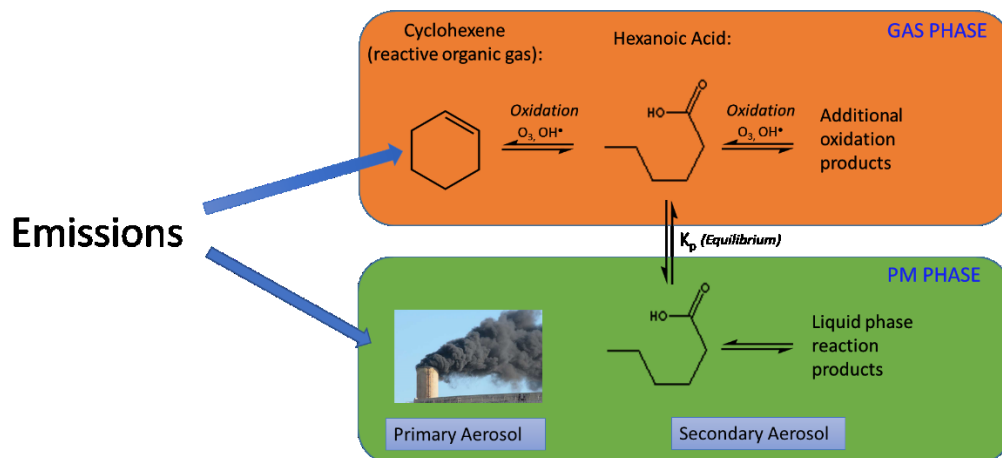


Figure 1. Formation of organic particulate matter.

PM is not static in its composition, but is constantly evolving, in part because SOA ages in the atmosphere. Individual organic compounds become functionalized, fragmented, and/or oligomerized (Barsanti and Pankow, 2006; Chacon-Madrid and Donahue, 2011; Daumit et al., 2013; Jimenez et al., 2009; Shiraiwa et al., 2014; Song and Ng, 2005). As SOA ages and moves downwind of an emission source, the products become more oxidized, more polar, and more hygroscopic, and tend to grow in size and mass (Duplissy et al., 2011; Jimenez et al., 2009). Changes in meteorological variables such as relative humidity and temperature can alter the viscosity and the phase state of the particles (Li et al., 2015). Finally, the chemical constituents of the particles may undergo chemical reactions, such as acid-base reactions (Pankow, 2015, 2003).

Both atmospheric and tobacco smoke PM are complex mixtures of organic and inorganic components. In some cases, aerosol particles are composed primarily of inorganics such as nitrates, sulfates, ammonium, and water (Bassett and Seinfeld, 1983). Commonly, though, PM_{2.5} (which includes aerosols < 2.5 nm in diameter) contains significant amounts of organic matter, including alkanes, alkenes, alcohols, carbonyls, peroxides, organic acids, organic nitrates, and many more. Amounts of organic PM reported are 20% - 50% by mass at mid-latitudes (Kanakidou et al., 2005) and 80% - 95% in the tropics, with 45% - 75% of the organics being water soluble (Trebs et al., 2005). In tobacco smoke, at least 70% of the PM mass is composed of organic compounds, and about 16% is water (Thielen et al., 2008). Provided the organic and inorganic components are all sufficiently miscible with one another (e.g., the organics are fairly water-soluble), aerosol particles are internally mixed and no separation into organic/inorganic phases occurs (Marcolli et al., 2004). For such mixed aerosols, the bulk phase of the particle may be more akin to a non-aqueous organic solution than to an aqueous solution, particularly when relative humidity is low (Clegg et al., 2001).

1.2. Equilibrium Gas/Particle Partitioning of Acids and Bases to Organic PM

Several models have been developed to predict the equilibrium partitioning of matter from the gas to the particulate phase, and inorganic PM is generally modeled separately from organic PM (e.g. Griffin et al., 2003; Zhang et al., 2000). Organic absorptive equilibrium partitioning models parameterize the partitioning of an organic atmospheric

compound, i , from the gas to the particle phase using the equilibrium partitioning constant, K_p ($\text{m}^3/\mu\text{g}$):

$$K_{p,i} = \frac{c_{p,i}}{c_{g,i}} \quad (1)$$

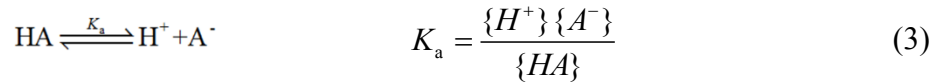
where $c_{p,i}$ is the concentration of i in the gas phase, in μg of compound i per μg total particulate matter (TPM), and $c_{g,i}$ is the concentration of i in the gas phase, in μg of compound i/m^3 of air (Pankow, 1994). This absorptive gas/particle partitioning model represents conditions at thermodynamic equilibrium. In general, whether an atmospheric compound exists as a gas, a particle, or both depends on its volatility and the characteristics of the existing PM. K_p is determined using the equation (Pankow, 1994):

$$K_{p,i} = \frac{f_{om} RT}{10^6 \overline{MW} \zeta_i p_i^0} \quad (2)$$

where f_{om} is the fraction of total particulate matter present that can absorb condensing organic species, R is the universal gas constant ($8.2 \times 10^{-5} \text{ m}^3 \text{ atm mol}^{-1} \text{ K}^{-1}$), T is the temperature in Kelvin, \overline{MW} is the average molecular weight of the total particulate matter present in g/mol , ζ_i is the unitless activity coefficient of compound i in the PM, and p_i^0 is the sub-cooled liquid vapor pressure of i in atm (Pankow, 1994).

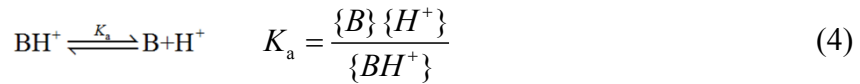
Current SOA models using the above parameterization treat all partitioning compounds as if they existed only in their neutral forms. However, some partitioning compounds are

capable of ionization, and their ionized forms are not able to partition into the gas phase. The theoretical equation for K_p would be more representative of reality for acids and bases if it represented the equilibrium between the concentration of the free, un-ionized fraction in the particle phase and the total concentration in the gas phase (Pankow, 2003). The acid-base equilibrium (and the extent of ionization) for an acid j is described by its thermodynamic acid dissociation constant, K_a . The acid dissociation constant is formally defined in terms of the thermodynamic equilibrium between the protonated and deprotonated forms of the acid:



where $\{\text{H}^+\}$, $\{\text{A}^-\}$ and $\{\text{HA}\}$ are the activities of the hydrogen ion, the acid anion, and the neutral form of the acid. Activity is equal to γC , where C is the molar concentration and γ is an activity coefficient dependent on the composition of the solution).

Similarly, for a protonated base:



The acid dissociation constant is often expressed as:

$$pK_a = -\log(K_a) \quad (5)$$

More acidic compounds have relatively lower pK_a values (higher K_a values).

For aqueous solutions, K_a values are well-established (γ is assumed to be 1 for a dilute aqueous solution), and pH ($-\log \{H^+\}$) can be easily measured with a calibrated glass electrode. In complex non-aqueous media such as atmospheric OPM, it is practical to measure the abundance of the hydrogen ion on the concentration scale, defining:

$$p_cH = -\log[H^+] \quad (6)$$

rather than using the definition:

$$pH = -\log \{H^+\} \quad (7)$$

The acid dissociation constant may also be redefined on a concentration scale by including the activity coefficients:

$${}^c K_a = \frac{[H^+][A^-]}{[HA]} = K_a \frac{\gamma_{HA}}{\gamma_{A^-} \gamma_{H^+}} \quad (8)$$

The concentrations $[H^+]$, $[HA]$ and $[A^-]$ can be determined experimentally.

The overall partitioning constant for the acid HA, $K_{p,j}$, can be revised to include the effect of the acid-base reaction (Pankow, 2003):

$$K_{p,HA} = \frac{K_{p,HA(fa)}}{\alpha_{fa}} \quad (9)$$

where $K_{p,j(fa)}$ is the partitioning constant for the neutral (free) form of HA (calculated as in Equation (2)), and α_{fa} represents the fraction of HA that is in the free form:

$$\alpha_{fa} = \frac{[HA]}{[HA]+[A^-]} \quad (10)$$

Similar equations can be developed for bases:

$$K_{p,B} = \frac{K_{p,B(fb)}}{a_{fb}} \quad (11)$$

$$\alpha_{fb} = \frac{[B]}{[B]+[HB^+]} \quad (12)$$

The value of α_{fa} depends on the acid-dissociation constant of the compound, K_a , as well as the acidity of the solvent, $\{H^+\}$:

$$\alpha_{fa} = \frac{\{H^+\}}{K_a + \{H^+\}} \quad (13)$$

$$\alpha_{fb} = \frac{K_a}{K_a + \{H^+\}} \quad (14)$$

In general, when SOA compounds ionize or form salts, the solubility of the acid or base in the particulate phase increases, because ions are not volatile (Mellouki et al., 2015; Pankow, 2003). By equations (9) - (14), a greater fraction of a weak acid exists in the ionic form under alkaline conditions, while a greater fraction of a weak base exists in the ionic form under acidic conditions. Thus, high pH encourages the partitioning of organic acids to the particulate phase and of bases to the gas phase, while low pH encourages the partitioning of bases to the particulate phase and of acids to the gas phase (Figure 2). The lower the α_{fa} value for a given acid (or the lower the α_{fb} value for a given base), the

greater the ionized fraction and the greater the expected partitioning to the particulate phase.

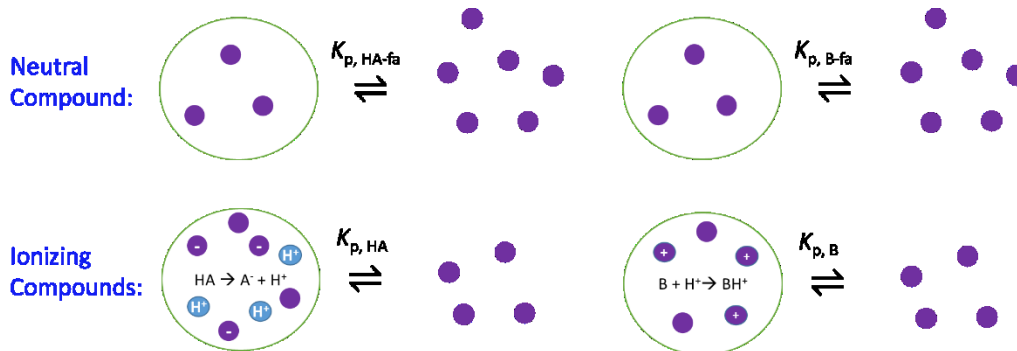


Figure 2. Partitioning behavior in neutral (top) and partially-ionized (bottom) acids and bases.

1.3. Acid-Base Chemistry in Non-Aqueous Systems

Acidity and acid-base equilibria are often discussed in terms of aqueous solutions; however, when the medium is organic PM, the reactions occur in a non-aqueous system. The equilibria of all chemical reactions depend on the medium in which they take place. Thus, the extent of ionization (or “strength”) of an acid or base, depends on the activity coefficients (γ) in that solution, which depend on the solvation energy (the energy required to achieve dissolution of a solute species) of each of the potential solute species (e.g. A^- , H^+ , and HA) in a particular solvent. Intermolecular forces between solvent molecules as well as between solute and solvent molecules determine the solvation energy. Ultimately, the dissociation extent of an acid or protonated base depends on the ability of the forces of attraction between solute-solvent molecules to overcome the forces of attraction between solute-solute and solvent-solvent molecules.

Dielectric constant, hydrogen-bonding ability, proton-donating capacity, electron-donating capacity, temperature, pressure, polarizability, and steric considerations all impact solvation energy to some extent, with dielectric constant and hydrogen-bonding ability generally considered to be the most important characteristics for amphiprotic solvents (Burger, 1983; Gyenes, 1967; Reichardt, 2003). The dielectric constant of a solvent represents the decrease in electric field strength due to the solvent – the higher the dielectric constant, the lower the energy state of the ion, and the more well-solvated it can be. Dielectric constant is generally a measure of the polarity and dissociation power of a solvent (Burger, 1983; Reichardt, 2003). In a solvent with a high dielectric constant (such as water) the energy state of ions is low and acids, which ionize when they dissociate, are generally more likely to dissociate than in non-aqueous solvents with lower dielectric constants (Reichardt, 2003). Solvents with lower dielectric constants, which include alcohols and most other organic solvents, favor neutral molecules over ionized forms. Iso-ionic reactions, such as the dissociation of the protonated base illustrated in Equation (4), have the same number and charge of ions on either side of the reaction. These equilibria are far less affected by changes in dielectric constant and electrostatic interactions than equilibria in which the number and charge of ions changes over the course of the reaction (represented by the dissociation of the neutral acid in Equation (3) (Gyenes, 1967; Trémillon, 1971). For example, the K_a of acetic acid (CH_3COOH) is five orders of magnitude lower in methanol ($\text{p}K_a = 9.63$) than it is in water ($\text{p}K_a = 4.75$), but the K_a of protonated methylamine (CH_3NH_3^+), changes by less than one order of magnitude ($\text{p}K_a = 11.00$ in methanol compared to $\text{p}K_a = 10.64$ in water; Rived et al.,

1998). Solvents like water and alcohol have strong interactions with solutes through the creation of hydrogen bonds and preferentially solvate anions, while non-polar solvents like dioxane have only weak interactions with the solute and solvate anions poorly (Burger, 1983; Trémillon, 1971).

2. Acid-Base Chemistry in Simulated Atmospheric OPM

2.1. Background

The distribution and composition of PM in the atmosphere affects global climate, human health, and visibility (Dockery and Pope, 1994; Pope et al., 2002; Pöschl and Shiraiwa, 2015; Stocker et al., 2013; Zhang et al., 2015). The gas/particle partitioning behavior of the semi-volatile and low-volatility organic compounds that comprise SOA remains a source of considerable uncertainty in air quality and climate models, with PM typically under-predicted (Hallquist et al., 2009; Kroll and Seinfeld, 2008; Stocker et al., 2013; Zhang et al., 2015). The ionization of organic acids and bases through acid-base reactions in atmospheric PM represents a mechanism that is relevant to gas/particle partitioning but is missing from current models.

Many important atmospheric partitioning compounds are capable of ionization, such as carboxylic acids (e.g. oxalic, succinic, malonic, and acetic acid) and weak bases (e.g. ammonia and amines). These may take part in acid-base neutralization reactions of the form:



Carboxylic acids are generally secondary pollutants derived from the oxidization of precursor gases, and can make up (by mass) ~3% of total fine PM (Trebs et al., 2005), ~10% of SOA (Bao et al., 2012), and ~50% of the water soluble organic carbon in PM (Mayol-Bracero et al., 2002). Amines are emitted by livestock operations and other types

of industry, by automobiles, and by natural sources such as biomass burning (Ge et al., 2011a). Near emission sources, total gaseous amines may exist in concentrations up to a few hundred ppb (Tang et al., 2013). Amines are less abundant than ammonia in the atmosphere, but are generally more basic and therefore could be more important in some circumstances (Ge et al., 2011b; Qiu et al., 2011).

In atmospheric systems, bases such as ammonia and amines first neutralize strong inorganic acids such as sulfuric and nitric acids, mechanisms accounted for by inorganic partitioning models (Zhang et al., 2000). If excess bases exist, however, they can potentially be neutralized by weaker, organic acids. The resulting ionization of both acid and base would cause α_{fb} and α_{fa} to fall below unity, and increase the K_p values of both compounds (Equations (9) and (11)). This scenario is most likely to occur in regions with high ammonia emissions and high concentrations of PM.

Experimental and field studies suggest that neutralization and salt formation occur in aerosol particles. The extent of the salt formation appears to depend on relative humidity, the pH of the particle, and the strength of the acid (Häkkinen et al., 2014; Paciga et al., 2014). In a charge-balance study of ambient PM in the tropics, Trebs et al. (2005) found that the inclusion of organic acid anions in the model was necessary to balance the positively-charged inorganic species, suggesting that not only the inorganic species were present in ionic form. Amines have also been shown to form salts with nitric acid in aerosol formed in chamber studies (Tang et al., 2013) and with acids in the atmosphere (Smith et al., 2010).

It is well-established that the water content of atmospheric organic PM, which is affected by relative humidity and increases as SOA becomes more oxidized (Li et al., 2015), has a significant effect on partitioning behavior through its effect on average molecular weight and activity coefficients (Pankow et al., 2015). Water content is also likely to influence partitioning through its effect on acid/base equilibria. The highly polar, amphiprotic, and hydrogen-bond-forming character of water tends to increase ion solvation and encourage the ionized form over the neutral form. For example, ammonia uptake by SOA (normalized to carboxylic acid mass) has been shown to increase with relative humidity, approaching the limiting value of full neutralization of ammonia by carboxylic acid (Li et al., 2015).

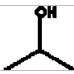

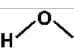
In this work, experiments were conducted to demonstrate the effects of varying PM water content on the acid-base equilibria of two representative partitioning compounds, hexanoic acid and benzylamine. Organic solvent/water mixtures were developed to approximate the characteristics of one type of theoretical atmospheric PM at different water contents, and two types of experiments elucidate the changes in acid-base behavior. First, acid-base titrations were used to estimate the $p^{\circ}K_a$ values of each partitioning compound in the solvent mixtures. Second, nuclear magnetic resonance imaging (NMR) spectra were used to determine the fraction of each partitioning compound present in ionic form, when both compounds are present in equal amounts.

2.2. Methods

2.2.1. Solution Design

A simple liquid solvent system was chosen to approximate organic PM, which is in reality a very complex mixture of thousands of compounds with a wide variety of molecular properties. The solvent was chosen such that the three properties most likely to affect intermolecular interactions and acid-base behavior (dielectric constant, hydrogen-bonding ability, and polarity) would be representative of those values in one hypothetical type of somewhat-oxidized organic PM. The chosen solvent mixture consists of equal parts of two organic solvents: isopropanol (IPA), representing the more polar organic compounds present in PM, and *p*-dioxane, representing the less-polar compounds present in PM, along with a varying amount of water (Table 1). The solvent is composed of pairs of molecules that interact strongly with one another (e.g. water/IPA) as well as pairs of molecules that interact weakly with one another (e.g. IPA/*p*-dioxane), as would be the case in somewhat-oxidized SOA.

Table 1. Properties of the solvents chosen for the liquid mixture to simulate atmospheric organic PM (ϵ = dielectric constant; δ_h = Hansen solubility parameter for hydrogen bonding; D = dipole moment).

Solvent	Relative Permittivity	Hydrogen-bonding capability	Polarity	Structure
isopropyl alcohol	ϵ =19.9	δ_h = 16.4	D = 1.66	
<i>p</i> -dioxane	ϵ =2.25	δ_h = 9.0	D = 0.45	
water	ϵ =78.5	δ_h = 42.3	D = 1.85	

The water content range for the three solvents intended to represent organic PM (between ~6% and 33% by weight), was chosen to capture a range of expected water contents of

organic PM under atmospheric conditions. Estimates of the total liquid water content of PM_{2.5} range from 13% - 50% by weight, depending on relative humidity and particle composition (Ho et al., 1974; Hueglin et al., 2005; McMurry, 2000; Rees et al., 2004), with 35% - 50% of the total PM_{2.5} water associated with the organic fraction (Guo et al., 2014). Hexanoic acid and benzylamine were chosen as the representative partitioning acid and base, respectively.

2.2.2. Acid-Base Titrations

2.2.2.1. Solution Preparation

Three solvent mixtures were prepared to approximate OPM using equal volume proportions of *p*-dioxane (TCI) and IPA (Sigma-Aldrich) and a varying amount of water (18.2 MΩ·cm at 25 °C, Millipore) (Table 2). A mostly-aqueous solvent mixture (~95% water by volume) was also prepared for comparison (Table 2). Hexanoic acid (Sigma-Aldrich) and benzylamine (TCI) and were each added to the solutions in concentrations between 0.05F and 0.06F, along with enough NaOH to bring each solution to a high pH prior to titration (Table 3). The NaOH solution (10F) was prepared from a 1.0 mole concentrate (Fluka, Sigma-Aldrich), which was diluted with a 50/50 mix of *p*-dioxane/IPA. The water content of this solution was determined gravimetrically and accounted for in the listed water content of each solution (Table 2). Listed purity of all reagents used was >99%. The solutions were titrated with 2.0F HCl, prepared by diluting 4.0F HCl in *p*-dioxane (Sigma-Aldrich) with IPA.

Table 2. Concentrations of the three solvent components used in titration and NMR experiments, varying in percent water content. In the solution ID, H denotes hexanoic acid and B denotes benzylamine.

	Solution ID	Solvent % by weight (25°C)		Solvent mole fraction		
		Organic mix (50/50 IPA and <i>p</i> -dioxane)	Water	Dioxane	IPA	Water
Acid-Base Titrations	H-95	94%	6.3%	0.37	0.41	0.21
	H-85	83%	17%	0.26	0.29	0.45
	H-70	67%	33%	0.16	0.18	0.66
	H-5	5.7%	94%	0.0069	0.0077	0.98
	B-95	94%	5.9%	0.38	0.42	0.20
	B-85	83%	17%	0.26	0.29	0.45
	B-70	68%	32%	0.16	0.18	0.66
	B-5	4.8%	95%	0.0058	0.0064	0.99
NMR Experiments	HB-95	95%	4.8%	0.42	0.41	0.17
	HB-85	84%	16%	0.28	0.27	0.45
	HB-70	66%	34%	0.16	0.16	0.68

Table 3. Concentrations (*F*) of solutes representing partitioning compounds (hexanoic acid and benzylamine) used in titration and NMR experiments, and concentration of sodium hydroxide (*F*) added to initial solution prior to titration.

	Solution Name	Hexanoic Acid	Benzylamine	NaOH
Acid-Base Titrations	H-95	0.060		0.10
	H-85	0.060		0.10
	H-70	0.060		0.10
	H-5	0.060		0.10
	B-95		0.051	0.05
	B-85		0.051	0.05
	B-70		0.051	0.05
	B-5		0.051	0.05
NMR Experiments	HB-95	0.047	0.047	
	HB-85	0.048	0.047	
	HB-70	0.050	0.049	

2.2.2.2. Analysis

A titration curve was developed for each solution, plotting p_cH as a function of the fraction of initial acid or base titrated (this fraction, f , was back-calculated using the equivalence points of the titration curve). A pK_a value for each solution was determined from the inflection point of the titration curve, where $f = 0.5$. These were estimated using the Gran technique (described in (Pankow, 1991)).

Titration curves were carried out using a T-50 automatic titrator system (Mettler-Toledo). 5 mL of each solution was titrated with a total of 0.3 mL of 2.0F HCl, in increments ranging from 0.5 μ L to 10 μ L. Electrode potential (ΔE) was measured with a silver chloride glass electrode (Mettler-Toledo InLab® Ultra-Micro). 1.0F LiCl in ethanol (Mettler-Toledo) was used as a reference solution to minimize drift in junction potential. The electrode was calibrated using aqueous buffer solutions (Nernst slope >96% of theoretical) at pH 4.00 and 10.00 (Fischer Scientific). Automatic titrator parameters were chosen to accommodate a slower electrode response in organic solutions (Avdeef et al., 1999; Scherrer and Donovan, 2009): a change in ΔE of less than 1.0 mV over 10 seconds was required for equilibration after each addition of titrant before the recording of each datapoint. The target change in electrode potential per aliquot was 6.0 mV, and the threshold for detection of an equivalence point was 4500 mV/mL titrant. The total difference in the mole fraction of water between the beginning and end of each titration, accounting for both the titrant volume added and the water produced by neutralization of

strong base during the titration, was less than 0.02. All titrations were carried out at ~20°C.

p_cH was calculated from the ΔE measured by the instrument through calibration with known values of strong acid and base. For a solution containing one weak acid, the electroneutrality equation is (Pankow, 1991):

$$[\text{H}^+] + \text{NSB} = (1 - \alpha_{\text{fa}})A_{\text{T}} + [\text{OH}^-] \quad (16)$$

Where A_{T} is the total weak acid in the system, α_{fb} is the fraction of acid that is in the protonated form (HA), and NSB is the net strong base added by titration. When pH is very low, $[\text{OH}^-] \approx 0$, $\alpha_{\text{fa}} \approx 1$, and $[\text{H}^+] \approx -\text{NSB}$, which is known from the amount of titrant added.

Similarly, for a solution containing one weak base, the electroneutrality equation is (Pankow, 1991):

$$[\text{H}^+] + \text{NSB} + (1 - \alpha_{\text{fb}})B_{\text{T}} = [\text{OH}^-] \quad (17)$$

Where B_{T} is the total weak base in the system, α_{fb} is the fraction of base that is in the unprotonated form (B), and NSB is the net strong base added by titration. When pH is very low, $[\text{OH}^-] \approx 0$, $\alpha_{\text{fb}} \approx 0$, and $[\text{H}^+] \approx -(B_{\text{T}} + \text{NSB})$, which is known from the amount of titrant added (NSB) and the initial amount of weak base (B_{T}).

The calculated $[H^+]$ can be related to the measured electrode potential, ΔE , by the Nernst equation:

$$\Delta E = E - E_0 = S \times (\log \gamma_{H^+}) - S \times (\log [H^+]) \quad (18)$$

Where E_0 includes the half-cell potential of the reference electrode, the standard half-cell potential of the glass pH electrode, and the liquid junction potential; E is the standard half-cell potential of the glass pH electrode (both in volts); and γ_{H^+} is the ionic activity coefficient of the solution. S is the Nernst slope, and depends on temperature and solvent composition. Assuming a constant γ_{H^+} gives:

$$\Delta E = E - E_0 = b + S \times (\text{pH}) \quad (19)$$

The slope S and intercept b of Equation (19) were determined using a linear least-squares fit for the $[H^+]$ values calculated using Equations (16) and (17) at the low end of the pH titration. This slope was applied to the remainder of the datapoints in order to calculate $[H^+]$ from the measured electrode potential for the entire titration curve.

2.2.3. NMR Experiments

2.2.3.1. Solution Preparation

For ^1H NMR, solvents were prepared using perdeuterated chemicals so that ^1H NMR spectra could be achieved without interference from oversized solvent peaks. Three solvent mixtures to approximate organic PM were prepared using equal volume proportions of *p*-dioxane-d8 (TCI) and IPA-d8 (Sigma-Aldrich) and a varying amount of

deuterium hydroxide (all Cambridge Isotope Laboratories) (Table 2). Both benzylamine and hexanoic acid were added to each solvent mixture, in proportions of approximately 1:1, at concentrations of $\sim 0.05F$ (Table 3).

2.2.3.2. Analysis

Each ~ 0.7 mL sample was prepared in a 2.5 mm o.d. NMR tube (Bruker), and tetramethylsilane was added as a reference solvent at a concentration of 0.1%. ^1H NMR, ^{13}C NMR (Carbon-13 NMR), and HSQC (Heteronuclear Single Quantum Correlation) spectra were obtained using a Bruker AMX-600 NMR spectrometer and analyzed using Bruker Topspin software (version 2.1).

^1H NMR spectroscopy uses the nuclear resonance of protons in a magnetic field to reveal the structure of a compound. The resonance frequency (δ) of each proton (normalized to the operation frequency of the spectrometer and reported in units of ppm), provides information about the proton's surrounding environment. For protonated and unprotonated species of the same compound, the resonances of the protons nearest the protonation site (Figure 3; shown in blue for benzylamine and hexanoic acid) resonate at different frequencies. For example, when hexanoic acid is fully protonated, its methylene groups resonate at a frequency of $\delta_{\text{max}} \approx 2.27$ ppm, compared to a frequency of $\delta_{\text{min}} \approx 2.11$ when fully deprotonated.



Figure 3. Unprotonated and protonated forms of benzylamine (left) and hexanoic acid (right). The ^1H NMR shift of the protons shown in blue gives information about the protonation state of the compound in solution.

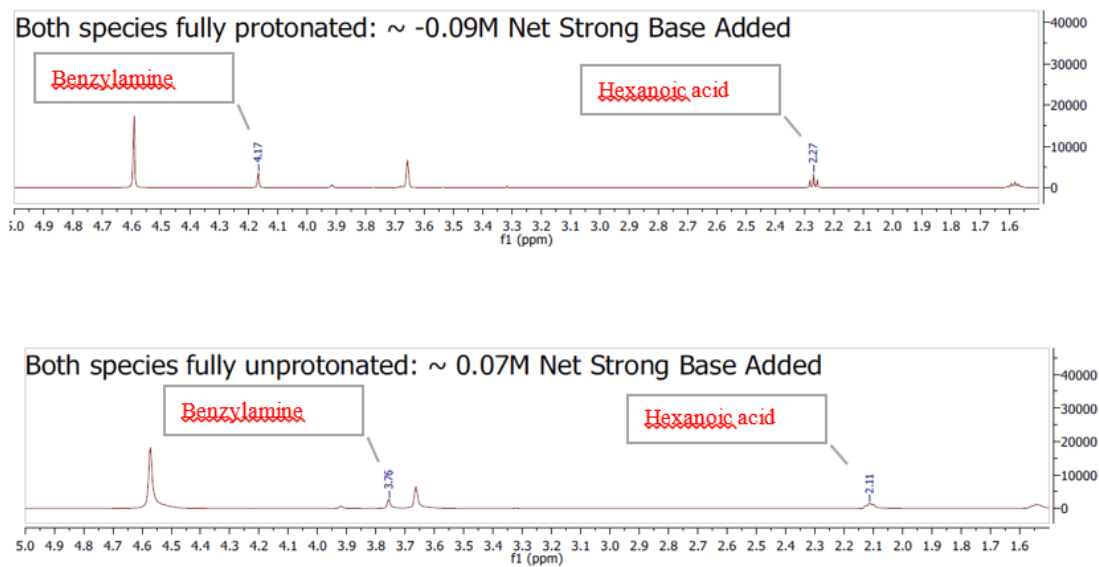


Figure 4. ^1H NMR spectra of fully protonated (top) and fully unprotonated (bottom) hexanoic acid (0.05F) and benzylamine (0.05F), dissolved in 35% IPA/35% *p*-dioxane/30% water (v/v/v).

When only some of the molecules in a compound are protonated, the resonance frequency falls between the δ_{\max} and δ_{\min} , in a manner proportional to unprotonated portion of the compound, α_{fb} (Bezençon et al., 2014; Kim et al., 2013; Shivapurkar and Jeannerat, 2011). Thus, the fraction ionized ($1-\alpha_{\text{fb}}$ or $1-\alpha_{\text{fa}}$) can be calculated using:

$$1 - \alpha_{fa} = 1 - \left(\frac{(\delta - \delta_{\min})}{(\delta_{\max} - \delta_{\min})} \right) \quad (20)$$

$$1 - \alpha_{fb} = 1 - \left(\frac{(\delta_{\max} - \delta)}{(\delta_{\max} - \delta_{\min})} \right) \quad (21)$$

The resonance frequencies of carbon atoms in ^{13}C NMR were used in a manner analogous to the frequencies of the protons in ^1H NMR to verify the results. Two-dimensional HSQC spectra were also obtained to verify that the target protons and carbon atoms were identified correctly. HSQC spectra provide more information about molecular structure by showing how protons are associated with nearby carbon atoms.

For each of the three 1:1 hexanoic acid/benzylamine solutions tested (Table 3), initial ^1H NMR, ^{13}C NMR, and HSQC spectra were collected. After each initial collection, δ_{\max} was determined by adding excess (0.09 F) strong acid (DCI, Cambridge Isotope Laboratories), and δ_{\min} was then determined by adding excess (0.1 F) net strong base (NaOD, Cambridge Isotope Laboratories). In this way, a single sample was used to collect all six spectra.

2.3. Results

The changing shape of the titration curves show hexanoic acid becoming weaker with increased organic content in the solvent. The calculated $\text{p}^{\text{c}}K_{\text{a}}$ increased from 4.9 in the near-aqueous solution to 8.8 in the 94% organic solution (Figure 5). The $\text{p}^{\text{c}}K_{\text{a}}$ of benzylamine decreased from 9.3 in the near-aqueous solution to 8.4 in the 70% organic

solution, and then increased slightly to 8.6 in the 94% organic solution (Figure 6). The benzylamine titration curves show a less pronounced change than for hexanoic acid, especially for the three solutions with mostly-organic composition.

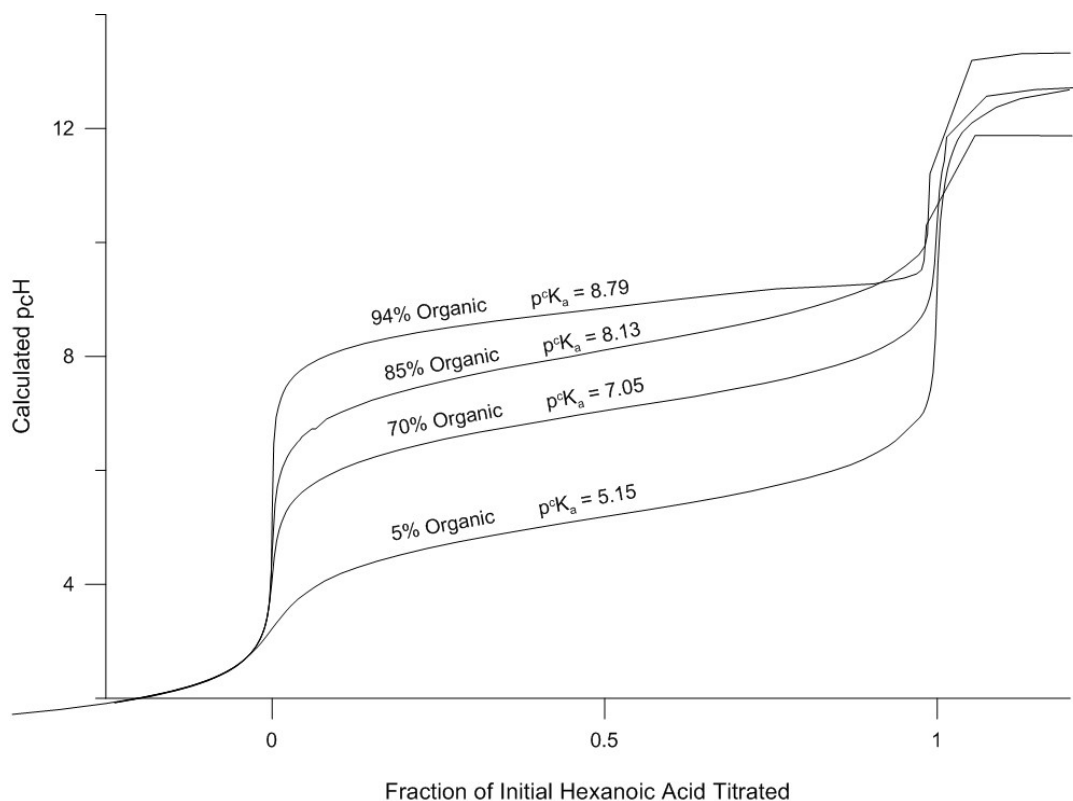


Figure 5. Titration curves for 0.06F hexanoic acid dissolved in solutions consisting of between 6% and 94% (by weight) organic solvent (equal parts *p*-dioxane and IPA) and water. The first equivalence point (fraction titrated = 0) represents a solution of pure hexanoic acid, the second equivalence point (fraction titrated = 1) represents a solution of pure sodium hexanoate, and the inflection point (fraction titrated = 0.5) occurs where $p^cH = p^cK_a$.

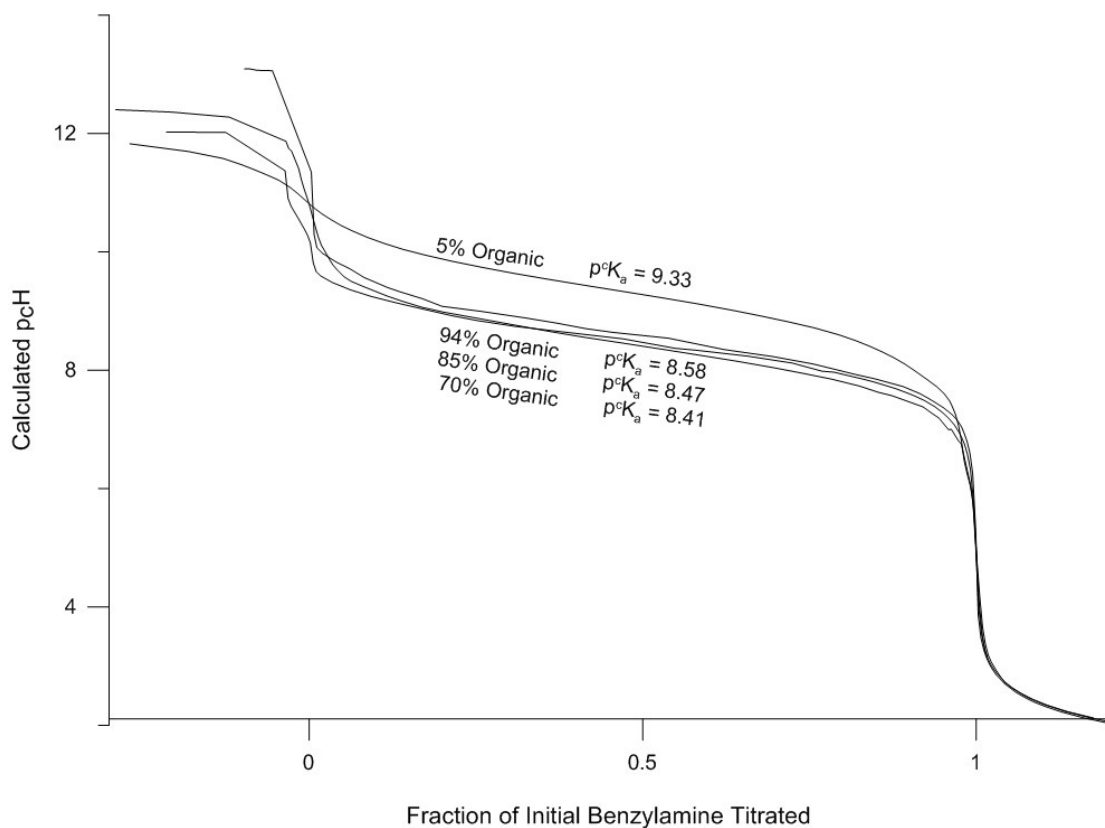


Figure 6. Titration curves for 0.05F benzylamine dissolved in solutions consisting of between 6% and 95% (by weight) organic solvent (equal parts *p*-dioxane and IPA) and water. The first equivalence point (fraction titrated = 0) represents a solution of pure benzylamine, the second equivalence point (fraction titrated = 1) represents a solution of benzylamine plus enough strong acid to protonate it fully, and the inflection point (fraction titrated = 0.5) occurs where $p^cH = p^cK_a$.

The ^1H NMR data for both hexanoic acid and benzylamine show that the fraction present in the ionized form decreases with increasing organic content (Table 4; see Appendix A for spectra). However, even at the highest level of organic content measured, which corresponds to a simulated organic PM particle with water content = 0.17 (mole fraction), 46% of the hexanoic acid and 39% of the benzylamine are ionized. No difference in was found between the results from ^1H NMR data and results calculated from ^{13}C NMR data, and HSQC spectra verified that protons were identified correctly.

Table 4. Fraction of hexanoic acid and benzylamine that are ionized in 1:1 molar solutions consisting of various portions of organic solvent (equal parts *p*-dioxane and IPA) and water, as determined by ¹HNMR.

% organic solvent (by mass)	% Ionized at 1:1 Ratio	
	Hexanoic Acid	Benzylamine
95%	46%	39%
84%	74%	75%
66%	95%	90%

2.4. Discussion

Hexanoic acid behaves as a weaker acid in organic PM with lower water content than in aqueous PM or organic PM with higher water content. The rise in $p^{\circ}K_a$ of hexanoic acid demonstrated by the titrations and the decreased fraction in the ion form seen in the ¹HNMR experiments both indicate that the ability of hexanoic acid to ionize decreases with the organic content of the solvent mixture. These results agree with several other studies that have demonstrated increased pK_a with increased organic solvent content (e.g. in methanol/water, ethanol/water, isopropanol/water, tetrahydrofuran/water, and acetonitrile/water systems; Bosch et al., 1995; Cox, 2015; Rosés and Bosch, 2002). The findings also agree with intermolecular attraction theory, in that organic mixtures are poor solvators of ions compared to water (Cox, 2015; Sarmini and Kenndler, 1999). The calculated near-aqueous $p^{\circ}K_a$ for hexanoic acid (5.15) is larger than its value in aqueous solution (4.88), suggesting that even a small amount (~5%) of these organics in the solvent measurably impacts the acid-base equilibria by altering the relative strength of intermolecular attractions in the solution.

The p^cK_a values of benzylamine indicate that, when organic content is 70% or greater, it behaves as a weaker base than in aqueous solution, although it slightly increases in strength with organic contents between 70% and 95%. The strength of the base in pure aqueous solution, at $p^cK_a = 9.33$, is equal to the calculated near-aqueous p^cK_a . The difference is much less pronounced than for hexanoic acid, which is in agreement with other studies that demonstrated a similar pattern for protonated bases in organic solvent/water mixtures (e.g. in methanol/water, ethanol/water, and acetonitrile/water systems; Cox, 2015; Sarmini and Kenndler, 1999). This can be explained by the fact that iso-ionic reactions, such as the protonation of a neutral base, are not strongly affected by changes in the solution's ability to solvate ions.

In the 94%-organic solution, hexanoic acid is no longer sufficiently acidic to protonate benzylamine (as it does in water); in fact, the protonated benzylamine and the hexanoic acid have similar p^cK_a values. As a result, hexanoic acid only partially protonates benzylamine, which is demonstrated for an equimolar acid/base solution by the ^1H NMR results. Although the majority of the hexanoic acid does not protonate the benzylamine in this solution (as it does in the solutions with higher water content), the significant fraction of base and acid ionized (39% and 46%, respectively) shows that acid/base neutralization does occur even in the most-organic solution tested. Regarding the gas/particle partitioning of these two organic species to atmospheric PM, the ^1H NMR data provide evidence that neutralization reactions are likely to be important when excess base exists, and should be considered in air quality models.

Including acid/base reactions in equilibrium organic partitioning models is expected to increase predicted total concentrations of SOA. For both hexanoic acid and benzylamine partitioning to a neutral, mostly organic particle phase, including acid-base reactions could theoretically cause K_p to increase nearly ten-fold in a particle that is 70% organic (mole fraction water = 0.69), and about two-fold in a particle that is 30% organic (mole fraction water = 0.19). This is based on the percent ionized in the ^1H NMR experiments and Equations (9) and (11), and assumes that the solvent characteristics of the PM are similar to those of the experimental mixture. The effect would become increasingly important for organic acids in more basic particles, and would become increasingly important for ammonia and amines in more acidic particles. The overall effect is expected to be strongest in alkaline conditions (when bases exist in concentrations higher than required to neutralize strong inorganic acids), and when water content is high. It should be noted that, because both K_p and α values in organic PM are coupled to the composition of the PM (by Equation (2) and by $[\text{H}^+]$, respectively), a true predicted increase in K_p would incorporate an iterative algorithm to solve simultaneously for individual K_p values, individual α values, and total PM mass (Pankow, 2003).

The accuracy of the p^cK_a values calculated from the titration data results could be determined and possibly improved by repeating the experiments with a few alterations. First, the titrations should be replicated several times. Second, the concentrations of solute added should be reduced so that any differences in γ_{H^+} (assumed constant in the calculation of p^cH) will be minimized. Finally, the calibration of the p^cH scale to the

measured electrode potential would be improved if a separate titration was carried out over the whole of the p_cH range using only strong acid and strong base.

The ¹H NMR data may be subject to isotope effects. The strength of hydrogen bonds varies among isotopes, which could bias the results slightly in favor of solvation of the neutral form in deuterated solvents (Reichardt, 2003). The impact of changes in ionic strength, concentration, and other solvent conditions is unlikely to have affected the analysis significantly. No difference in was found between the results from ¹H NMR data and another set of results calculated from ¹³C NMR, which is less sensitive to these changes (Reichardt, 2003).

3. Acid-Base Chemistry of Tobacco Smoke PM

3.1. Background

3.1.1. Free Base Nicotine, Nicotine Delivery, and Tobacco Smoke “pH”

Mainstream cigarette smoke is an aerosol composed of thousands of organic and inorganic compounds, including the addictive compound nicotine, and water. In cigarette smoke PM, nicotine can theoretically exist in three forms: unprotonated, or “free-base” (Nic), monoprotonated (NicH^+), and diprotonated (NicH_2^{2+}) (Figure 7). At typical acidities, the diprotonated form is expected to exist in such small proportions as to be considered negligible (Pankow et al., 2003). Because ions are not volatile, only the unprotonated form is present in the gas phase.

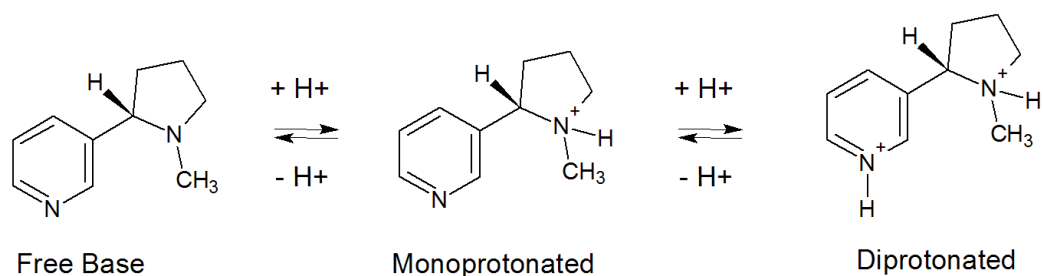


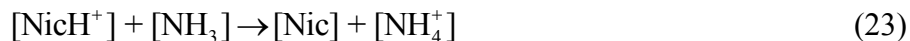
Figure 7. The three forms of nicotine potentially present in solution.

The addictive properties of nicotine are related to the efficiency of delivery to the brain (Henningfield and Keenan, 1993). Because gaseous molecules are more bioavailable to the tissues of the respiratory tract than particles, free base nicotine is more easily absorbed than monoprotonated nicotine (Tomar and Henningfield, 1997). The fraction free base, α_{fb} , is related to the pH of the smoke and the $\text{p}K_{\text{a}}$ of nicotine (Equation (14)).

Theory suggests, as do tobacco industry documentation and independent research, that the amount of nicotine in the free base form depends on the pH of the PM phase of the smoke (Henningfield et al., 2004; Pankow et al., 1997; Watson et al., 2015; Wayne et al., 2006). If acids with sufficiently low pK_a values are present, some or all of the free base nicotine molecules become protonated and the fraction of free base nicotine is decreased:



Similarly, if bases with sufficiently high pK_a values are present, the fraction of free-base nicotine is increased:



Tobacco additives that have been investigated in terms of their ability to alter the pH of the PM phase include ammonia, urea, diammonium phosphate (DAP), sodium hydroxide, sodium carbonate, levulinic acid, lactic acid, and various nicotine salts of organic acids (Henningfield et al., 2004; Lakritz et al., 2014; RJ Reynolds, 1991; Steele, 1989).

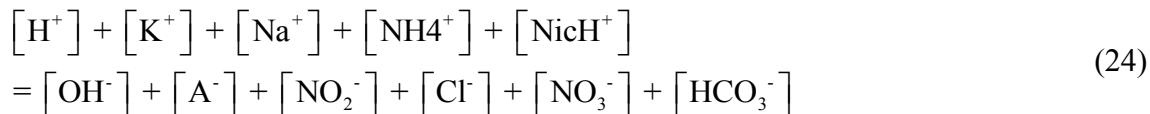
Through acid-base chemistry, cigarette composition effects the amount of free-base nicotine in the smoke and, consequently, the addictive properties of tobacco.

Despite its direct relevance to public health, the acid-base balance of tobacco smoke PM is not well-understood. Like atmospheric PM, tobacco smoke PM is not an aqueous solution but an extremely complex liquid mixture composed primarily of condensed organic compounds. Attempts to directly measure the pH of tobacco smoke PM have

been unsuccessful, except possibly as a method for measuring relative acidity between smoke samples (Pankow, 2001; Watson et al., 2004; Wayne et al., 2006). The difficulty of measuring “smoke pH” has led researchers to focus on other ways of characterizing the acid-base chemistry of tobacco smoke PM. The fraction of free-base nicotine in tobacco smoke PM (α_{fb}) has been measured directly using volatility-based techniques, and falls in the range of 0.01 – 0.36 (Lauterbach et al., 2010; Pankow et al., 2003; Watson et al., 2004). The wide variability in α_{fb} values among brands suggests that the acid-base chemistry imparted to smoke PM by different tobacco formulations has a significant impact on the efficiency of nicotine absorption by smokers. Further characterization of this acid-base balance will improve our understanding of the underlying causes of this variability.

3.1.2. Toward a Comprehensive Acid-Base Balance of Tobacco Smoke PM

An acid-base balance for tobacco smoke PM can be developed using the electroneutrality equation (ENE). The ENE equates the positively-charged species and the negatively-charged species in an uncharged solution such as tobacco smoke PM. Positively charged species include $[H^+]$, protonated weak bases, and cation tracers for strong bases, while negatively charged species include $[OH^-]$, deprotonated weak acids or anion tracers for strong acids. For tobacco smoke PM, a potential ENE is:



Where $[A^-]$ is the combined concentration of anions formed from several organic acids. For weak acid and weak base species, total concentrations of compounds are more easily measured than ions alone. Substituting total concentrations of partially-ionized compounds for the ion concentrations, and expressing $[OH^-]$ in terms of $[H^+]$ gives:

$$\begin{aligned}
 & [K^+] + [Na^+] + (1-\alpha_1^{NH_3})NH_{3(T)} + (1-\alpha_1) Nic_T + [H^+] \\
 & = \alpha_1^{HA} Ac_T + \alpha_1^{FA} F_T + \alpha_1^{LA} L_T + \alpha_1^{GA} G_T + \alpha_1^{NO_2} NO_{2(T)} + [Cl^-] \\
 & \quad + [NO_3^-] + K_H^{HCO_3} K_1^{HCO_3} \frac{pCO_2}{[H^+]} + \frac{K_w}{[H^+]}
 \end{aligned}
 \tag{25}$$

Where α_1 is the fraction of unprotonated base or acid present in the PM and the superscripts denote the chemical system (HA = acetic acid system (Ac_T = total acetic acid), FA = formic acid system (F_T = total formic acid), LA = lactic acid system (L_T = total lactic acid), GA = glycolic acid system (G_T = total glycolic acid), NO_2 = nitrous acid system, and NH_3 = ammonia system), $K_H^{HCO_3}$ is the Henry's law constant for carbon dioxide in tobacco smoke PM, $K_1^{HCO_3}$ is the acid dissociation constant for H_2CO_3 , pCO_2 is the atmospheric pressure of carbon dioxide, and K_w is the autoprotolysis constant of tobacco smoke PM.

The work that follows provides some of the data needed to populate Equation (25) by extracting smoke PM from 5 brands of cigarettes. Total concentrations of the organic acids (acetic, formic, lactic, and glycolic), ammonia, and tracer ions potassium, sodium, chloride, nitrite, and nitrate were determined using ion chromatography. To provide

assurance that all of the important organic acids and bases have been accounted for in the ENE, the total titratable acids and bases were determined using acid-base titrations. Concurrent work by colleagues will provide values for total nicotine and α_{fb} . Several previous studies have reported concentrations of acids and ions in tobacco smoke, including several organic acids, nitrite, nitrate, chloride, ammonia, potassium, and sodium (Chen and Pankow, 2009; Lagoutte et al., 1994; Nanni et al., 1990; Quin and Hobbs, 1958; Swauger et al., 2002). One previous study (Cundiff et al., 1962) quantified strong acids (e.g. HCl), weak acids (e.g. organic acids), and very weak acids (e.g. phenols) in tobacco smoke PM. Ultimately, the data presented here could be used, along with a good estimation of the values of the constants $K_H^{HCO_3}$ and K_w , to develop a general predictive model for the acid dissociation constants of organic acids in tobacco smoke PM.

3.1.3. “Stealth” Acids and Bases

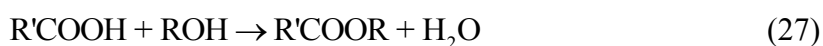
Ammonia may exist in “bound” or “unbound” forms in tobacco smoke (Chen and Pankow, 2009). Unbound ammonia includes NH_3 and NH_4^+ , while bound ammonia includes compounds which may be converted to NH_3 or NH_4^+ under certain conditions. For example, amides may be converted to unbound ammonia via hydrolysis:



The accuracy of some tobacco smoke ammonia measurements has been called into question because it is not always clear whether the measurement applies to the bound

form of ammonia only, or to a combination of the bound and unbound forms (Chen and Pankow, 2009). Bound ammonia is important to the overall acid-base balance of tobacco smoke PM because, when the above reaction occurs, the released amines may increase the basicity of smoke PM.

Another reaction of possible interest in tobacco smoke PM is the esterification of organic acids:



Organic acid esters represent a potential source of basicity in tobacco smoke PM, because acids are converted to a non-acid form through esterification. In order to determine amounts of these “stealth” acids and bases, a portion of each smoke PM sample was acidified to encourage the hydrolysis of amines and the esterification of organic acids and then re-analyzed by ion chromatography.

3.2. Methods

3.2.1. Sampling and Extraction

Five brands of filtered cigarettes (Kool Superlongs, Marlboro Red 100s (soft pack), American Spirit Blue Box, Camel 99's, and Basic Red Pack 100's) were examined in this study, and three replicate samples were collected for each brand. Cigarettes were purchased in Portland, OR in December, 2015. Cigarette packs were left at ambient laboratory conditions prior to sampling, opened within a month of purchase, and sampled within five hours of opening.

For each sample, two cigarettes were lit simultaneously and smoked into a Teflon bag using a pump and timer to evacuate puffs of air from an air-tight 4L chamber surrounding the bag (Figure 8). The smoking apparatus consisted of the following parts in series: (i) a glass dual cigarette holder (Clear Concepts, Bend, OR); (ii) a 0.25" TFE Teflon Swagelok union (Solon, OH); (iii) a glass/TFE tee stopcock (Clear Concepts/Swagelok); (iv) a 0.25" brass Swagelok union; (v) a 1" section of 0.25" I.D. flexible tubing (Nalgene); (vi) an empty, pre-weighed 1L Tedlar gas sampling bag (Supelco). Teflon tape was placed around the filter ends of the cigarettes for ease of placement and sealing. Following the FTC smoking protocol (Marian et al., 2009), a 70 mL puff (35 mL per cigarette) of 2-second duration was taken every 60 seconds. After the initial lighting puff, five puffs were drawn, and then the bag was sealed to allow PM to accumulate on the walls of the bag. After ten minutes, the bag was opened, the gaseous portion of the smoke allowed to escape, and the bag weighed to determine the mass of wet total particulate matter (WTPM) collected.

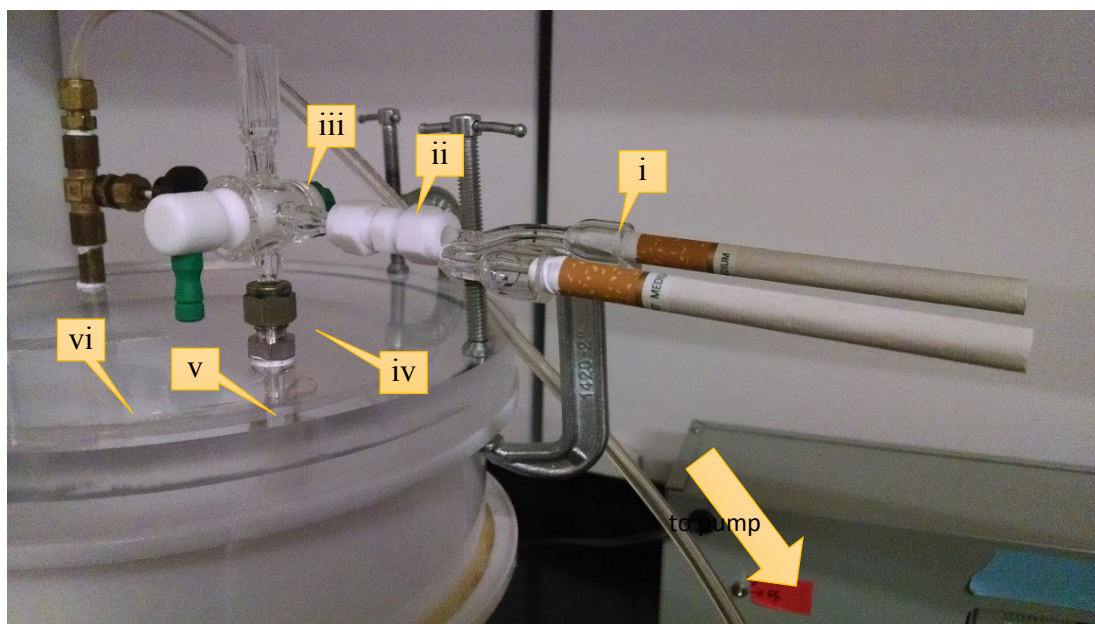


Figure 8. Cigarette smoking apparatus used for sampling of tobacco smoke PM.

To extract the PM, 14 mL of 98% IPA (>99%, Sigma-Aldrich) / 2% nanopure water (18.2 M Ω ·cm at 25 °C, Millipore) were added to the bag. Using 98% IPA as a solvent for the tobacco smoke PM ensures that both hydrophilic and hydrophobic components of the smoke PM are dissolved. Because water content affects acid-base chemistry, 2% water was included in the extraction solvent to ensure a constant level of water regardless of water content in the PM. The amount of water in tobacco smoke PM ranges from 9% to 23% by mass, and is variable between brands (Chen and Pankow, 2009). The tobacco smoke extract was poured into a glass beaker and distributed for analysis as follows: 3.0 mL unfiltered into a glass titration beaker for titration with strong acid; 3.0 mL unfiltered into a glass titration beaker for titration with strong base; 3 mL filtered (0.2 μ m filter; National Scientific) for later analysis by ion chromatography. After the acid-side titration,

an aliquot of acidified sample was filtered and refrigerated for later analysis by ion chromatography, for determination of stealth acids and bases.

3.2.2. Acid-Base Titrations

Separate acid-side and base-side titrations were carried out at ambient temperature ($\sim 20^{\circ}\text{C}$) using a T-50 automatic titrator system (Mettler-Toledo). Each 3.0 mL aliquot of sample was titrated with a total of 2.0 mL of titrant (5.0 mN), in increments ranging from 5.0 μL to 50 μL . The acid titrant, a 5.0 mN solution of hydrochloric acid (Fischer Scientific), was prepared in 95% IPA/5% nanopure water. The base titrant, a 5.0 mN solution of lithium phenoxide (Sigma Aldrich), was prepared in 99.5% IPA/0.5% THF. Lithium phenoxide as a moderately-strong base was chosen for its ability to titrate organic acids without also titrating phenols, which are common constituents of tobacco smoke PM and would be deprotonated by a stronger base. The titer of the lithium phenoxide titrant was determined at the start of each sampling day against the concentration-certified HCl titrant.

The electrode potential (ΔE) of the solution was measured after each addition of titrant with a silver chloride glass electrode (Mettler-Toledo InLab® Ultra-Micro). 1.0M LiCl in ethanol (Mettler Toledo) was used as a reference solution to minimize drift in junction potential. Automatic titrator parameters were chosen to accommodate the relatively sluggish electrode response of organic solutions (Avdeef et al., 1999; Scherrer and Donovan, 2009): a change in ΔE of less than 0.5 mV over 10 seconds was required for equilibration after each addition of titrant before the recording of each datapoint. The

target change in electrode potential per aliquot was 10.0 mV, and the threshold for detection of an equivalence point (EP) was 200 mV/mL of titrant for the acid titration and 450 mV/mL of titrant for the base titration. The concentrations (v/v) of IPA in the sample at the end of the titrations were 96.8% for the acid side and 98.6% for the base side.

The amounts of titratable acids and bases were determined by examination of the EPs of the titration, which are located at the maxima of the first derivative of the titration curve (Figure 9). There are three visible EPs in the titration curves: the leftmost equivalence point (EP1) represents the point at which all of the organic acids and nicotine are fully protonated (RCOOH and NicH^+), the middle equivalence point (EP2) represents the point at which all of the organic acids are fully protonated and the nicotine is fully unprotonated (RCOOH and Nic), and the rightmost equivalence point (EP3) represents the point at which all of the organic acids and nicotine are fully unprotonated (RCOO^- and Nic). Organic acids behave as very weak acids in isopropanol, and nicotine is not protonated by organic acids at EP2 in these samples. This was verified by a $^1\text{HNMR}$ analysis which showed that, when dissolved in a 95% IPA solution with 1:1 with acetic acid, nicotine remains fully unprotonated (Appendix C).

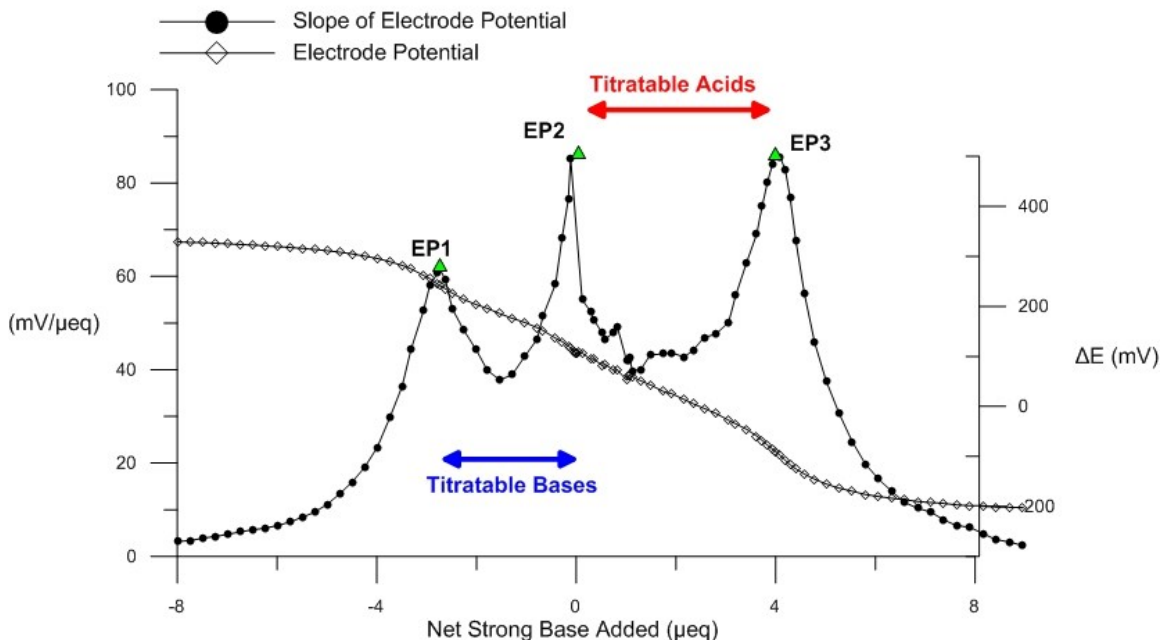


Figure 9. Example of a tobacco smoke titration curve (electrode potential vs. equivalents of net strong base added) and the slope of the titration curve (slope of electrode potential). Equivalence points (green triangles) are used to determine concentrations of weak (titratable) acids and weak (titratable) bases.

The total titratable (weak) acids, A_T , is given by:

$$A_T = NSB_{EP3} - NSB_{EP2} \quad (28)$$

where NSB_{EP3} is the net strong base that has been added at EP3, and NSB_{EP2} is the net strong base that has been added at EP2 (all in units of equivalents). The total titratable (weak) bases, B_T , is given by:

$$B_T = -(NSB_{EP1} - NSB_{EP2}) \quad (29)$$

where NSB_{EP1} is the net strong base that has been added at EP1. All acid and base concentrations were normalized to equivalents per mg WTPM for reporting.

EP1 and EP3 were calculated automatically by the titrator software (LabX, version 5; Mettler-Toledo) using an algorithm that considers the 10 surrounding datapoints to determine the derivative of the titration curve at each point. Due to software limitations, EP2 could not be calculated this way (the surrounding points were gathered from two separate titrations). The location of EP2 was determined manually using the Gran technique (described in Pankow, 1991) and the points on the acid-side titration curve. The base-side titration curve points were not used because the acid-side titration curves were smoother and provided a more suitable dataset for the Gran technique (see Appendix B).

A test of the titration method using known quantities of acetic acid and nicotine dissolved in 95% IPA gave percent error values of -2.4% (for nicotine) and -5.9% (for acetic acid), for concentrations similar to those expected in the samples. However, when the extraction solvent was titrated alone alongside the samples, some titratable acids were quantified. The amounts of titratable acids in four blank samples (two obtained after pouring into the sampling bag), were measured and the average (0.58 ueq per 3 mL sample; RSD=7%) was subtracted from the total titrated acids in each sample to calculate the titratable acids in the tobacco smoke PM. The most likely source of the acids in the blank samples is carbon dioxide, which dissolves in isopropanol and creates titratable carbonic acid (the solubility of carbon dioxide is nearly ten times greater in isopropanol than in water (Tokunaga, 1975)). No titratable bases were identified in the extraction solvent by titration with HCl.

3.2.3. Ion Chromatography

Stock ion standard solutions were prepared in nanopure water (18.2 MΩ·cm at 25 °C, Millipore) with the following ACS reagents: sodium chloride (>99.0%, Sigma Aldrich), sodium nitrate (>98.1%, Mallinckrodt Chemical Works), potassium nitrite (>99.0%, JT Baker), sodium sulfate (>99.0%, Sigma Aldrich), potassium acetate (>99.0%, Fischer Scientific), sodium formate (99.4%, JT Baker), glycolic acid (99%, Sigma Aldrich), potassium chloride (>99.0%, Chem Products), and ammonium chloride (99.5%, Acros). Chloroform (0.2%) was added to the anion stock solution to preserve the nitrate and nitrite. For calibration, the stock solution was diluted in 98% IPA, and linear calibration curves (five point curves for anions and a seven point curve for cations) were constructed with respect to peak height (Table 5). After the initial calculation in mg/L, sample ion concentrations were converted to equivalents per mg WTPM for reporting.

Analyses of anions for both initial and acidified samples were made within 24 hours of sample collection. Samples were run with cell and column temperatures of 40°C and a compartment temperature of 35°C on a 4-mm IC-5000 ion chromatography system with a 25 uL sample loop (Dionex). The anion method used an AS-15 anion column with an AG-15 guard column, a CR-ATC continuously regenerated anion trap column, and ASRS-300 suppressor (current = 71 mA). Elution was with KOH at a flow rate of 0.75 mL/min and the following concentration gradient: hold at 10mM KOH for 10 minutes, steadily increase to 22 mM from 10 to 12.5 minutes, step-increase to 45 mM at 12.5, and hold at 45 mM for 25.5 minutes.

Analyses of cations for both initial and acidified samples were made within 28 days of sample collection. Samples were run at ambient temperature on a 4-mm IC-5000 ion chromatography system with a 25 uL sample loop (Dionex). The analysis used a CS-12A cation column, a CG 12A guard column, and a CSRS 300 suppressor (current = 51 mA). Elution occurred at 1.0 mL/min with 20 mM methanesulfonic acid (MSA) for 15 minutes.

Table 5. Range of analytical method and linear calibration curve R² values for tobacco smoke PM analytes quantified using ion chromatography. Curves were run on five separate days for anion analysis, so minimum and maximum R² is given for anion standards.

Analyte	Concentration Range (mg/L)		R ²	
	Low	High	Min	Max
Glycolate	0.94	15.0	0.9977	0.9996
Acetate	3.13	50.0	0.9930	0.9960
Formate	1.25	20.0	0.9830	0.9962
Chloride	0.62	10.0	0.9965	0.9995
Nitrite	3.12	50.0	0.9953	0.9996
Nitrate	1.25	20.0	0.9972	0.9996
Sulfate	0.62	10.0	N/A	N/A
Lactate	0.94	15.1	0.9937	0.9995
Potassium	0.67	20.1	0.9964	
Sodium	1.00	30.1	0.9975	
Ammonium	0.33	9.9	0.9980	

3.3. Results

The mass of WTPM from the first 5 puffs (plus lighting puff) of two cigarettes ranged from 14-27 mg for the five brands sampled (Table 6). Total titrated bases ranged from 532-610 neq/mg WTPM, and total titrated acids ranged from 449-763 neq/mg WTPM (Table 6; Figure 10; see Appendix B for titration curves).

Table 6. Measured WTPM extracted from two cigarettes of each brand (first 5 puffs plus lighting puff only), and total weak acids and total weak bases measured by titration. N=3 for all brands.

Brand	WTPM (mg)		Total Weak Acids (neq/mg WTPM)		Total Weak Bases (neq/mg WTPM)	
	mean	std. dev	mean	std. dev	mean	std. dev
Am. Spirit	14 +/-	1.9	559 +/-	27.8	582 +/-	64.2
Basic	27 +/-	1.3	763 +/-	16.5	543 +/-	17.3
Camel	22 +/-	2.3	632 +/-	30.3	556 +/-	23.7
Kool	20 +/-	2.3	449 +/-	97.0	532 +/-	92.5
Marlboro	22 +/-	0.64	707 +/-	29.1	610 +/-	21.2

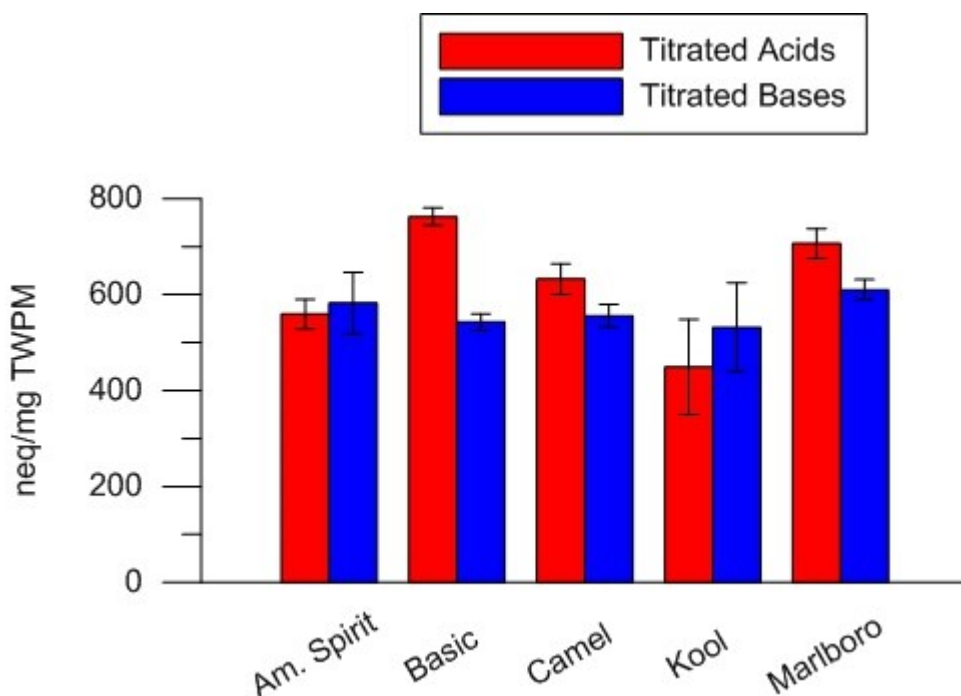


Figure 10. Measured titratable acids and bases in the first five puffs (plus lighting puff) for five cigarette brands. Error bars give the standard error (n=3 for all brands).

Ion chromatography identified weak acid anions in amounts corresponding to between 50-89% of the weak acids quantified by the titrations (Figure 11). These acids include

acetic acid (acetate ion), formic acid (formate ion), glycolic acid (glycolate ion), lactic acid (lactate ion), and nitrous acid (nitrite ion) (Table 9). Acetate and nitrite were the most abundant anions, followed by formate and lactate (see Appendix D for chromatograms). The proportions of the acid anions among brands were similar, but the American Spirit brand contained nitrite at levels below the method detection limit, while nitrite was abundant in other brands. Sulfate was present at trace levels in some brands but was not quantified (see Appendix D). Several smaller peaks on the chromatogram were not identified. Potassium, sodium, and ammonium were the only cation peaks in the chromatograms from the initial sample, but a very small lithium peak (likely from trace contamination introduced during titration) appeared in many of the acidified samples. Sodium, ammonium, and potassium were identified in the cation analysis, although sodium was present at concentrations below the method detection limit and was estimated (Table 7; see Appendix D for chromatograms).

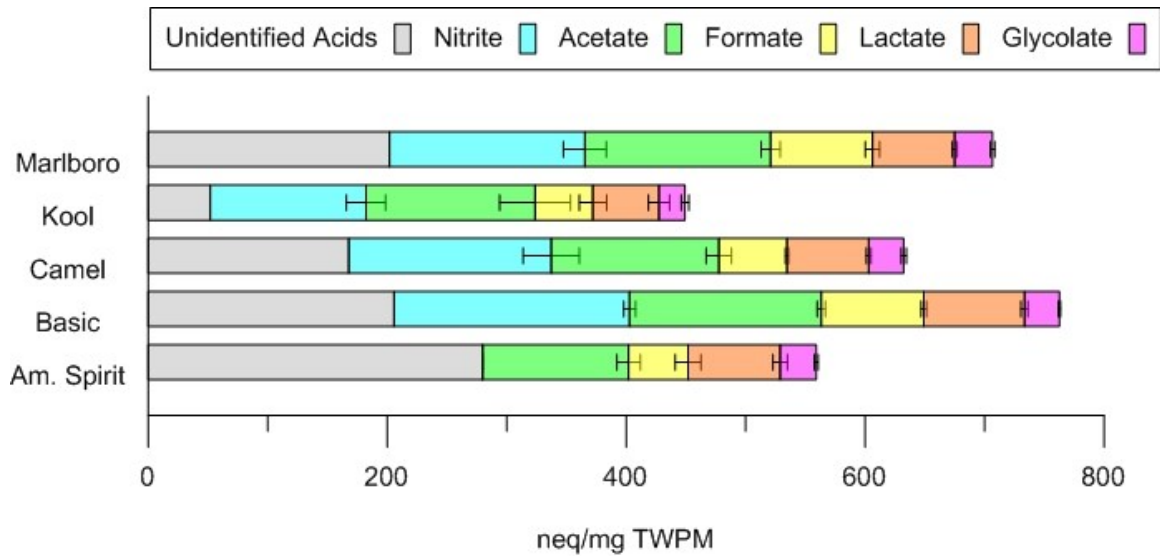


Figure 11. Identified and unidentified weak acids in the first five puffs (plus lighting puff) for five cigarette brands. Error bars give the standard error for ion chromatography measurements ($n=3$ for all brands). The unidentified portion is equal to the titrated acids less the weak acids identified by ion chromatography.

Table 7. Cation concentrations measured in the first five puffs (plus lighting puff) for five cigarette brands (n=3 for all brands). Concentrations highlighted in grey are below the quantitation limit of the method and are estimated.

Cations (neq/mg WTPM) - Initial Sample						
Brand	Sodium		Ammonium		Potassium	
	mean	std. dev	mean	std. dev	mean	std. dev
Am. Spirit	4.71	+/- 3.41	7.82	+/- 2.72	13.04	+/- 2.34
Basic	3.29	+/- 0.59	20.3	+/- 1.92	84.1	+/- 12.1
Camel	5.55	+/- 1.12	15.0	+/- 0.76	31.0	+/- 3.75
Kool	6.21	+/- 0.99	15.6	+/- 2.22	21.1	+/- 8.02
Marlboro	3.98	+/- 0.34	21.0	+/- 0.44	54.0	+/- 4.30

Table 8. Cation concentrations measured after acidification in the first five puffs (plus lighting puff) for five cigarette brands (n=3 for all brands). Concentrations highlighted in grey are below the quantitation limit of the method and are estimated.

Cations (neq/mg WTPM) - Acidified Sample						
Brand	Sodium		Ammonium		Potassium	
	mean	std. dev	mean	std. dev	mean	std. dev
Am. Spirit	7.03	+/- 3.18	17.6	+/- 2.01	13.9	+/- 3.54
Basic	4.48	+/- 0.43	47.0	+/- 6.14	71.5	+/- 14.4
Camel	7.51	+/- 0.49	30.6	+/- 1.08	27.4	+/- 3.51
Kool	8.89	+/- 1.42	34.2	+/- 4.69	21.5	+/- 7.87
Marlboro	7.62	+/- 2.33	48.6	+/- 0.70	43.4	+/- 5.83

Table 9. Anion concentrations measured in the first five puffs (plus lighting puff) for five cigarette brands (n=3 for all brands). Concentrations highlighted in grey are below the quantitation limit of the method and are estimated.

Anions (neq/mg WTPM) - Initial Sample										
Brand	Glycolate			Lactate			Acetate			
	mean	+/-	std. dev	mean	+/-	std. dev	mean	+/-	std. dev	std. dev
Am. Spirit	30.1	+/-	1.65	77.0	+/-	6.12	122	+/-	9.91	
Basic	29.2	+/-	0.96	84.4	+/-	3.00	161	+/-	3.50	
Camel	29.1	+/-	2.21	68.5	+/-	2.11	140	+/-	10.6	
Kool	21.8	+/-	3.23	55.3	+/-	8.75	142	+/-	29.6	
Marlboro	31.7	+/-	1.98	68.9	+/-	2.11	155	+/-	8.01	

Brand	Formate			Chloride			Nitrite			Nitrate		
	mean	+/-	std. dev	mean	+/-	std. dev	mean	+/-	std. dev	mean	+/-	std. dev
Am. Spirit	49.9	+/-	10.7	17.9	+/-	4.02	ND	+/-		ND	+/-	
Basic	85.7	+/-	2.25	60.2	+/-	6.90	197	+/-	5.05	14.8	+/-	2.13
Camel	57.0	+/-	1.26	39.1	+/-	4.30	170	+/-	23.5	17.4	+/-	1.55
Kool	48.5	+/-	11.4	31.7	+/-	3.84	130	+/-	16.4	13.7	+/-	2.06
Marlboro	85.2	+/-	6.00	42.8	+/-	3.57	164	+/-	18.0	11.7	+/-	1.50

Table 10. Anion concentrations measured after acidification in the first five puffs (plus lighting puff) for five cigarette brands (n=3 for all brands). Concentrations highlighted in grey are below the quantitation limit of the method and are estimated.

Anions (neq/mg WTPM) - Acidified Sample									
Brand	Glycolate			Lactate			Acetate		
	mean	+/-	std. dev	mean	+/-	std. dev	mean	+/-	std. dev
Am. Spirit	31.7	+/-	3.17	76.2	+/-	5.03	79.9	+/-	20.6
Basic	31.4	+/-	1.45	81.8	+/-	0.43	154	+/-	3.52
Camel	31.0	+/-	4.24	63.9	+/-	1.31	119	+/-	14.6
Kool	24.5	+/-	1.85	57.2	+/-	10.9	129	+/-	28.9
Marlboro	34.8	+/-	0.76	67.4	+/-	0.59	148	+/-	10.5

Brand	Formate			Nitrate			Nitrite		
	mean	+/-	std. dev	mean	+/-	std. dev	mean	+/-	std. dev
Am. Spirit	39.9	+/-	12.1	5.12	+/-	0.39	ND	+/-	
Basic	86.2	+/-	2.08	33.9	+/-	4.64	23.2	+/-	3.57
Camel	39.9	+/-	2.12	33.7	+/-	0.74	41.1	+/-	3.43
Kool	31.1	+/-	9.45	23.3	+/-	3.00	15.0	+/-	3.00
Marlboro	87.1	+/-	6.65	35.7	+/-	1.60	20.5	+/-	3.40

The net measured base (Figure 12) includes the total titrated (weak) bases and strong base tracers (sodium and potassium), less the total titrated (weak) acids and strong acid tracers (chloride and nitrate). The Basic Red brand had the greatest excess of acids and the menthol brand Kool had the greatest excess of bases, with the other brands having a smaller excess of base (American Spirit) or acid (Marlboro Red, Camel).

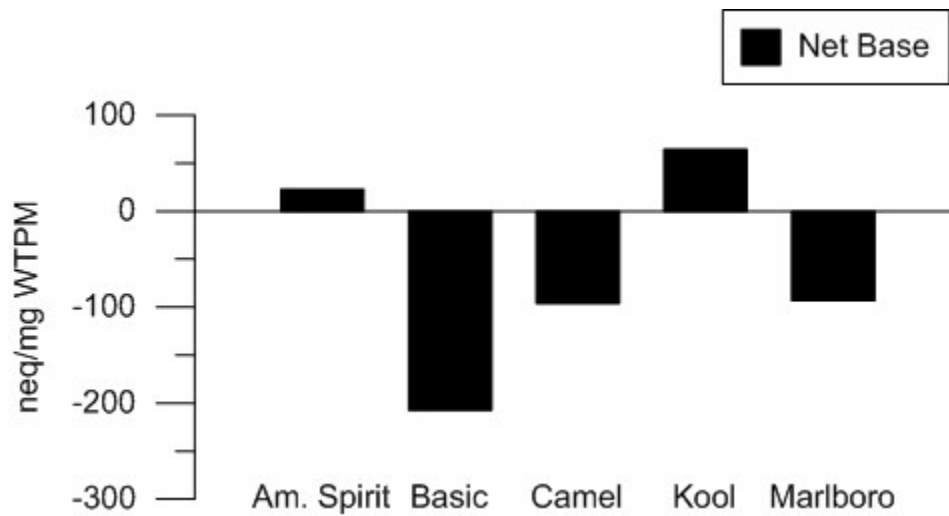


Figure 12. Total measured acids less total measured bases in the first five puffs (plus lighting puff) for five cigarette brands. Total measured acids includes titrated acids and the strong acid tracers, chloride and nitrate. Total measured bases includes titrated bases and the strong base tracers, potassium and sodium.

Levels of both strong acid tracers and strong base tracers were smallest for the American Spirit brand and largest for the Basic Red brand. The Camel and Kool brands both had higher concentrations of strong acid tracers than strong base tracers, while the Basic Red brand had higher concentrations of strong base tracers, and Marlboro and American Spirit brands had similar concentrations of each (Figure 13). Chloride and potassium were more abundant in all samples than nitrate and sodium.

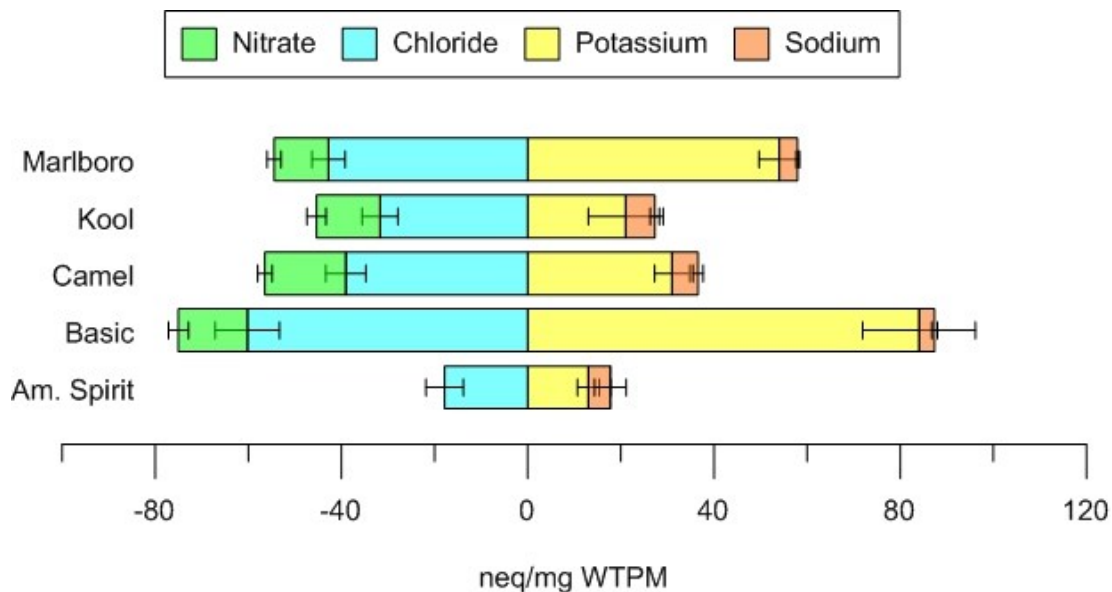


Figure 13. Concentrations of strong base tracers (sodium and potassium, shown as positive values) and strong acid tracers (chloride and nitrate, shown as negative values) in the first five puffs (plus lighting puff) for five cigarette brands. Error bars show standard deviation ($n=3$ for all brands).

Ammonia concentrations after acidification approximately doubled over initial ammonia concentrations (Figure 14; Table 8). Aside from a decrease in formate in the Camel brand samples, concentrations of organic acids did not change appreciably with acidification (Figure 15; Table 10).

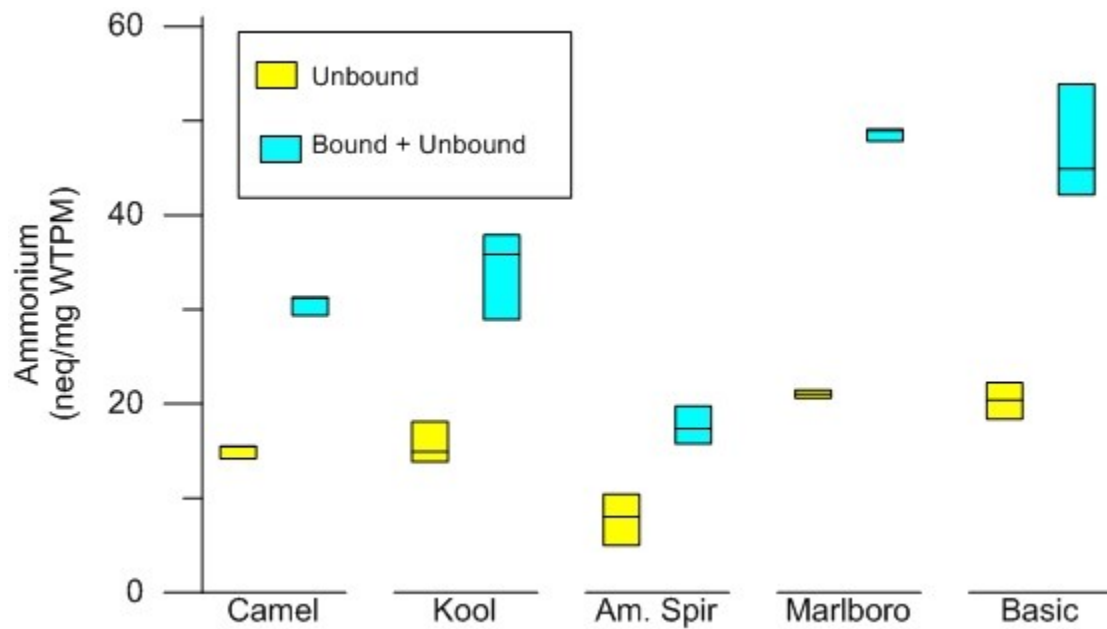


Figure 14. Concentrations of ammonium in initial and acidified samples in the first five puffs (plus lighting puff) for five cigarette brands, showing contribution of bound “stealth” ammonia. Measurements for all three replicates are shown; box height indicates the range and the center line represents the median sample.

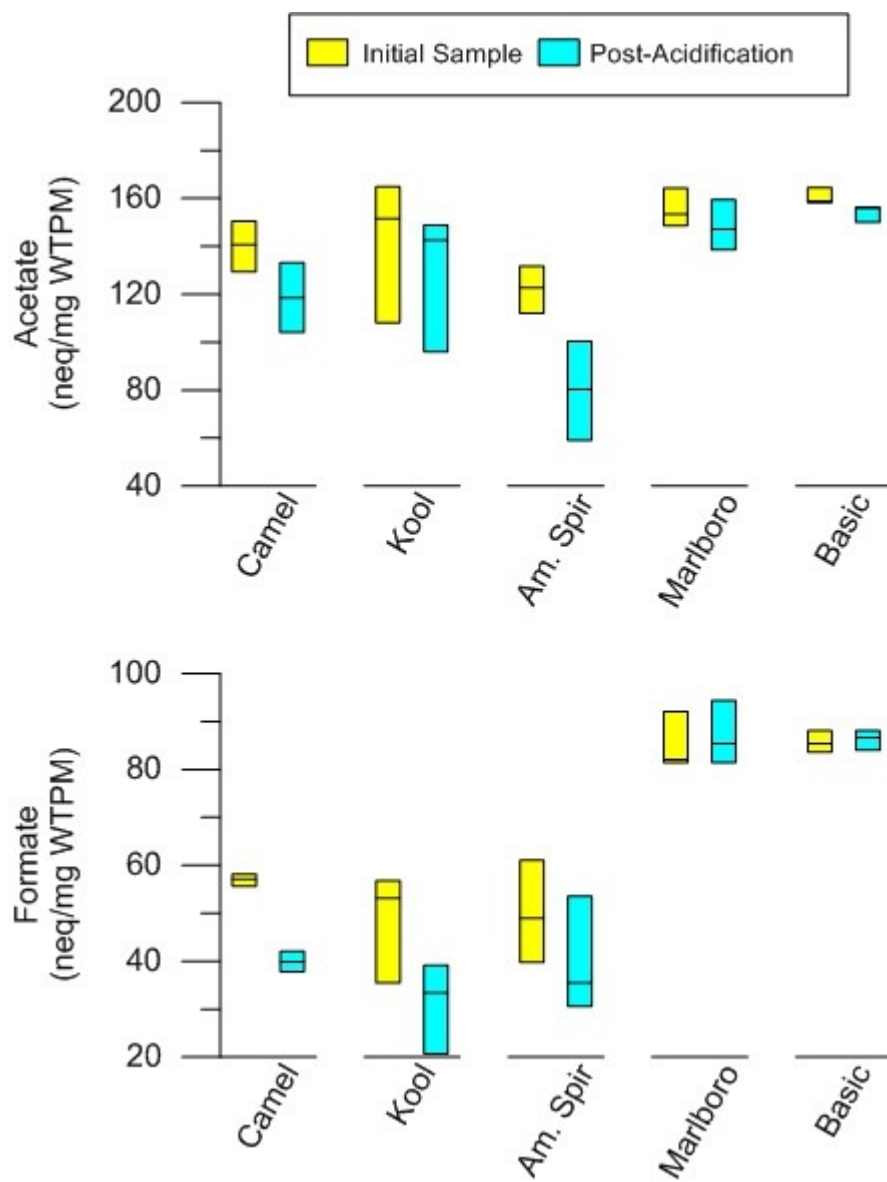


Figure 15. Concentrations of acetate and formate in initial and acidified samples in the first five puffs (plus lighting puff) for five cigarette brands, showing no consistent evidence of esterification. Measurements for all three replicates are shown; box height indicates the range and the center line represents the median sample.

3.4. Discussion

Comparison of the total weak acid concentration from the titration equivalence points with the total weak acid concentrations from the ion chromatography data suggests that, on average, about 30% of the weak acids in tobacco smoke PM are unaccounted for by the proposed ENE (Equation(25)). In fresh tobacco smoke, there are ~230 carboxylic acids and ~200 amines. Propionic, butyric, valeric, oxalic, levulinic, succinic, malic, malonic, and quinic acids are among the acids that have been identified and may contribute to the missing portion (Borgerding and Klus, 2005; Lu et al., 2003; Moldoveanu, 2012; Schumacher et al., 1977). Dicarboxylic acids such as oxalic acid and those with low molecular weight (such as propionic and butyric acids) potentially contribute more base-neutralizing power for their mass. If the unidentified peaks in the anion chromatogram can be identified as organic acids and quantified, they may account for some of the discrepancy. The majority of the weak base titrated is expected to be accounted for by nicotine when that data becomes available, but ammonia and other amines will make some contribution to total bases.

Comparison of total acids and bases indicates that American Spirit and Kool are the most basic brands tested. This is at least partially consistent with an earlier free base nicotine study (Pankow et al., 2003), which reported that the American Spirit brand had the highest free base values of 12 cigarette brands studied. Marlboro and Camel brands are shown here to be about equally acidic, while in the earlier study, early puffs of Marlboro

cigarettes had more free base nicotine than Camel cigarettes. However, brand formulations change over time, so comparisons between studies done over a range of years may not valid in all cases. In general, the wide range of results in net basicity over just the five brands sampled here lends support to the hypothesis that the proportions of free base and monoprotonated nicotine in smoke PM vary widely among brands. The variation in net basicity may be the result of differences among brands in the types and amounts of additive used, tobacco curing practices, and/or tobacco type.

The increase in ammonium measured after acidification indicates that about half of the ammonia in tobacco smoke PM is present in “bound” form, most likely as amines which may be converted to ammonia under acidic conditions. This amount corresponds to the amount of base needed to neutralize 2-4% of the weak acids titrated. Decreases in organic acid concentrations after acidification were not large or consistent enough to suggest that a significant amount of organic acids is becoming “bound” through esterification.

If tobacco smoke PM behaves similarly to the atmospheric organic PM, comparisons may be drawn between the nicotine and the organic acids in tobacco smoke and the benzylamine and hexanoic acid studied in Section 2. In solutions composed of 85% organics (tobacco smoke PM has about 15% water), we might expect about 75% of the organic acid and base to participate in neutralization reactions with one another, assuming the solution is nearly neutral in terms of acidity (as, for example, the American Spirit sample appears to be). In this case, both the weak acids and the nicotine are

probably partially protonated. Further data collection, particularly of α_{fb} values, will help to further populate the ENE and shed light on the extent of protonation of specific acids and bases in tobacco smoke PM.

4. Conclusions

The acid-base chemistry of atmospheric organic particulate matter has the potential to impact the gas/particle partitioning of organic compounds through the formation of ions. Ionization favors partitioning to the particulate phase over partitioning to the gas phase. The experiments presented here, through estimation of pK_a values and direct observation of ionization through ^1H NMR, show hexanoic acid and benzylamine undergo neutralization reactions in aqueous solutions with organic content as high as 95% by mass. Although increasing the organic content of a solution decreases the amount of ionization relative to that which occurs in a purely aqueous solution, a significant fraction of organic acid and base is likely to ionize in an organic/aqueous mixture like atmospheric PM. These results apply to solutions with equal amounts of acid and base, and are relevant to atmospheric situations in which PM is approximately neutral; however, the extent of ionization is dependent on the acidity of the PM as well as the amount of organic content. Because atmospheric PM is generally acidic and organic acids ionize to a greater extent under basic conditions, the effect of acid-base chemistry on partitioning is likely to be strongest in areas with significant alkaline emissions relative to acidic emissions. These acid-base reactions are chemical processes that are not represented in current atmospheric organic PM models, and models may be improved by incorporating them.

The acid-base chemistry of tobacco smoke effects the protonation state and bioavailability of nicotine, and is therefore relevant to public health and tobacco regulation. The ion concentration and titration data presented here from five cigarette brands indicates a range in the net basicity of cigarette smoke PM among brands, suggesting that nicotine delivery efficiency also varies among brands. While the extent of protonation of the individual acids and bases (including nicotine) was not determined, future research relating these protonation states to the acid/base composition of tobacco smoke could allow for improved prediction of the addictive properties of various cigarette formulations.

Due to its impact on the ionization and volatility of acidic and basic organic compounds, non-aqueous acid-base chemistry is highly relevant to current research in gas/particle partitioning problems, including atmospheric particulate matter modeling and tobacco science. It is important for atmospheric modelers and tobacco scientists to recognize the importance of the nature of the “solvent” that is particulate matter, as it drastically impacts the behavior of compounds in the PM, particularly acid-base reactions and gas/particle partitioning behavior.

5. References

- Abramson, E., Imre, D., Beránek, J., Wilson, J., Zelenyuk, A., 2013. Experimental determination of chemical diffusion within secondary organic aerosol particles. *Phys. Chem. Chem. Phys.* 15, 2983–2991. doi:10.1039/C2CP44013J
- Arp, H.P.H., Schwarzenbach, R.P., Goss, K.U., 2008. Ambient gas/particle partitioning. 1. Sorption mechanisms of apolar, polar, and ionizable organic compounds. *Environ. Sci. Technol.* 42, 5541–5547. doi:10.1021/es703094u
- Avdeef, A., Box, K.J., Comer, J.E.A., Gilges, M., Hadley, M., Hibbert, C., Patterson, W., Tam, K.Y., 1999. pH-metric log P 11. pKa determination of water-insoluble drugs in organic solvent–water mixtures. *J. Pharm. Biomed. Anal.* 20, 631–641. doi:10.1016/S0731-7085(98)00235-0
- Bao, L., Matsumoto, M., Kubota, T., Sekiguchi, K., Wang, Q., Sakamoto, K., 2012. Gas/particle partitioning of low-molecular-weight dicarboxylic acids at a suburban site in Saitama, Japan. *Atmos. Environ.* 47, 546–553. doi:10.1016/j.atmosenv.2009.09.014
- Barsanti, K.C., Luo, W., Isabelle, L.M., Pankow, J.F., Peyton, D.H., 2007. Tobacco smoke particulate matter chemistry by NMR. *Magn. Reson. Chem.* 45, 167–170. doi:10.1002/mrc.1939
- Barsanti, K.C., Pankow, J.F., 2006. Thermodynamics of the formation of atmospheric organic particulate matter by accretion reactions—Part 3: Carboxylic and dicarboxylic acids. *Atmos. Environ.* 40, 6676–6686. doi:10.1016/j.atmosenv.2006.03.013
- Bassett, M., Seinfeld, J.H., 1983. Atmospheric equilibrium model of sulfate and nitrate aerosols. *Atmos. Environ.* 17, 2237–2252. doi:10.1016/0004-6981(83)90221-4
- Bezençon, J., Wittwer, M.B., Cutting, B., Smieško, M., Wagner, B., Kansy, M., Ernst, B., 2014. pKa determination by ¹H NMR spectroscopy – An old methodology revisited. *J. Pharm. Biomed. Anal., NMR Spectroscopy in Pharmaceutical and Biomedical Analysis* 93, 147–155. doi:10.1016/j.jpba.2013.12.014
- Borgerding, M., Klus, H., 2005. Analysis of complex mixtures – Cigarette smoke. *Exp. Toxicol. Pathol.* 57, Supplement 1, 43–73. doi:10.1016/j.etp.2005.05.010
- Bosch, E., Ràfols, C., Rosés, M., 1995. Variation of acidity constants and pH values of some organic acids in water—2-propanol mixtures with solvent composition.

- Effect of preferential solvation. *Anal. Chim. Acta* 302, 109–119.
doi:10.1016/0003-2670(94)00435-O
- Burger, K., 1983. *Solvation, Ionic and Complex Formation Reactions in Non-Aqueous Solvents*. Elsevier.
- Chacon-Madrid, H.J., Donahue, N.M., 2011. Fragmentation vs. functionalization: chemical aging and organic aerosol formation. *AtmosChem Phys* 11, 10553–10563. doi:10.5194/acp-11-10553-2011
- Chang, E.I., Pankow, J.F., 2006. Prediction of activity coefficients in liquid aerosol particles containing organic compounds, dissolved inorganic salts, and water—Part 2: Consideration of phase separation effects by an X-UNIFAC model. *Atmos. Environ.* 40, 6422–6436. doi:10.1016/j.atmosenv.2006.04.031
- Chen, C., Pankow, J.F., 2009. Gas/particle partitioning of two acid–base active compounds in mainstream tobacco smoke: nicotine and ammonia. *J. Agric. Food Chem.* 57, 2678–2690. doi:10.1021/jf803018x
- Ciobanu, V.G., Marcolli, C., Krieger, U.K., Weers, U., Peter, T., 2009. Liquid–liquid phase separation in mixed organic/inorganic aerosol particles. *J. Phys. Chem. A* 113, 10966–10978. doi:10.1021/jp905054d
- Clegg, S.L., Seinfeld, J.H., Brimblecombe, P., 2001. Thermodynamic modelling of aqueous aerosols containing electrolytes and dissolved organic compounds. *J. Aerosol Sci.* 32, 713–738. doi:10.1016/S0021-8502(00)00105-1
- Cox, B.G., 2015. Acids, bases, and salts in mixed-aqueous solvents. *Org. Process Res. Dev.* 19, 1800–1808. doi:10.1021/op5003566
- Cundiff, R., Sensabaugh, Jr, A., Markunas, P., 1962. Titrimetric determination of acid fractions of tobacco smoke. *Tob. Sci.* 6, 25–27.
- Daumit, K.E., Kessler, S.H., Kroll, J.H., 2013. Average chemical properties and potential formation pathways of highly oxidized organic aerosol. *Faraday Discuss.* 165, 181–202. doi:10.1039/C3FD00045A
- Dockery, D.W., Pope, C.A., 1994. Acute respiratory effects of particulate air pollution. *Annu. Rev. Public Health* 15, 107–132.
doi:10.1146/annurev.pu.15.050194.000543

- Duplissy, J., DeCarlo, P.F., Dommen, J., Alfarra, M.R., Metzger, A., Barmapadimos, I., Prevot, A.S.H., Weingartner, E., Tritscher, T., Gysel, M., Aiken, A.C., Jimenez, J.L., Canagaratna, M.R., Worsnop, D.R., Collins, D.R., Tomlinson, J., Baltensperger, U., 2011. Relating hygroscopicity and composition of organic aerosol particulate matter. *AtmosChem Phys* 11, 1155–1165. doi:10.5194/acp-11-1155-2011
- Ge, X., Wexler, A.S., Clegg, S.L., 2011a. Atmospheric amines – Part I. A review. *Atmos. Environ.* 45, 524–546. doi:10.1016/j.atmosenv.2010.10.012
- Ge, X., Wexler, A.S., Clegg, S.L., 2011b. Atmospheric amines – Part II. Thermodynamic properties and gas/particle partitioning. *Atmos. Environ.* 45, 561–577. doi:10.1016/j.atmosenv.2010.10.013
- Griffin, R.J., Nguyen, K., Dabdub, D., Seinfeld, J.H., 2003. A coupled hydrophobic-hydrophilic model for predicting secondary organic aerosol formation. *J. Atmospheric Chem.* 44, 171–190. doi:10.1023/A:1022436813699
- Guo, H., Xu, L., Bougiatioti, A., Cerully, K.M., Capps, S.L., Hite, J.R., Carlton, A.G., Lee, S.-H., Bergin, M.H., Ng, N.L., Nenes, A., Weber, R.J., 2014. Particle water and pH in the southeastern United States. *AtmosChem Phys Discuss* 14, 27143–27193. doi:10.5194/acpd-14-27143-2014
- Gyenes, I., 1967. *Titration in Non-aqueous Media*. Iliffe.
- Häkkinen, S.A.K., McNeill, V.F., Riipinen, I., 2014. Effect of inorganic salts on the volatility of organic acids. *Environ. Sci. Technol.* 48, 13718–13726. doi:10.1021/es5033103
- Hallquist, M., Wenger, J.C., Baltensperger, U., Rudich, Y., Simpson, D., Claeys, M., Dommen, J., Donahue, N.M., George, C., Goldstein, A.H., Hamilton, J.F., Herrmann, H., Hoffmann, T., Iinuma, Y., Jang, M., Jenkin, M.E., Jimenez, J.L., Kiendler-Scharr, A., Maenhaut, W., McFiggans, G., Mentel, T.F., Monod, A., Prévôt, A.S.H., Seinfeld, J.H., Surratt, J.D., Szmigielski, R., Wildt, J., 2009. The formation, properties and impact of secondary organic aerosol: Current and emerging issues. *AtmosChem Phys* 9, 5155–5236. doi:10.5194/acp-9-5155-2009
- Henningfield, J.E., Keenan, R.M., 1993. Nicotine delivery kinetics and abuse liability. *J. Consult. Clin. Psychol.* 61, 743–750. doi:http://dx.doi.org.proxy.lib.pdx.edu/10.1037/0022-006X.61.5.743

- Henningfield, J.E., Pankow, J.F., Garrett, B.E., 2004. Ammonia and other chemical base tobacco additives and cigarette nicotine delivery: Issues and research needs. *Nicotine Tob. Res.* 6, 199–205. doi:10.1080/1462220042000202472
- Ho, W., Hidy, G.M., Govan, R.M., 1974. Microwave measurements of the liquid water content of atmospheric aerosols. *J. Appl. Meteorol.* 13, 871–879. doi:10.1175/1520-0450(1974)013<0871:MMOTLW>2.0.CO;2
- Hueglin, C., Gehrig, R., Baltensperger, U., Gysel, M., Monn, C., Vonmont, H., 2005. Chemical characterisation of PM_{2.5}, PM₁₀ and coarse particles at urban, near-city and rural sites in Switzerland. *Atmos. Environ.* 39, 637–651. doi:10.1016/j.atmosenv.2004.10.027
- Jimenez, J.L., Canagaratna, M.R., Donahue, N.M., Prevot, A.S.H., Zhang, Q., Kroll, J.H., DeCarlo, P.F., Allan, J.D., Coe, H., Ng, N.L., Aiken, A.C., Docherty, K.S., Ulbrich, I.M., Grieshop, A.P., Robinson, A.L., Duplissy, J., Smith, J.D., Wilson, K.R., Lanz, V.A., Hueglin, C., Sun, Y.L., Tian, J., Laaksonen, A., Raatikainen, T., Rautiainen, J., Vaattovaara, P., Ehn, M., Kulmala, M., Tomlinson, J.M., Collins, D.R., Cubison, M.J., Dunlea, E.J., Huffman, J.A., Onasch, T.B., Alfarra, M.R., Williams, P.I., Bower, K., Kondo, Y., Schneider, J., Drewnick, F., Borrmann, S., Weimer, S., Demerjian, K., Salcedo, D., Cottrell, L., Griffin, R., Takami, A., Miyoshi, T., Hatakeyama, S., Shimono, A., Sun, J.Y., Zhang, Y.M., Dzepina, K., Kimmel, J.R., Sueper, D., Jayne, J.T., Herndon, S.C., Trimborn, A.M., Williams, L.R., Wood, E.C., Middlebrook, A.M., Kolb, C.E., Baltensperger, U., Worsnop, D.R., 2009. Evolution of organic aerosols in the atmosphere. *Science* 326, 1525–1529. doi:10.1126/science.1180353
- Kanakidou, M., Seinfeld, J.H., Pandis, S.N., Barnes, I., Dentener, F.J., Facchini, M.C., Van Dingenen, R., Ervens, B., Nenes, A., Nielsen, C.J., Swietlicki, E., Putaud, J.P., Balkanski, Y., Fuzzi, S., Horth, J., Moortgat, G.K., Winterhalter, R., Myhre, C.E.L., Tsigaridis, K., Vignati, E., Stephanou, E.G., Wilson, J., 2005. Organic aerosol and global climate modelling: a review. *AtmosChem Phys* 5, 1053–1123. doi:10.5194/acp-5-1053-2005
- Kim, H., Babu, C.R., Burgess, D.J., 2013. Quantification of protonation in organic solvents using solution NMR spectroscopy: Implication in salt formation. *Int. J. Pharm.* 448, 123–131. doi:10.1016/j.ijpharm.2013.03.040
- Kroll, J.H., Seinfeld, J.H., 2008. Chemistry of secondary organic aerosol: Formation and evolution of low-volatility organics in the atmosphere. *Atmos. Environ.* 42, 3593–3624. doi:10.1016/j.atmosenv.2008.01.003

- Lagoutte, D., Lombard, G., Nisseron, S., Papet, M.P., Saint-Jalm, Y., 1994. Determination of organic acids in cigarette smoke by high-performance liquid chromatography and capillary electrophoresis. *J. Chromatogr. A* 684, 251–257. doi:10.1016/0021-9673(94)00593-1
- Lakritz, L., Stedman, R.L., Strange, E.D., 2014. Composition studies on tobacco XXXLX: changes in smoke composition and filtration by artificial alteration of smoke pH: formic and acetic acids and volatile phenols. *Contrib. Tob. Res.* 5, 104–108. doi:10.2478/cttr-2013-0224
- Lauterbach, J.H., Bao, M., Joza, P.J., Rickert, W.S., 2010. Free-base nicotine in tobacco products. Part I. Determination of free-base nicotine in the particulate phase of mainstream cigarette smoke and the relevance of these findings to product design parameters. *Regul. Toxicol. Pharmacol.* 58, 45–63. doi:10.1016/j.yrtph.2010.05.007
- Li, J., Cleveland, M., Ziemba, L.D., Griffin, R.J., Barsanti, K.C., Pankow, J.F., Ying, Q., 2015. Modeling regional secondary organic aerosol using the Master Chemical Mechanism. *Atmos. Environ.* 102, 52–61. doi:10.1016/j.atmosenv.2014.11.054
- Lu, X., Cai, J., Kong, H., Wu, M., Hua, R., Zhao, M., Liu, J., Xu, G., 2003. Analysis of cigarette smoke condensates by comprehensive two-dimensional gas chromatography/time-of-flight mass spectrometry I. Acidic fraction. *Anal. Chem.* 75, 4441–4451. doi:10.1021/ac0264224
- Marcilli, C., Luo, B., Peter, T., 2004. Mixing of the organic aerosol fractions: Liquids as the thermodynamically stable phases. *J. Phys. Chem. A* 108, 2216–2224. doi:10.1021/jp0360801
- Mayol-Bracero, O.L., Guyon, P., Graham, B., Roberts, G., Andreae, M.O., Decesari, S., Facchini, M.C., Fuzzi, S., Artaxo, P., 2002. Water-soluble organic compounds in biomass burning aerosols over Amazonia 2. Apportionment of the chemical composition and importance of the polyacidic fraction. *J. Geophys. Res. Atmospheres* 107, 8091. doi:10.1029/2001JD000522
- McMurry, P.H., 2000. A review of atmospheric aerosol measurements. *Atmos. Environ.* 34, 1959–1999. doi:10.1016/S1352-2310(99)00455-0
- Mellouki, A., Wallington, T.J., Chen, J., 2015. Atmospheric chemistry of oxygenated volatile organic compounds: Impacts on air quality and climate. *Chem. Rev.* 115, 3984–4014. doi:10.1021/cr500549n

- Moldoveanu, S., 2012. Analysis of quinic acid and of myo-inositol in tobacco. *Beitrag Zur Tab. Int. Contrib. Tob. Res.* 25, 498–506.
- Nanni, E.J., Lovette, M.E., Hicks, R.D., Fowler, K.W., Borgerding, M.F., 1990. Separation and quantitation of monovalent anionic and cationic species in mainstream cigarette smoke aerosols by high-performance ion chromatography. *J. Chromatogr. Sci.* 28, 432–436. doi:10.1093/chromsci/28.8.432
- Paciga, A.L., Riipinen, I., Pandis, S.N., 2014. Effect of ammonia on the volatility of organic diacids. *Environ. Sci. Technol.* 48, 13769–13775. doi:10.1021/es5037805
- Pankow, J.F., 2015. Phase considerations in the gas/particle partitioning of organic amines in the atmosphere. *Atmos. Environ.* 122, 448–453. doi:10.1016/j.atmosenv.2015.09.056
- Pankow, J.F., 2003. Gas/particle partitioning of neutral and ionizing compounds to single and multi-phase aerosol particles. 1. Unified modeling framework. *Atmos. Environ.* 37, 3323–3333. doi:10.1016/S1352-2310(03)00346-7
- Pankow, J.F., 2001. A consideration of the role of gas/particle partitioning in the deposition of nicotine and other tobacco smoke compounds in the respiratory tract. *Chem. Res. Toxicol.* 14, 1465–1481. doi:10.1021/tx0100901
- Pankow, J.F., 1994. An absorption model of gas/particle partitioning of organic compounds in the atmosphere. *Atmos. Environ.* 28, 185–188. doi:10.1016/1352-2310(94)90093-0
- Pankow, J.F., 1991. *Aquatic Chemistry Concepts*. CRC Press.
- Pankow, J.F., Mader, B.T., Isabelle, L.M., Luo, W., Pavlick, A., Liang, C., 1997. Conversion of nicotine in tobacco smoke to its volatile and available free-base form through the action of gaseous ammonia. *Environ. Sci. Technol.* 31, 2428–2433. doi:10.1021/es970402f
- Pankow, J.F., Marks, M.C., Barsanti, K.C., Mahmud, A., Asher, W.E., Li, J., Ying, Q., Jathar, S.H., Kleeman, M.J., 2015. Molecular view modeling of atmospheric organic particulate matter: Incorporating molecular structure and co-condensation of water. *Atmos. Environ.* 122, 400–408. doi:10.1016/j.atmosenv.2015.10.001
- Pankow, J.F., Tavakoli, A.D., Luo, W., Isabelle, L.M., 2003. Percent free base nicotine in the tobacco smoke particulate matter of selected commercial and reference cigarettes. *Chem. Res. Toxicol.* 16, 1014–1018. doi:10.1021/tx0340596

- Pope, C.A., Burnett, R.T., Thun, M.J., Calle, E.E., Krewski, D., Ito, K., Thurston, G.D., 2002. Lung cancer, cardiopulmonary mortality, and long-term exposure to fine particulate air pollution. *J. Am. Med. Assoc.* 287, 1132–1141.
- Pöschl, U., Shiraiwa, M., 2015. Multiphase chemistry at the atmosphere–biosphere interface influencing climate and public health in the anthropocene. *Chem. Rev.* 115, 4440–4475. doi:10.1021/cr500487s
- Qiu, C., Wang, L., Lal, V., Khalizov, A.F., Zhang, R., 2011. Heterogeneous reactions of alkylamines with ammonium sulfate and ammonium bisulfate. *Environ. Sci. Technol.* 45, 4748–4755. doi:10.1021/es1043112
- Quin, L.D., Hobbs, M.E., 1958. Analysis of nonvolatile acids in cigarette smoke by gas chromatography of their methyl esters. *Anal. Chem.* 30, 1400–1405. doi:10.1021/ac60140a032
- Rees, S.L., Robinson, A.L., Khlystov, A., Stanier, C.O., Pandis, S.N., 2004. Mass balance closure and the federal reference method for PM_{2.5} in Pittsburgh, Pennsylvania. *Atmos. Environ., Findings from EPA’s Particulate Matter Supersites Program* 38, 3305–3318. doi:10.1016/j.atmosenv.2004.03.016
- Reichardt, C., 2003. *Solvents and Solvent Effects in Organic Chemistry*, 3rd ed. John Wiley & Sons.
- Rived, F., Rosés, M., Bosch, E., 1998. Dissociation constants of neutral and charged acids in methyl alcohol. The acid strength resolution. *Anal. Chim. Acta* 374, 309–324. doi:10.1016/S0003-2670(98)00418-8
- RJ Reynolds, 1991. Levulinic Acid. RJ Reynolds. Truth Tobacco Industry Documents. <https://industrydocuments.library.ucsf.edu/tobacco/docs/rymk0089>
- Rosés, M., Bosch, E., 2002. Influence of mobile phase acid–base equilibria on the chromatographic behaviour of protolytic compounds. *J. Chromatogr. A* 982, 1–30. doi:10.1016/S0021-9673(02)01444-9
- Sarmini, K., Kenndler, E., 1999. Ionization constants of weak acids and bases in organic solvents. *J. Biochem. Biophys. Methods* 38, 123–137. doi:10.1016/S0165-022X(98)00033-5
- Scherrer, R.A., Donovan, S.F., 2009. Automated potentiometric titrations in KCl/water-saturated octanol: Method for quantifying factors influencing ion-pair partitioning. *Anal. Chem.* 81, 2768–2778. doi:10.1021/ac802729k

- Schumacher, J.N., Green, C.R., Best, F.W., Newell, M.P., 1977. Smoke composition. An extensive investigation of the water-soluble portion of cigarette smoke. *J. Agric. Food Chem.* 25, 310–320. doi:10.1021/jf60210a003
- Shiraiwa, M., Berkemeier, T., Schilling-Fahnestock, K.A., Seinfeld, J.H., Pöschl, U., 2014. Molecular corridors and kinetic regimes in the multiphase chemical evolution of secondary organic aerosol. *AtmosChem Phys* 14, 8323–8341. doi:10.5194/acp-14-8323-2014
- Shivapurkar, R., Jeannerat, D., 2011. Determination of the relative pKa's of mixtures of organic acids using NMR titration experiments based on aliased 1H–13C HSQC spectra. *Anal. Methods* 3, 1316–1322. doi:10.1039/C0AY00771D
- Smith, J.N., Barsanti, K.C., Friedli, H.R., Ehn, M., Kulmala, M., Collins, D.R., Scheckman, J.H., Williams, B.J., McMurry, P.H., 2010. Observations of aminium salts in atmospheric nanoparticles and possible climatic implications. *Proc. Natl. Acad. Sci.* 107, 6634–6639. doi:10.1073/pnas.0912127107
- Song, G., Ng, N.L., 2005. Particle phase acidity and oligomer formation in secondary organic aerosol. *Environ. Sci. Amp Technol.* 38, 6582–9. doi:10.1021/es049125k
- Song, M., Marcolli, C., Krieger, U.K., Zuend, A., Peter, T., 2012. Liquid-liquid phase separation and morphology of internally mixed dicarboxylic acids/ammonium sulfate/water particles. *AtmosChem Phys* 12, 2691–2712. doi:10.5194/acp-12-2691-2012
- Steele, R., 1989. Chemical Evaluation of Levulinic Acid. RJ Reynolds. Truth Tobacco Industry Documents. <https://industrydocuments.library.ucsf.edu/tobacco/docs/rsbd0095>
- Stocker, T., Qin, D., Plattner, G., Tignor, M., Allen, S., Boschung, J., Nauels, A., Xia, Y., Bex, B., Midgley, B., 2013. Climate change 2013: the physical science basis. Contribution of working group I to the fifth assessment report of the intergovernmental panel on climate change.
- Swauger, J.E., Steichen, T.J., Murphy, P.A., Kinsler, S., 2002. An analysis of the mainstream smoke chemistry of samples of the U.S. cigarette market acquired between 1995 and 2000. *Regul. Toxicol. Pharmacol.* 35, 142–156. doi:10.1006/rtph.2001.1521
- Tang, X., Price, D., Praske, E., Lee, S.A., Shattuck, M.A., Purvis-Roberts, K., Silva, P.J., Asa-Awuku, A., Cocker III, D.R., 2013. NO₃ radical, OH radical and O₃-initiated

- secondary aerosol formation from aliphatic amines. *Atmos. Environ.* 72, 105–112. doi:10.1016/j.atmosenv.2013.02.024
- Thielen, A., Klus, H., Müller, L., 2008. Tobacco smoke: Unraveling a controversial subject. *Exp. Toxicol. Pathol.* 60, 141–156. doi:10.1016/j.etp.2008.01.014
- Tomar, S.L., Henningfield, J.E., 1997. Review of the evidence that pH is a determinant of nicotine dosage from oral use of smokeless tobacco. *Tob. Control* 6, 219–225. doi:10.1136/tc.6.3.219
- Trebs, I., Metzger, S., Meixner, F.X., Helas, G., Hoffer, A., Rudich, Y., Falkovich, A.H., Moura, M.A.L., da Silva, R.S., Artaxo, P., Slanina, J., Andreae, M.O., 2005. The NH_4^+ - NO_3^- - Cl^- - SO_4^{2-} - H_2O aerosol system and its gas phase precursors at a pasture site in the Amazon Basin: How relevant are mineral cations and soluble organic acids? *J. Geophys. Res. Atmospheres* 110, D07303. doi:10.1029/2004JD005478
- Trémillon, B., 1971. *Chemistry in Non-Aqueous Solvents*. Springer Science & Business Media.
- Wania, F., Lei, Y.D., Wang, C., Abbatt, J.P.D., Goss, K.-U., 2015. Using the chemical equilibrium partitioning space to explore factors influencing the phase distribution of compounds involved in secondary organic aerosol formation. *AtmosChem Phys* 15, 3395–3412. doi:10.5194/acp-15-3395-2015
- Watson, C.H., Trommel, J.S., Ashley, D.L., 2004. Solid-phase microextraction-based approach to determine free-base nicotine in trapped mainstream cigarette smoke total particulate matter. *J. Agric. Food Chem.* 52, 7240–7245. doi:10.1021/jf049455o
- Watson, C.V., Valentin-Blasini, L., Damian, M., Watson, C.H., 2015. Method for the determination of ammonium in cigarette tobacco using ion chromatography. *Regul. Toxicol. Pharmacol.* 72, 266–270. doi:10.1016/j.yrtph.2015.04.019
- Wayne, G.F., Connolly, G.N., Henningfield, J.E., 2006. Brand differences of free-base nicotine delivery in cigarette smoke: the view of the tobacco industry documents. *Tob. Control* 15, 189–198. doi:10.1136/tc.2005.013805
- You, Y., Bertram, A.K., 2015. Effects of molecular weight and temperature on liquid–liquid phase separation in particles containing organic species and inorganic salts. *AtmosChem Phys* 15, 1351–1365. doi:10.5194/acp-15-1351-2015

- Zhang, R., Wang, G., Guo, S., Zamora, M.L., Ying, Q., Lin, Y., Wang, W., Hu, M., Wang, Y., 2015. Formation of urban fine particulate matter. *Chem. Rev.* 115, 3803–3855. doi:10.1021/acs.chemrev.5b00067
- Zhang, Y., Seigneur, C., Seinfeld, J.H., Jacobson, M., Clegg, S.L., Binkowski, F.S., 2000. A comparative review of inorganic aerosol thermodynamic equilibrium modules: Similarities, differences, and their likely causes. *Atmos. Environ.* 34, 117–137. doi:10.1016/S1352-2310(99)00236-8
- Ziemann, P.J., Atkinson, R., 2012. Kinetics, products, and mechanisms of secondary organic aerosol formation. *Chem. Soc. Rev.* 41, 6582–6605. doi:10.1039/C2CS35122F
- Zuend, A., Seinfeld, J.H., 2012. Modeling the gas-particle partitioning of secondary organic aerosol: the importance of liquid-liquid phase separation. *AtmosChem Phys* 12, 3857–3882. doi:10.5194/acp-12-3857-2012

6. Appendices

6.1. Appendix A: ^1H NMR and HSQC Spectra for Simulated Organic PM

0.05 M hexanoic acid and 0.05 M benzylamine
in 66% organic solvent / 34% water (by mass):

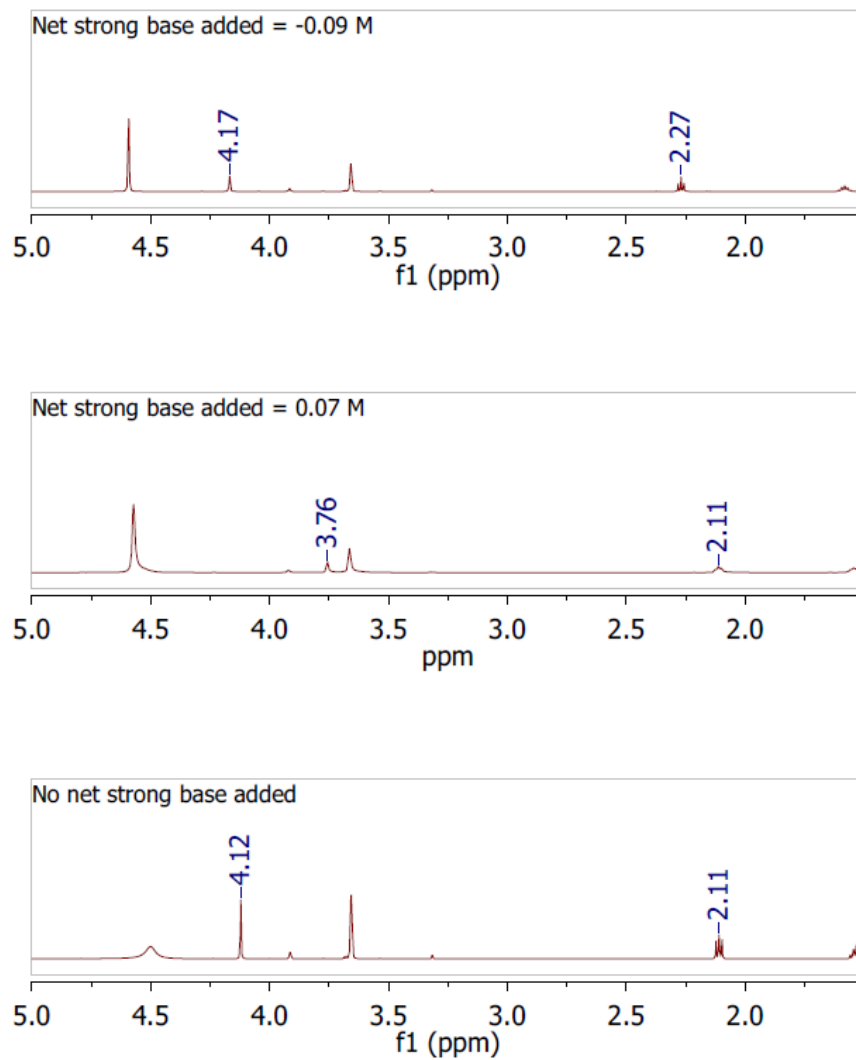


Figure 16. ^1H NMR spectra for simulated organic PM with 66% organic content, showing δ values for the target protons of benzylamine (downfield) and hexanoic acid (upfield) in fully acidified (top), fully basified (middle) and neutral (1:1 hexanoic acid and benzylamine with no net strong base added) samples.

**0.05 M hexanoic acid and 0.05 M benzylamine
in 84% organic solvent / 16% water (by mass):**

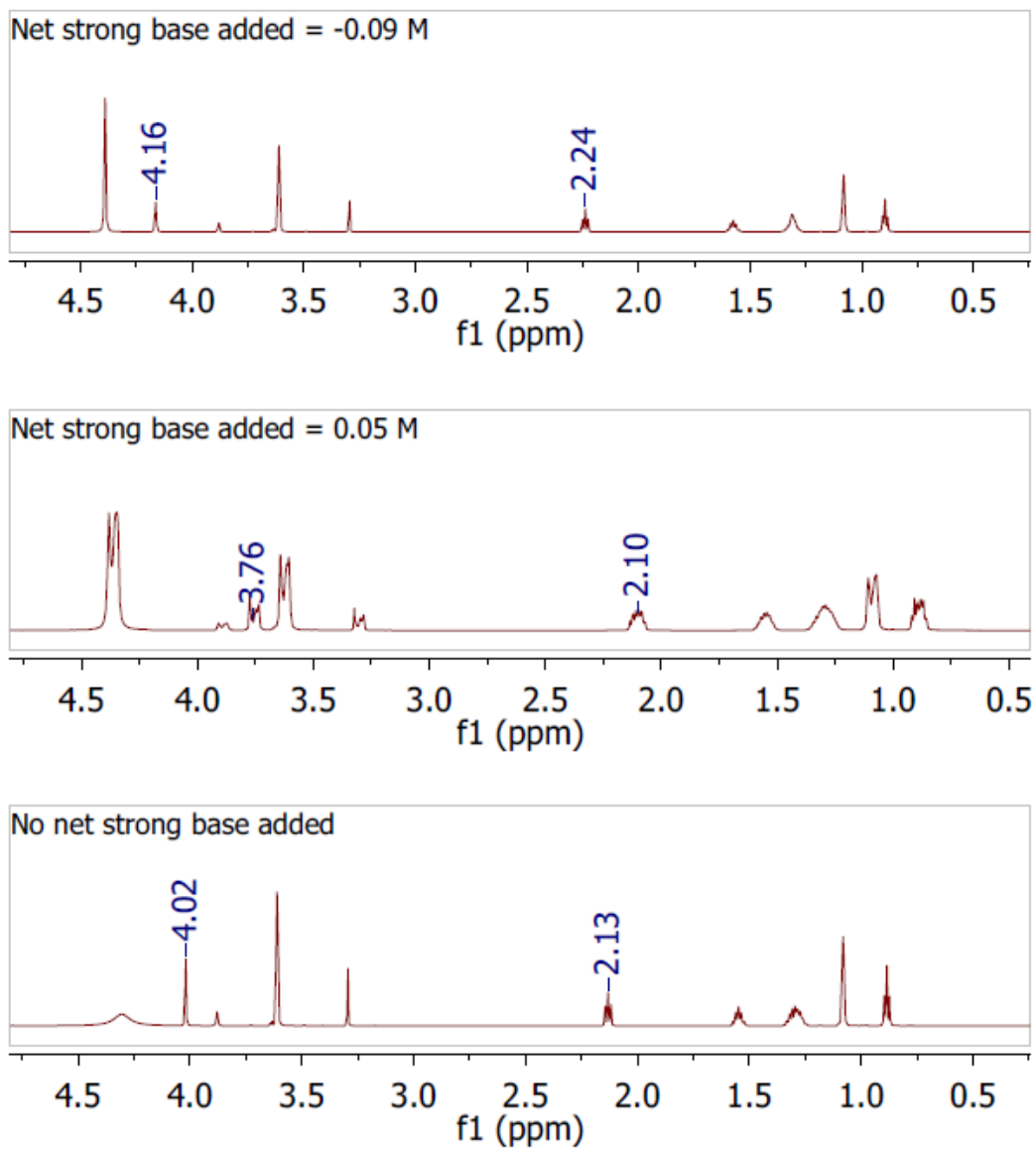


Figure 17. ¹H NMR spectra for simulated organic PM with 84% organic content, showing δ values for the target protons of benzylamine (downfield) and hexanoic acid (upfield) in fully acidified (top), fully basified (middle) and neutral (1:1 hexanoic acid and benzylamine with no net strong base added) samples.

**0.05 M hexanoic acid and 0.05 M benzylamine
in 95% organic solvent / 5% water (by mass):**

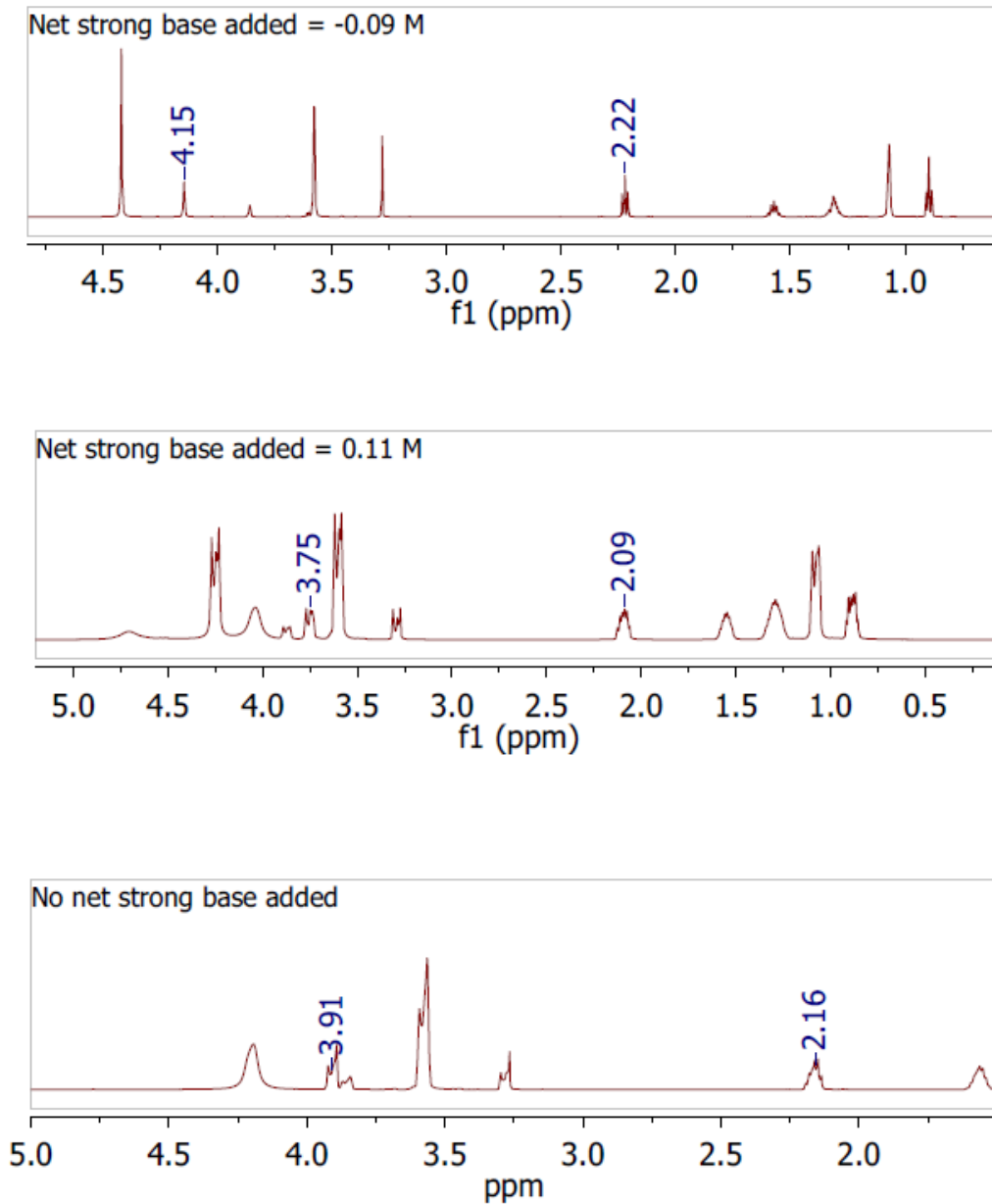


Figure 18. ¹H NMR spectra for simulated organic PM with 95% organic content, showing δ values for the target protons of benzylamine (downfield) and hexanoic acid (upfield) in fully acidified (top), fully basified (middle) and neutral (1:1 hexanoic acid and benzylamine with no net strong base added) samples.

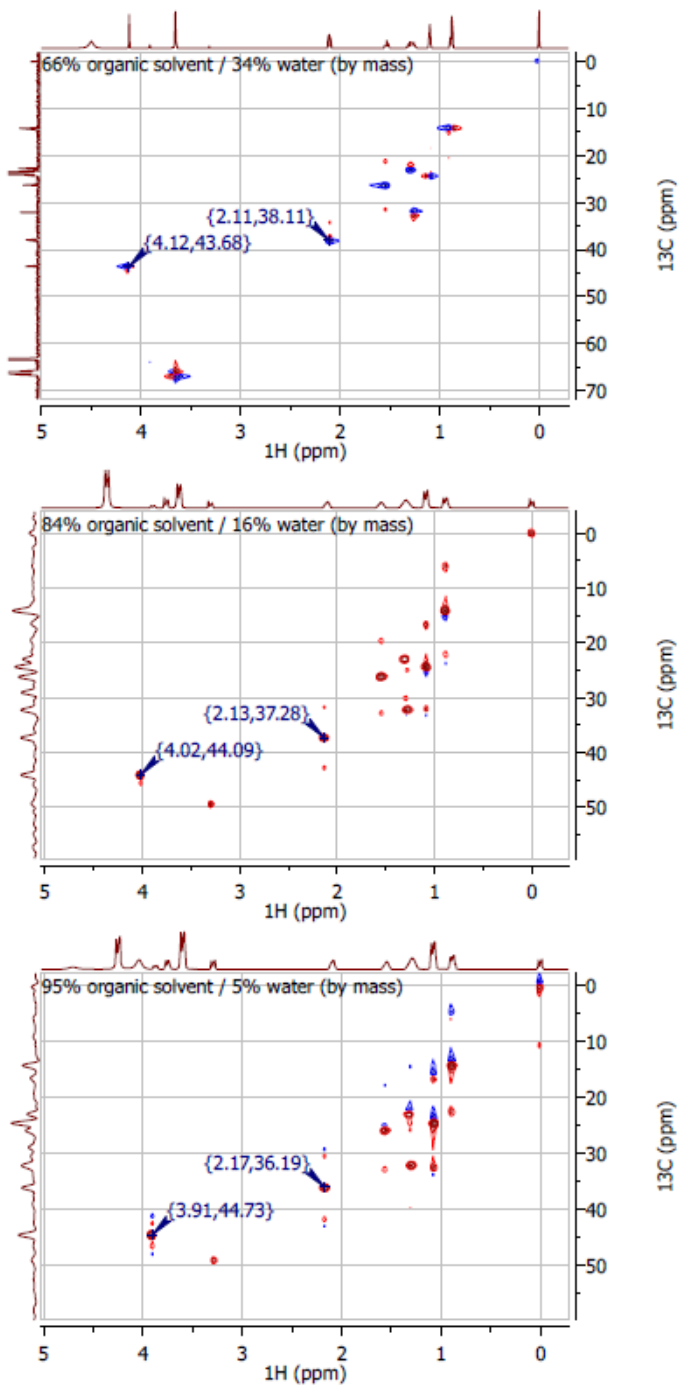


Figure 19. HSQC spectra showing the identification of target protons (proton δ on the x-axis) by their association with nearby carbon atoms (carbon δ on the y-axis). Simulated organic PM has 66% organic solvent (top), 84% organic solvent (middle), or 95% organic solvent (bottom).

6.2. Appendix B: Titration Curves for Tobacco Smoke PM

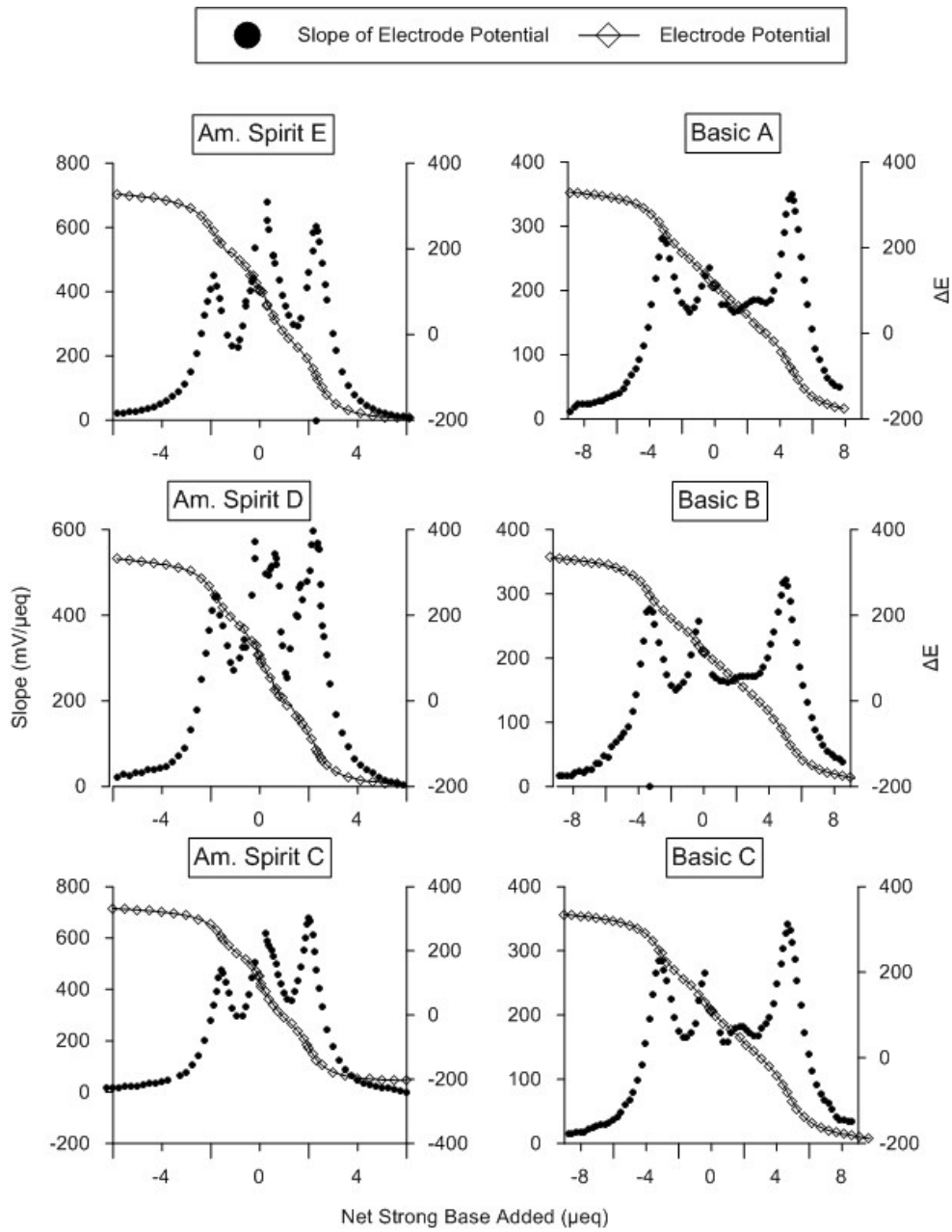


Figure 20. Titration curves and slopes of titration curves for smoke PM extracted from the first five puffs (plus lighting puff) of American Spirit and Basic brand cigarettes. Titration to the left of zero is with HCl and titration to the right of zero is with lithium phenoxide.

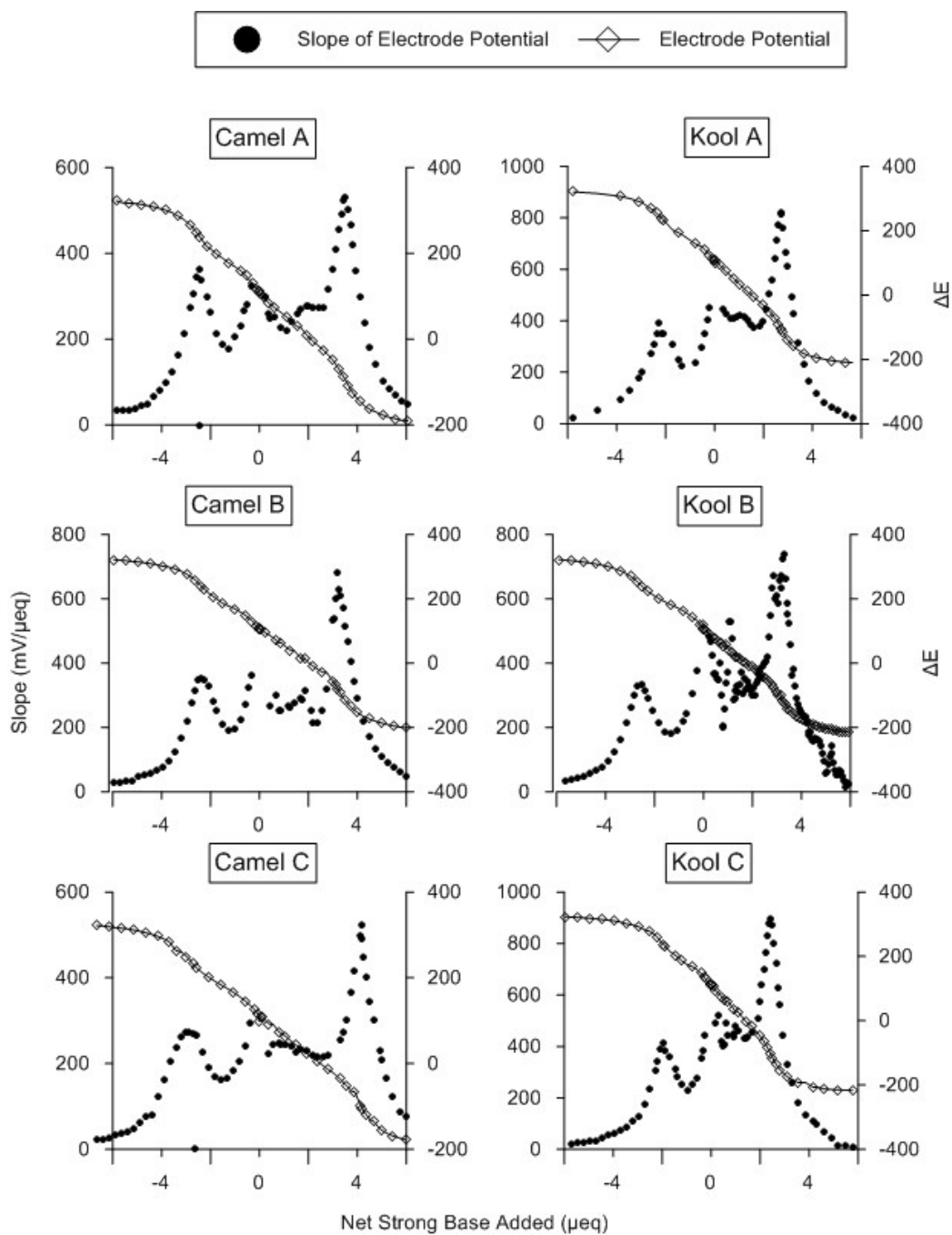


Figure 21. Titration curves and slopes of titration curves for smoke PM extracted from the first five puffs (plus lighting puff) of Camel and Kool brand cigarettes. Titration to the left of zero is with HCl and titration to the right of zero is with lithium phenoxide.

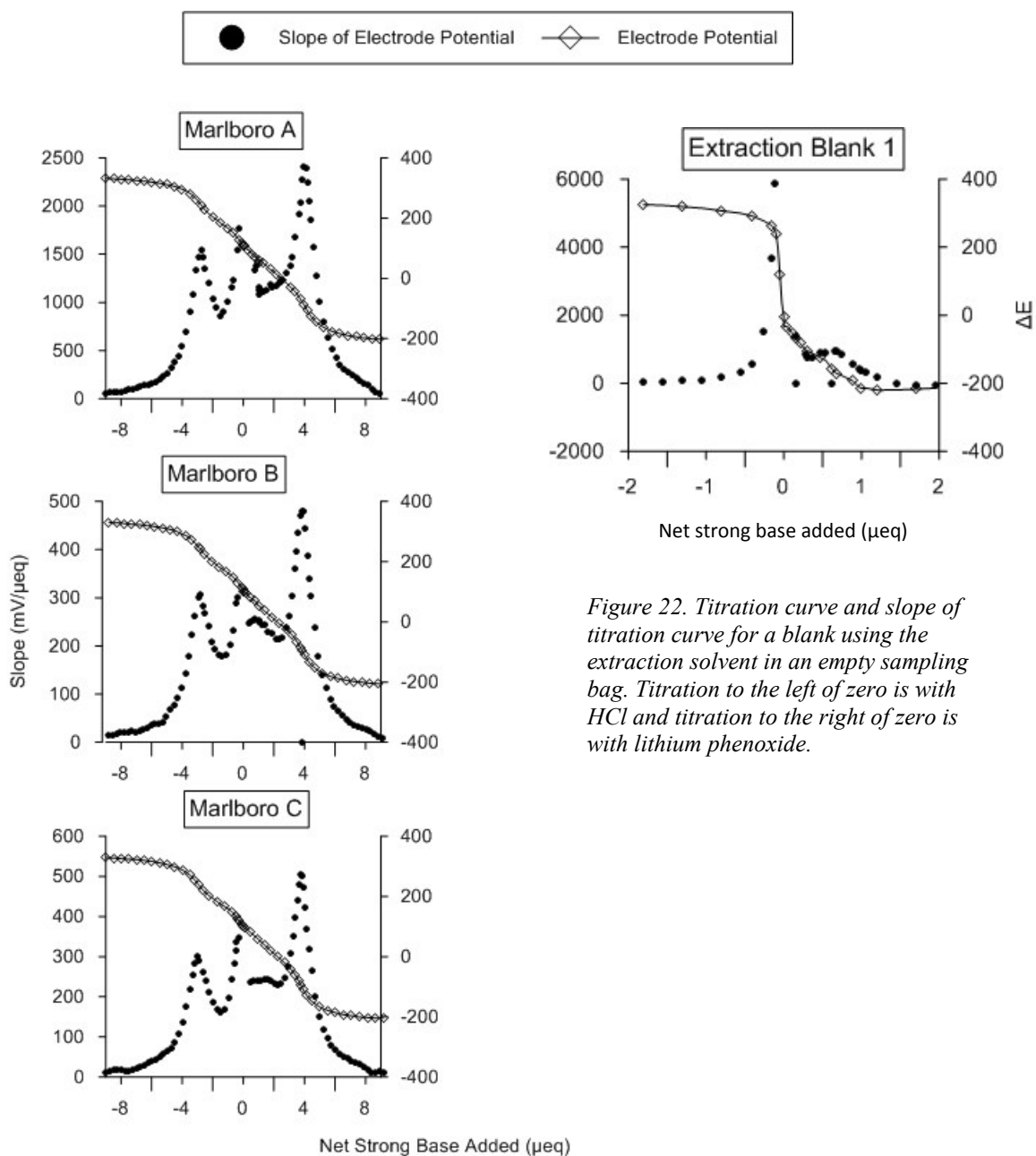


Figure 22. Titration curve and slope of titration curve for a blank using the extraction solvent in an empty sampling bag. Titration to the left of zero is with HCl and titration to the right of zero is with lithium phenoxide.

Figure 23. Titration curves and slopes of titration curves for smoke PM extracted from the first five puffs (plus lighting puff) of Marlboro brand cigarettes. Titration to the left of zero is with HCl and titration to the right of zero is with lithium phenoxide.

6.3. Appendix C: ^1H NMR Data for Acetic Acid and Nicotine in 95% IPA

In 98% IPA, the pK_a values of organic acids increase to such an extent that they no longer protonate bases such as nicotine in approximately neutral solutions. The pK_a of acetic acid increases from 4.75 in water to 11.35 in pure IPA (Bosch et al., 1995). The pK_a of nicotine in IPA is not precisely known, but the following NMR data demonstrates that acetic acid does not protonate nicotine at a 1:1 concentration in a 95% IPA solution.

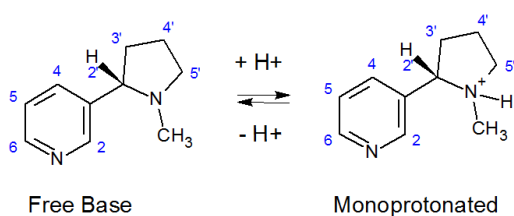


Figure 24. Free base and monoprotonated forms of nicotine

Whether nicotine is in the free base or monoprotonated form can be determined by subtracting the NMR frequencies (δ) of two of its protons (2' and 5 in Figure 23) to obtain a $\Delta\delta$ (Barsanti et al., 2007). Protonation is indicated by a shift of proton 2' downfield relative to proton 5 (smaller $\Delta\delta$), and fully-protonated and fully-unprotonated bounds can be determined by the addition of excess acid and excess base, respectively.

^1H NMR spectra of nicotine alone and nicotine/acetic acid d-4 show similar $\Delta\delta$ values with and without the addition of acid, demonstrating that a stronger acid than acetic acid (HCl) is required in both cases to achieve protonation of nicotine (Figure 25, Figure 26).

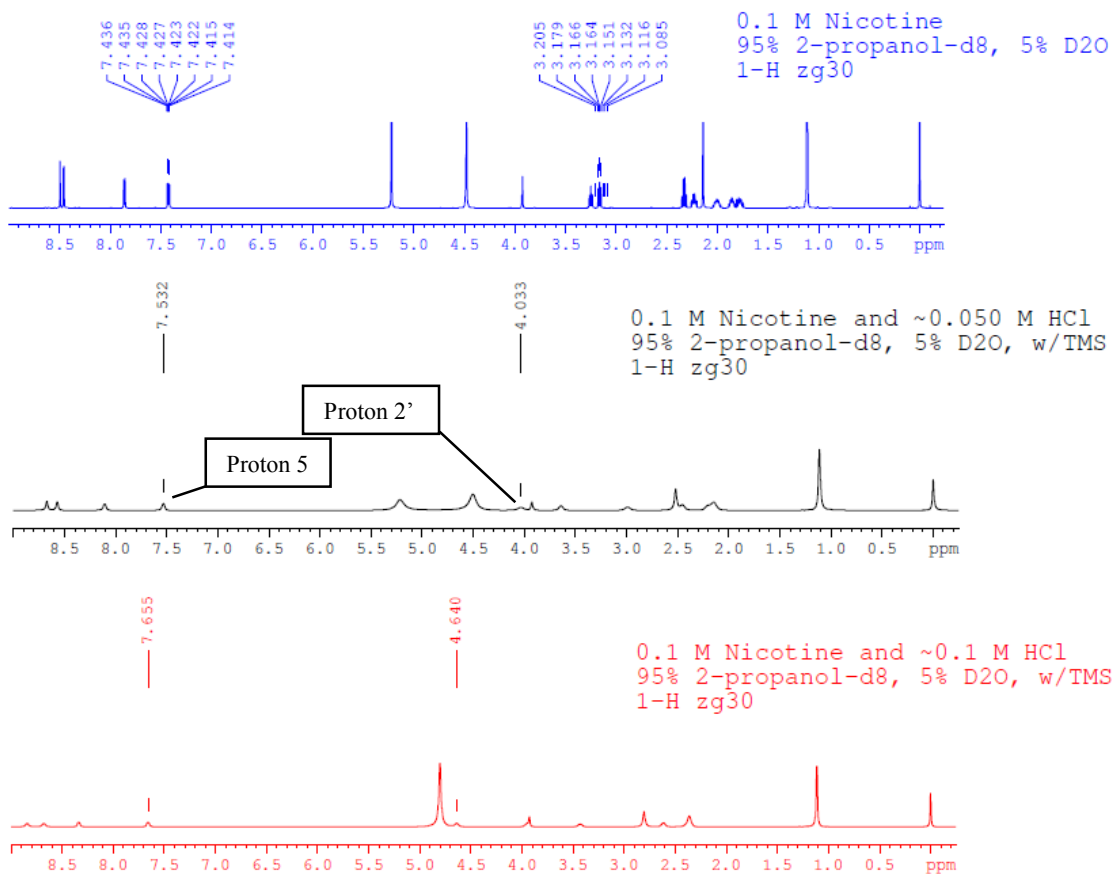


Figure 25. ^1H NMR spectra for nicotine in 95% IPA. Proton 2' can be seen moving downfield relative to the proton 5 with the addition of acid. In the top spectrum, nicotine is fully unprotonated, with $\Delta\delta = 7.42 - 3.16 = 4.26$; in the bottom spectrum, nicotine is fully protonated by HCl, with $\Delta\delta = 7.66 - 4.64 = 3.02$.

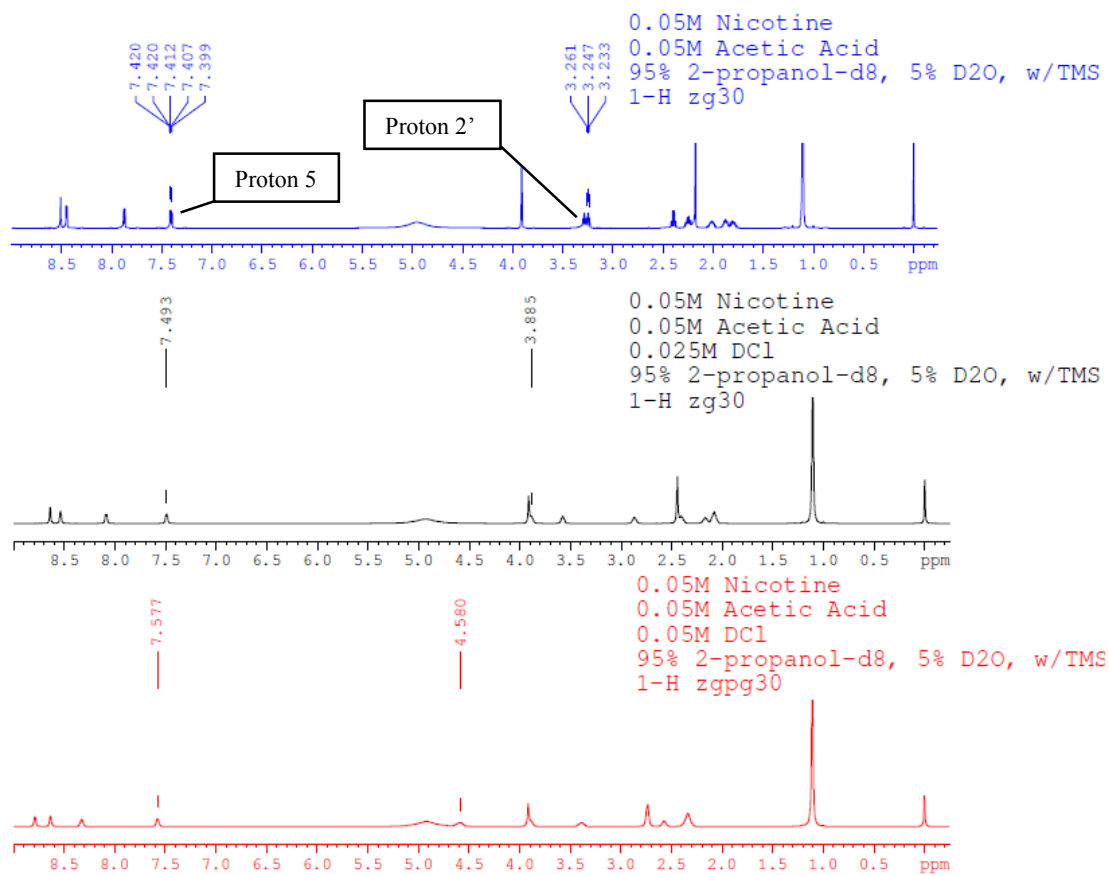


Figure 26. ^1H NMR spectra for nicotine and acetic acid- d_4 in 95% IPA. Proton 2' can be seen moving downfield relative to the proton 5 with the addition of acid. In the top spectrum, $\Delta\delta = 7.41 - 3.25 = 4.16$; in the bottom spectrum, $\Delta\delta = 7.57 - 4.58 = 2.99$.

6.4. Appendix D: Ion Chromatograms

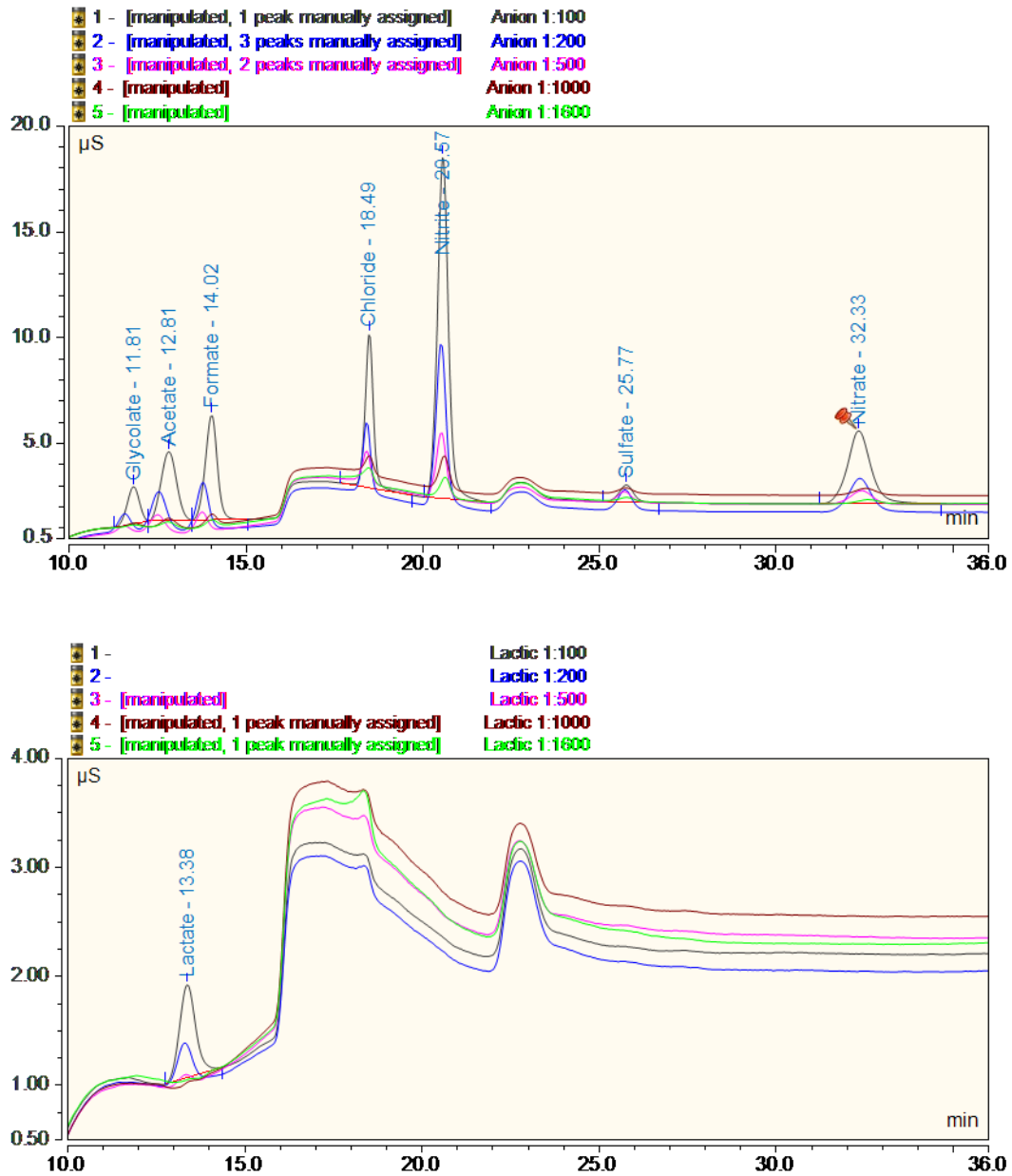


Figure 27. Ion chromatograms for anion standards at five concentrations used to construct calibration curves. Lactate (bottom) was measured as a separate standard due to its poor peak resolution in a mixed standard.

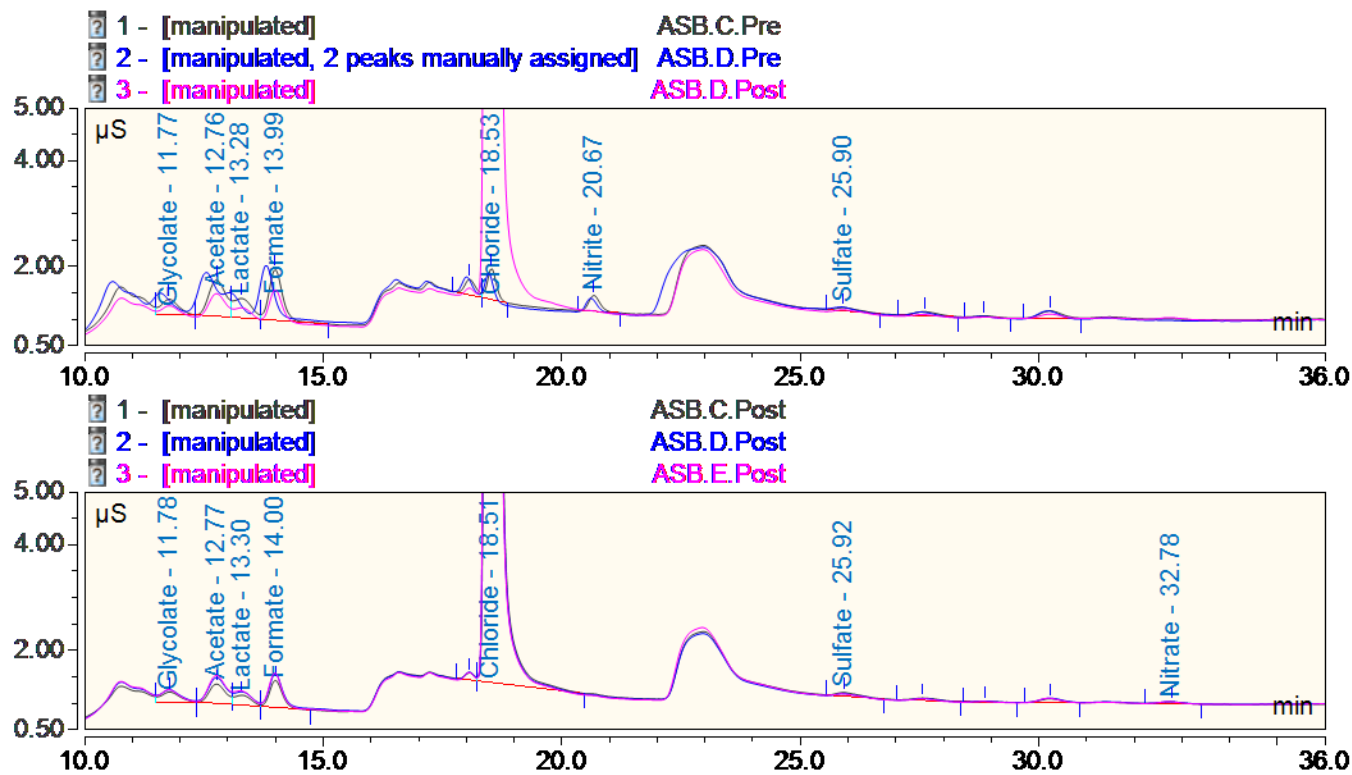


Figure 28. Anion chromatograms for smoke PM extracted from the first five puffs (plus lighting puff) for American Spirit brand cigarettes from initial sample (top) and acidified sample (bottom). X-axis = run-time and y-axis = signal in μS . Retention times are given for each analyte peak.

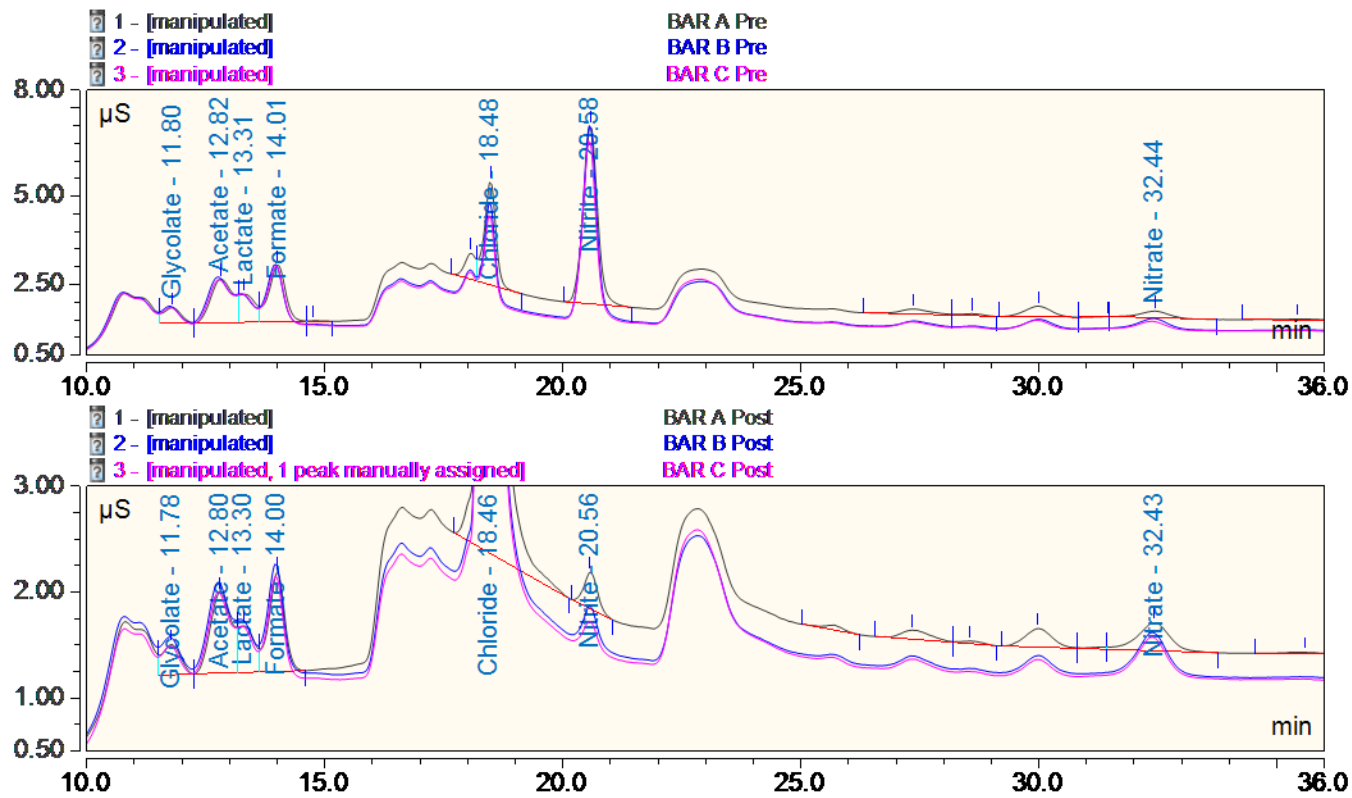


Figure 29. Anion chromatograms for smoke PM extracted from the first five puffs (plus lighting puff) for Basic brand cigarettes from initial sample (top) and acidified sample (bottom). X-axis = run-time and y-axis = signal in μS . Retention times are given for each analyte peak.

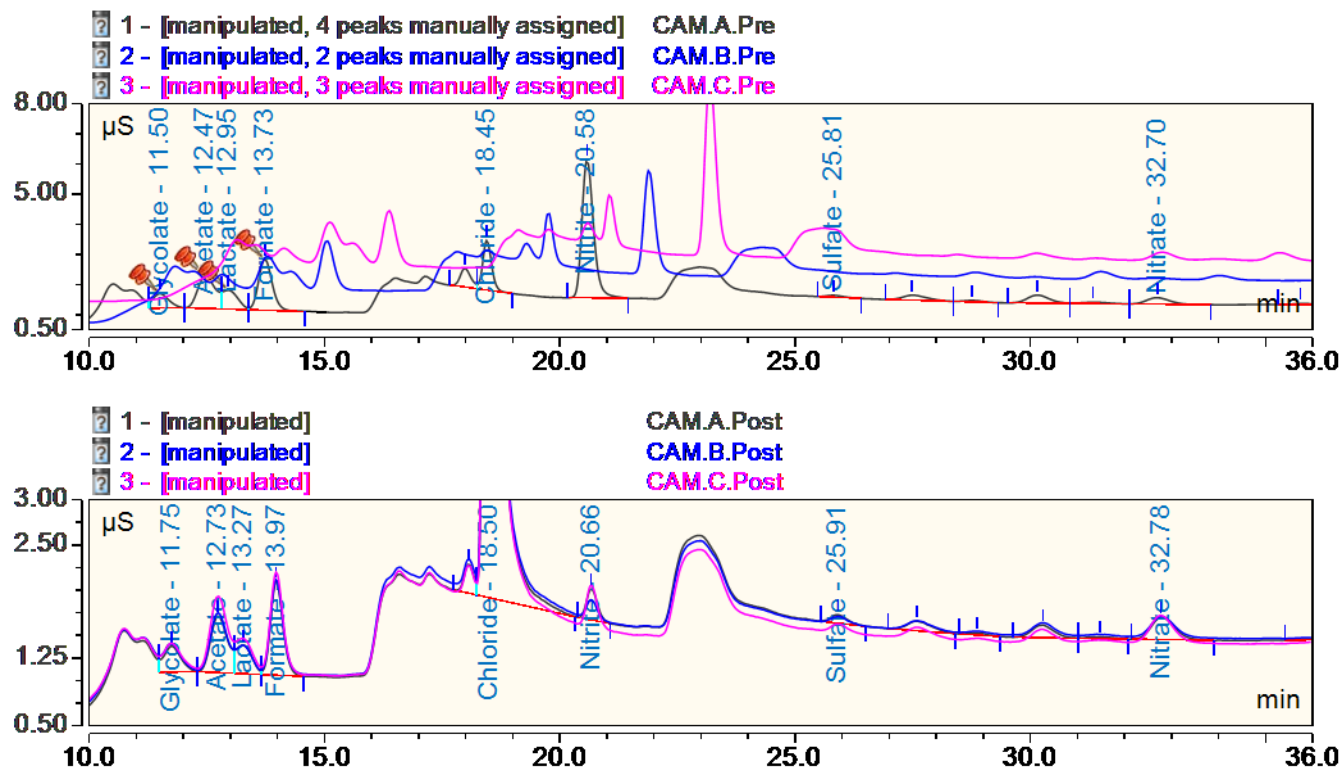


Figure 30. Anion chromatograms for smoke PM extracted from the first five puffs (plus lighting puff) for Camel brand cigarettes from initial sample (top) and acidified sample (bottom). X-axis = run-time and y-axis = signal in μS . Retention times are given for each analyte peak.

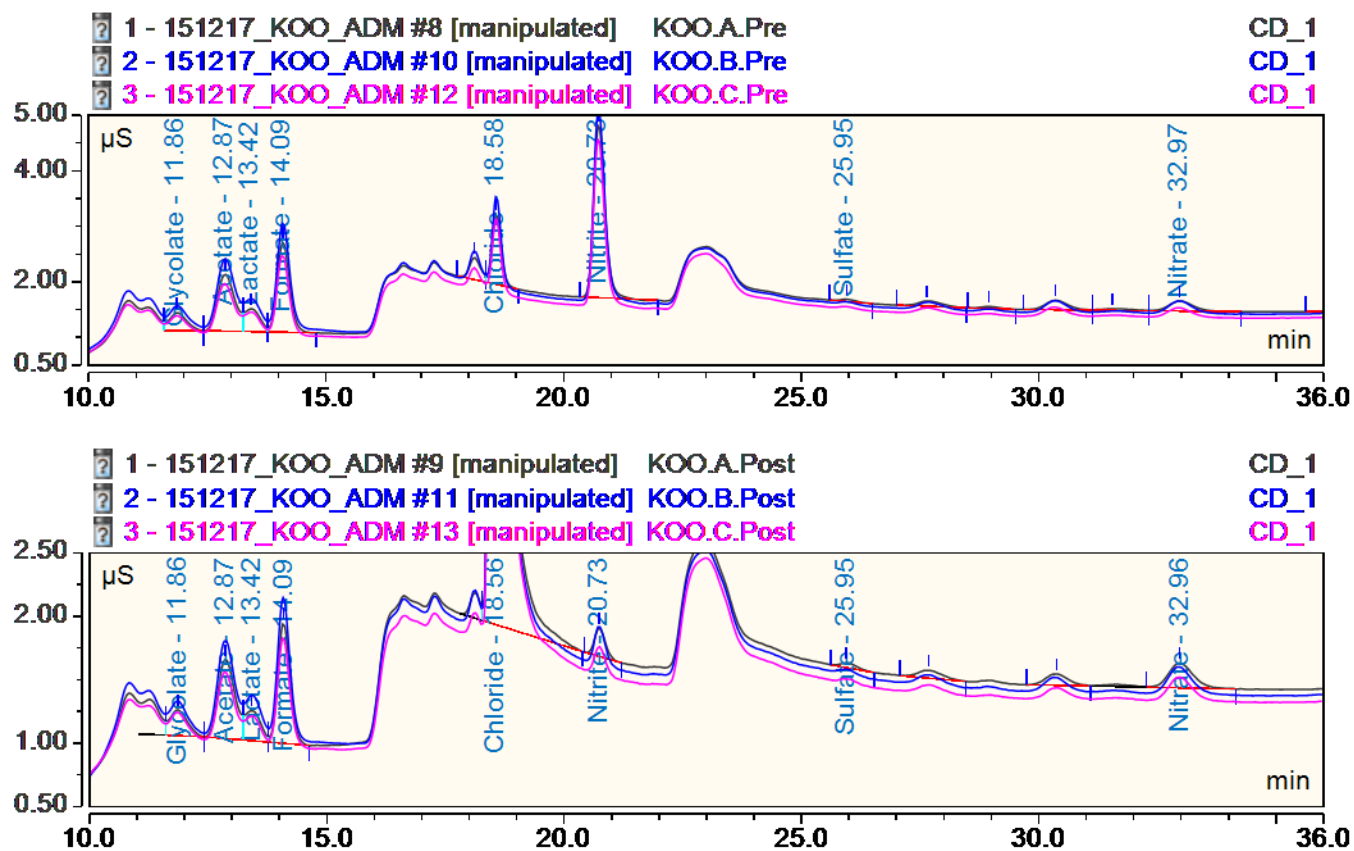


Figure 31. Anion chromatograms for smoke PM extracted from the first five puffs (plus lighting puff) for Kool brand cigarettes from initial sample (top) and acidified sample (bottom). X-axis = run-time and y-axis = signal in μS . Retention times are given for each analyte peak.

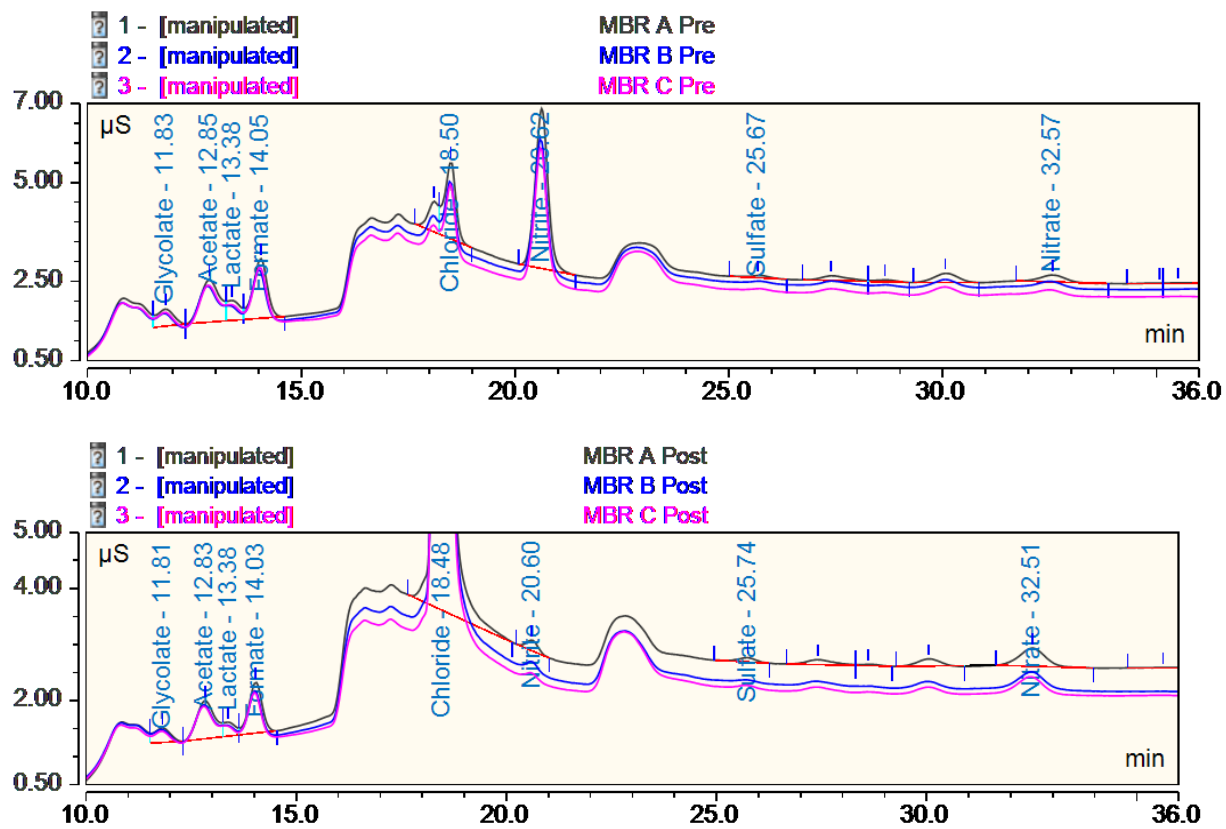


Figure 32. Anion chromatograms for smoke PM extracted from the first five puffs (plus lighting puff) for Marlboro brand cigarettes from initial sample (top) and acidified sample (bottom). X-axis = run-time and y-axis = signal in μS . Retention times are given for each analyte peak.

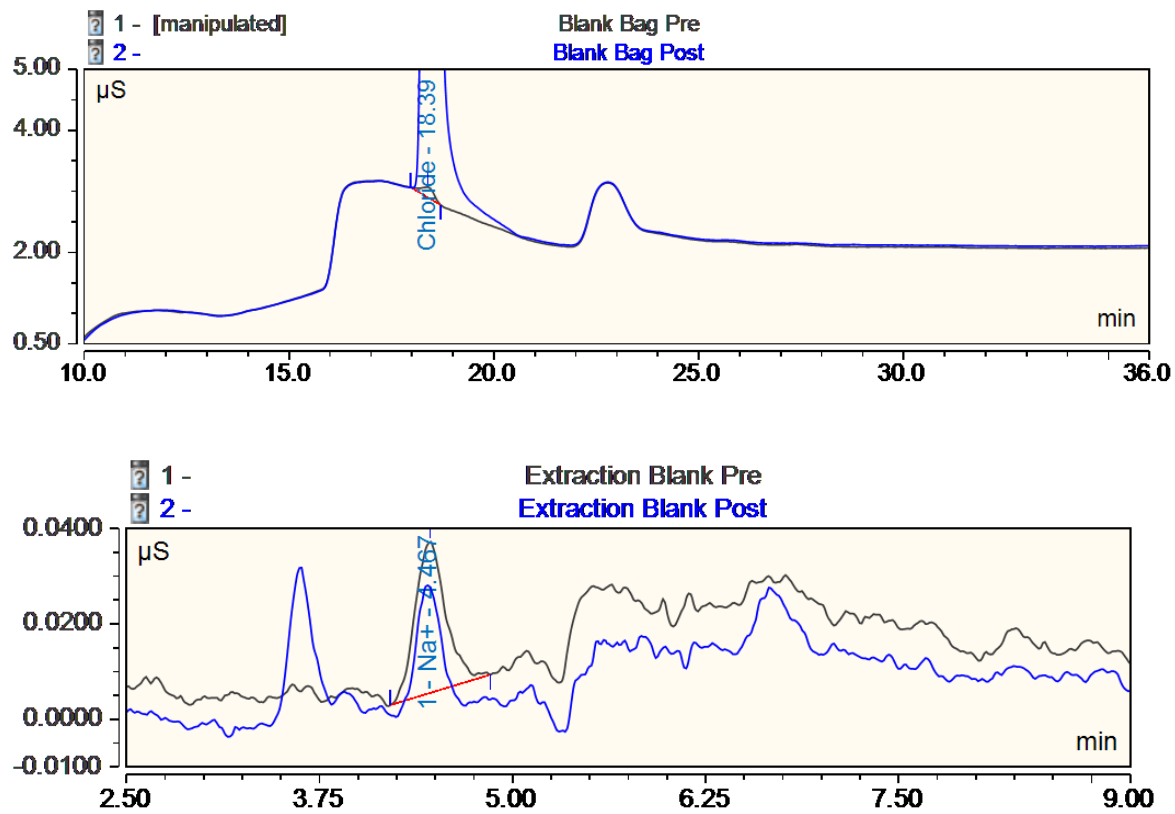


Figure 33. Anion (top) and cation (bottom) chromatograms for initial (black line) and acidified (blue line) blanks made using the extraction solvent to extract from an empty sampling bag. A trace amount of sodium chloride is detected.

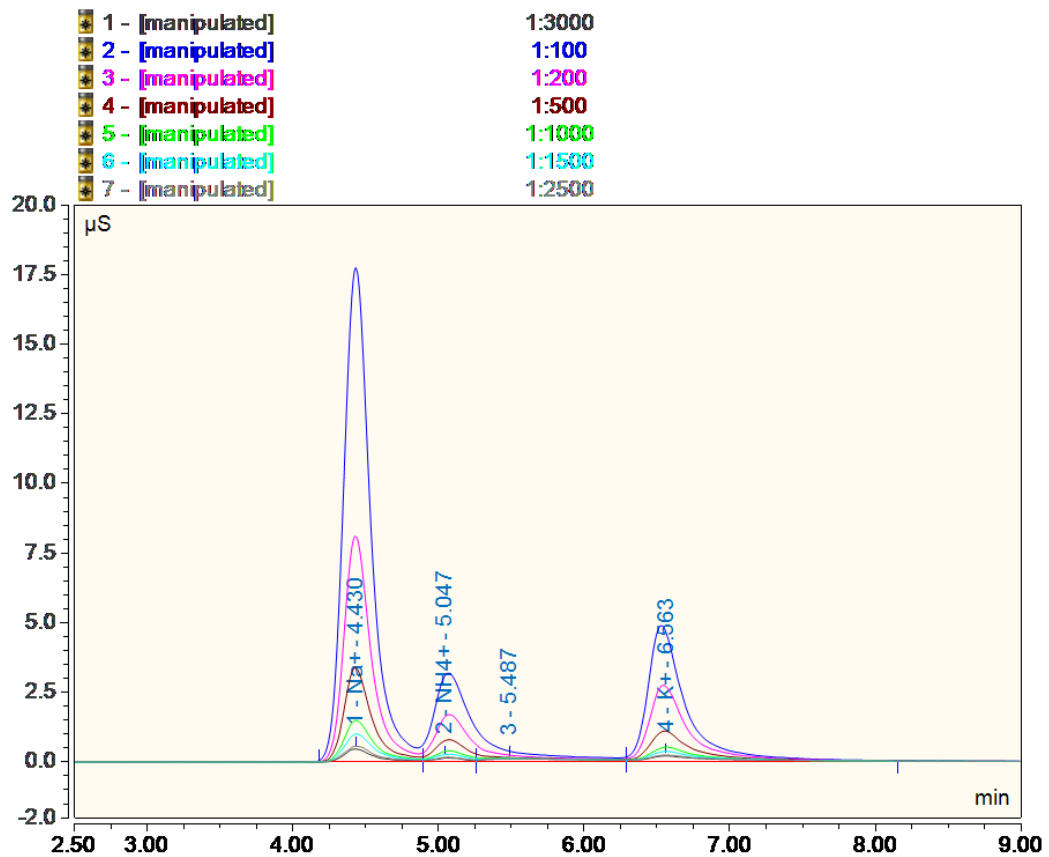


Figure 34. Ion chromatograms for cation standards at seven concentrations used to construct the calibration curve.

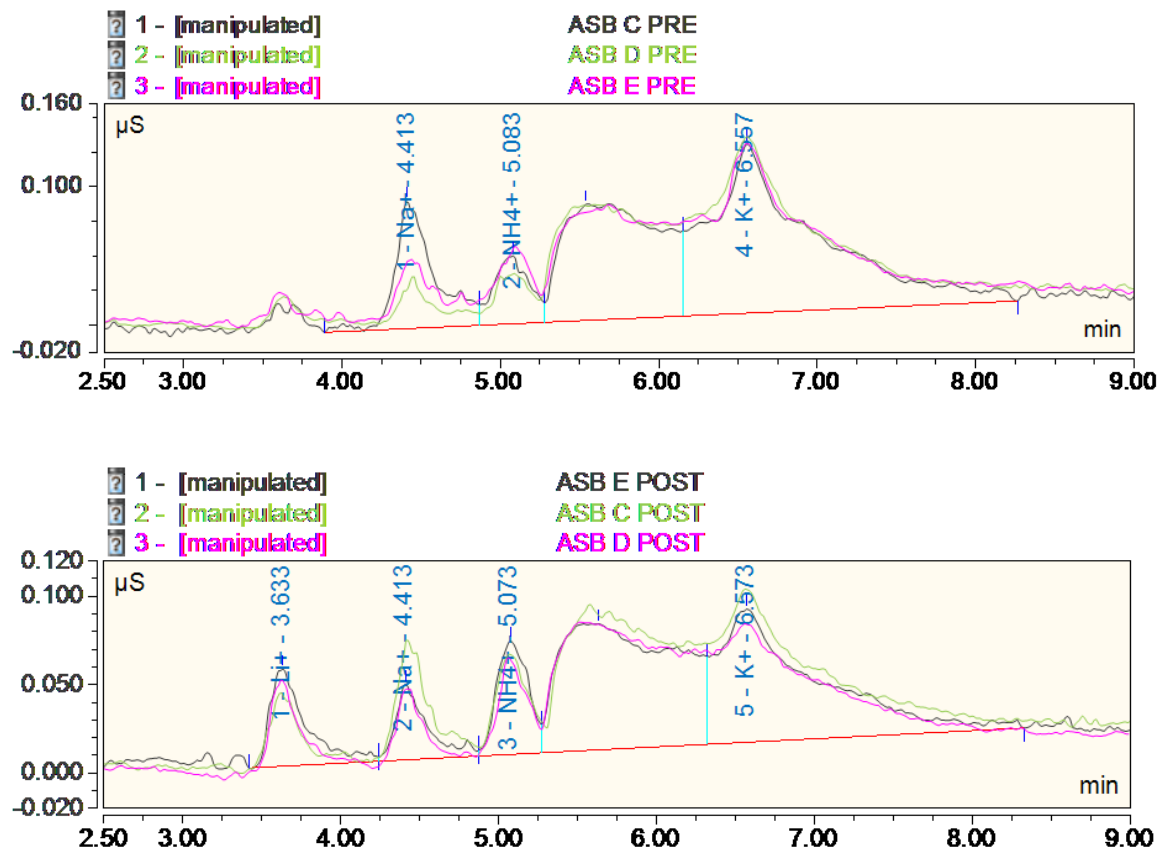


Figure 35. Cation chromatograms for smoke PM extracted from the first five puffs (plus lighting puff) for American Spirit brand cigarettes from initial sample (top) and acidified sample (bottom). X-axis = run-time and y-axis = signal in μS . Retention times are given for each analyte peak.

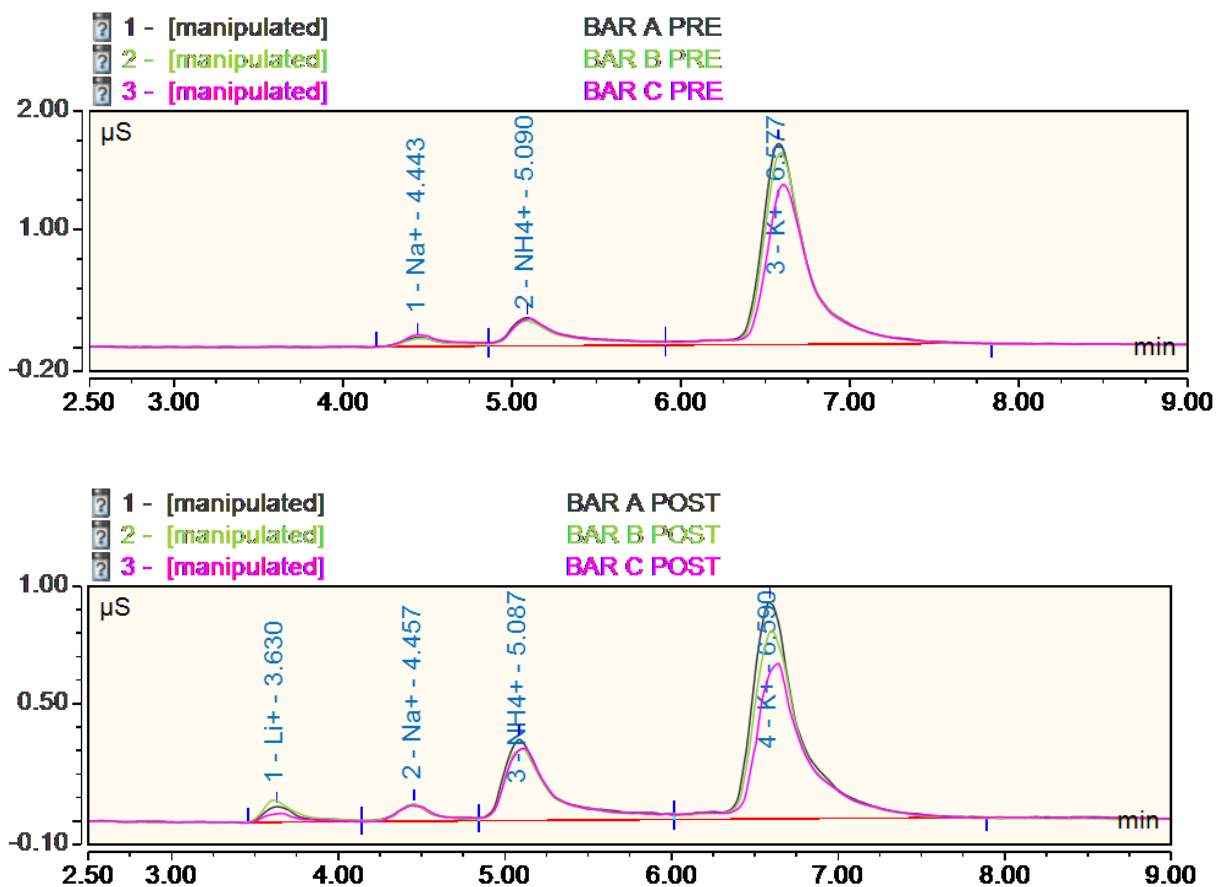


Figure 36. Cation chromatograms for smoke PM extracted from the first five puffs (plus lighting puff) for Basic brand cigarettes from initial sample (top) and acidified sample (bottom). X-axis = run-time and y-axis = signal in μS . Retention times are given for each analyte peak.

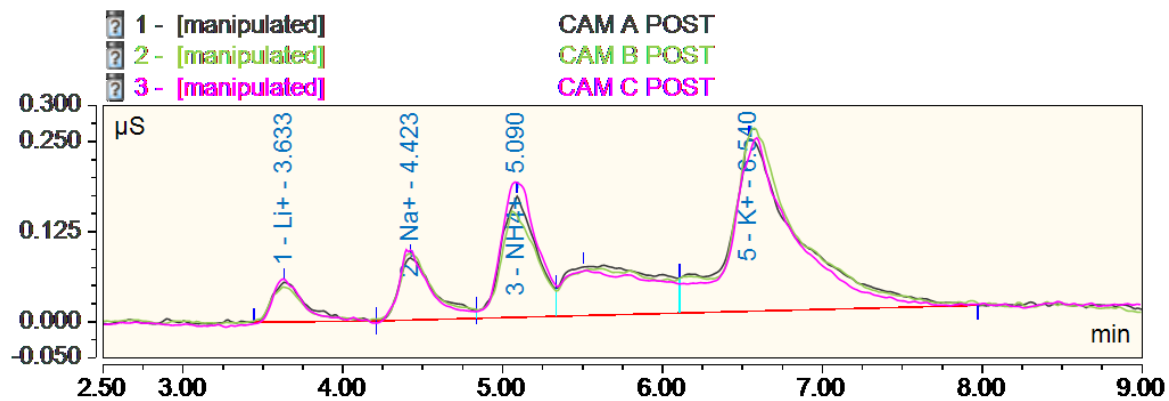
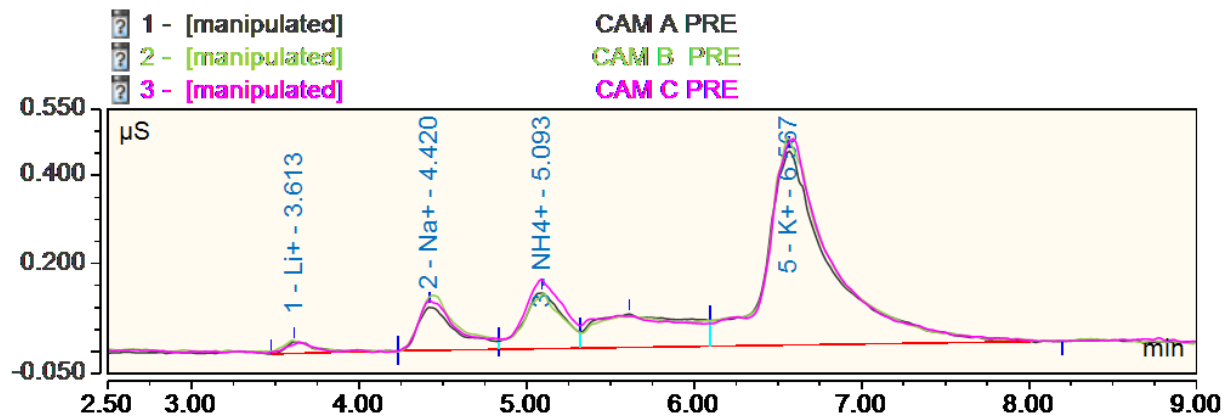


Figure 37. Cation chromatograms for smoke PM extracted from the first five puffs (plus lighting puff) for Camel brand cigarettes from initial sample (top) and acidified sample (bottom). X-axis = run-time and y-axis = signal in uS. Retention times are given for each analyte peak.

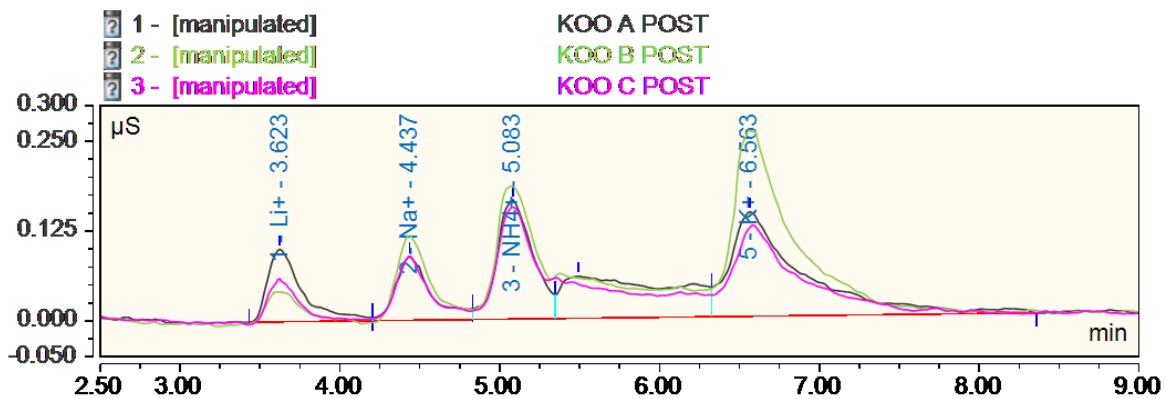
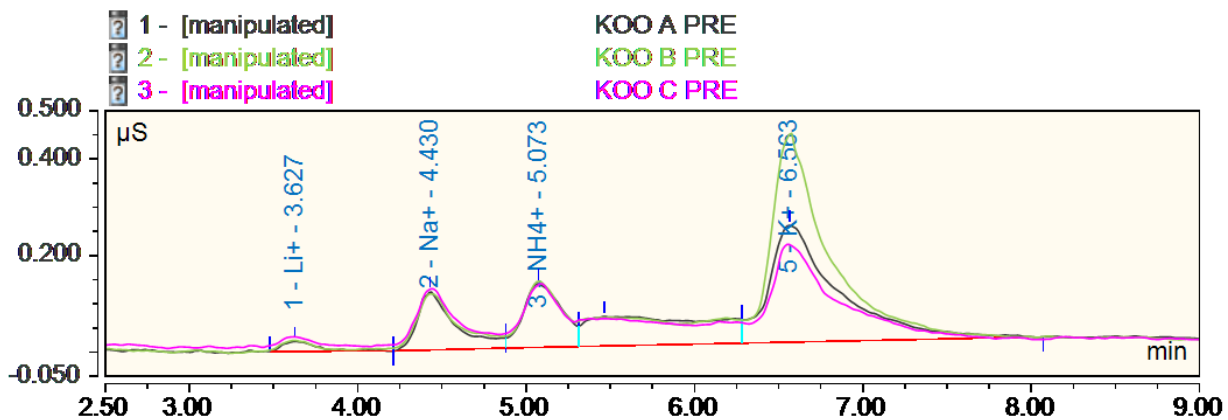


Figure 38. Cation chromatograms for smoke PM extracted from the first five puffs (plus lighting puff) for Kool brand cigarettes from initial sample (top) and acidified sample (bottom). X-axis = run-time and y-axis = signal in μS . Retention times are given for each analyte peak.

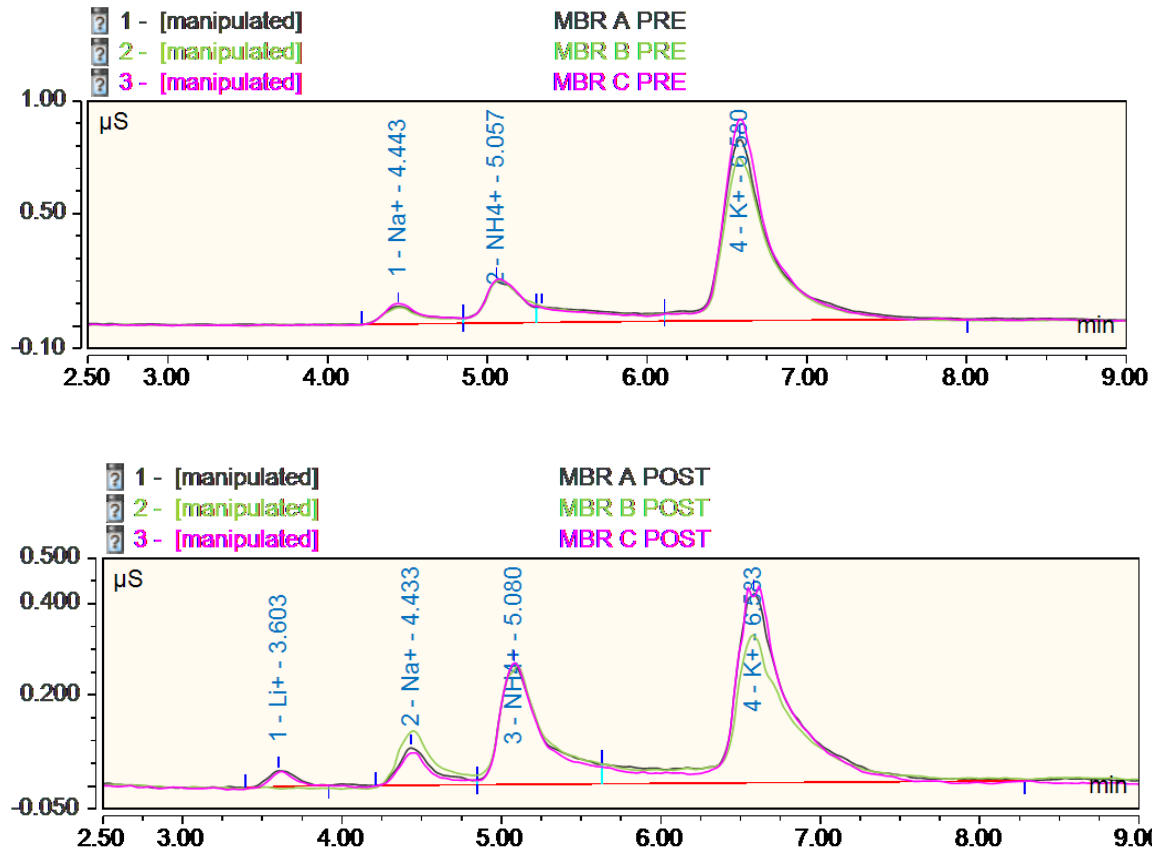


Figure 39. Cation chromatograms for smoke PM extracted from the first five puffs (plus lighting puff) for Marlboro brand cigarettes from initial sample (top) and acidified sample (bottom). X-axis = run-time and y-axis = signal in μS . Retention times are given for each analyte peak.